



Asymptotic behavior of quantum invariants

CLASSE DI SCIENZE
Corso di Perfezionamento in Matematica

Submitted by
Giulio Belletti

Advisors:

Professor Bruno Martelli
Università di Pisa

Professor Francesco Costantino
Université Paul Sabatier

Abstract

In this thesis we address the problem of the rate of growth of quantum invariants, specifically the Turaev-Viro invariants of compact manifolds and the related Yokota invariants for embedded graphs. We prove the recent volume conjecture proposed by Chen and Yang in two interesting families of hyperbolic manifolds. Furthermore we propose a similar conjecture for the growth of a certain quantum invariant of planar graphs, and prove it in a large family of examples.

This new conjecture naturally leads to the problem of finding the supremum of the volume function among all proper hyperbolic polyhedra with a fixed 1-skeleton; we prove that the supremum is always achieved at the rectification of the 1-skeleton.

Contents

Contents	2
1 Introduction	3
2 Three-manifolds and hyperbolic geometry	9
2.1 Dehn surgery and Kirby calculus	9
2.2 Hyperbolic geometry	12
2.3 Hyperbolic 3-manifolds	31
3 Quantum invariants	33
3.1 The Kauffman skein module	33
3.2 The Kauffman bracket of trivalent graphs	36
3.3 The Reshetikhin-Turaev invariants	41
3.4 The Turaev-Viro invariants	42
3.5 The Yokota invariant	44
4 The upper bound of the $6j$-symbol	49
4.1 Proof of the upper bound	49
4.2 Proofs of the technical lemmas	55
4.3 The Volume Conjecture for FSLs	63
5 The Maximum Volume Theorem	65
5.1 Related results	65
5.2 Proof of the Maximum Volume Theorem	67
5.3 Proof of Proposition 5.2	70
6 Volume conjecture for polyhedra	83
6.1 The volume conjecture for polyhedra	83
6.2 The Fourier Transform	85
6.3 The Turaev-Viro volume conjecture	92
A Numerical evidence for Conjecture 1.3	99
Bibliography	103

Chapter 1

Introduction

The Jones polynomial is an invariant of knots and links introduced in [24]; it quickly generated a strong interest and, thanks to insights of Witten [55], led to the construction of the colored Jones polynomials of knots and links [41], of the Reshetikhin-Turaev invariants of 3-manifolds [42] (and the related Turaev-Viro invariants [50]), and invariants of embedded graphs [28] and [56], among other things.

A major question about the invariants originated from the Jones polynomials has been the amount of information that they contain, especially with respect to their asymptotic behavior. An important motivating question in their study has been the Kashaev volume conjecture [25]:

Conjecture 1.1. *Let $K \subseteq S^3$ be a hyperbolic knot, and J_n^K the sequence of its colored Jones polynomials. Then,*

$$\lim_{n \rightarrow \infty} \frac{2\pi}{n} \log \left| J_n^K(e^{\pi i/n}) \right| = \text{Vol}(S^3 \setminus K)$$

where $\text{Vol}(S^3 \setminus K)$ is the volume of the unique hyperbolic structure of $S^3 \setminus K$.

This conjecture has been verified for knots with few crossings [37] [38] [40], still only in a finite number of examples.

As we mentioned, the colored Jones polynomials can be “enhanced” to give invariants of closed 3-manifolds (the Reshetikhin-Turaev invariants) or compact 3-manifolds (the Turaev-Viro invariants). These invariants are closely related (see Proposition 3.14), but for the purpose of this thesis we are going to concentrate on the Turaev-Viro invariants.

The Turaev-Viro invariants (see Section 3.4) take as input:

- an integer $r \geq 2$ called the *level*;

- a complex number $q \in \mathbb{C}$ that is either a primitive $2r$ -th root of unity or a primitive r -th root of unity if r is odd;
- a compact orientable manifold M

and give as output a real number $TV_r(M, q)$. The most natural choice for q is the first root of unity $q = e^{\pi i/r}$. This case, called *unitary*, is the most studied and the analog of the Volume Conjecture has been an open problem for a long time.

Conjecture 1.2 (The Witten expansion conjecture for Turaev-Viro invariants [55]). *Let M be a closed manifold, $r \geq 2$ and $q = e^{\pi i/r}$. Then*

$$TV_r(M, q) \sim_{r \rightarrow \infty} \left| \int_A e^{2\pi i CS(A)} r^{(h_A^1 - h_A^0)} e^{-2\pi i \left(\frac{2I_A + h_A^0}{8}\right)} \tau_M(A)^{\frac{1}{2}} \right|^2.$$

This conjecture is known for a few cases, most notably lens spaces [23] and an infinite family of Dehn surgeries on the figure eight knot [10], [9]. For a complete discussion of the known results about the Witten expansion conjecture, see the discussion in the introduction of [10]. The specific terms involved in the conjecture are not important for the purpose of this thesis, however it is important to notice two differences between the Volume Conjecture and the Witten expansion conjecture:

1. the growth of TV_r is polynomial (since the integrand is polynomial in r);
2. the growth of TV_r does not involve the hyperbolic volume (indeed, it only involves topological invariants).

The fact that the growth of TV_r in this case is at most polynomial is easy and has been known for a long time.

In stark contrast to the Witten expansion conjecture, Chen and Yang in [12] noticed that if we instead choose $q = e^{2\pi i/r}$ (notice that this is only allowed when r is odd) the growth of TV_r is in line with the Volume conjecture, and they proposed the following.

The Turaev-Viro Volume Conjecture. Let M be a hyperbolic 3-manifold, either closed, with cusps, or compact with geodesic boundary. Then as r varies along the odd natural numbers,

$$\lim_{r \rightarrow \infty} \frac{2\pi}{r} \log \left(TV_r \left(M, e^{\frac{2\pi i}{r}} \right) \right) = \text{Vol}(M) \quad (1.1)$$

Thus in this case the growth of TV_r is expected to be exponential and determined by the hyperbolic volume. As a matter of fact Chen and Yang

provide numerical evidence that this behavior is observed for any choice of root of unity which is not unitary. The conjecture has since been proven for the complements of the figure eight knot and the Borromean links [19] and for all integral (hyperbolic) Dehn surgeries on the figure eight knot [39].

The colored Jones polynomials can be also extended to define invariants of colored embedded graphs $\Gamma \subseteq M$, called the *Yokota invariants* $Y_r(M, \Gamma, col, q)$. In this general case a satisfying conjecture about the asymptotic growth of the Yokota invariant is not yet available; however an elegant formulation is possible for the case where Γ is a planar 3-connected graph.

Conjecture 1.3 (The Volume Conjecture for polyhedra). *Let P be a proper hyperbolic polyhedron with dihedral angles $\alpha_1, \dots, \alpha_m$ at the edges e_1, \dots, e_m , and 1-skeleton Γ . Let col_r be a sequence of r -admissible colorings $col_r(e_i)$ of the edges e_1, \dots, e_m of Γ such that*

$$2\pi \lim_{r \rightarrow +\infty} \frac{col_r(e_i)}{r} = \pi - \alpha_i.$$

Then

$$\lim_{r \rightarrow +\infty} \frac{\pi}{r} \log \left| Y_r(S^3, \Gamma, col, e^{2\pi i/r}) \right| = \text{Vol}(P).$$

This conjecture appeared in [16] [52] [29] in slightly different versions; here we propose a unified statement.

In this thesis we explore the asymptotics of these quantum invariants and their relation to the hyperbolic volume. The first main result is the fact that the Turaev-Viro Volume Conjecture holds for a large family of hyperbolic manifolds.

The following theorem is proved in a joint work with R. Detcherry, E. Kalfagianni and T. Yang:

Theorem 1.4. [7] *The Turaev-Viro Volume Conjecture holds for the complements of all Fundamental Shadow Links.*

Fundamental shadow links are links in $\#^g S^1 \times S^2$ whose complement are always hyperbolic; furthermore they are universal, in the sense that every closed oriented 3-manifold is obtained from one of their complements via Dehn filling. The fact that the Volume Conjecture holds for these manifolds has a few implications regarding other open problems in low dimensional topology, see [7, Section 6].

Regarding the Yokota invariant we introduce here a related invariant that is, in some sense, an analog for graphs to the Turaev-Viro invariants. This invariant, that we denote by $TV_r(\Gamma, q)$, is defined for any graph $\Gamma \subseteq S^3$ (not necessarily trivalent).

We formulate the following volume conjecture regarding its growth.

Conjecture 1.5 (The Maximum Volume Conjecture). [5] *Let $\Gamma \subseteq S^3$ be a 3-connected planar graph. Then*

$$\lim_{r \rightarrow +\infty} \frac{\pi}{r} \log \left(TV_r(\Gamma, e^{\frac{2\pi i}{r}}) \right) = \sup_P \text{Vol}(P)$$

where P varies among all proper generalized hyperbolic polyhedra (see Definition 2.7) with Γ as a 1-skeleton, and r ranges across all odd natural numbers.

The main feature of the Maximum Volume conjecture is that it does not involve any angles or colors, as in Conjecture 1.3, and instead it only sees the “global” geometry of a graph $\Gamma \subseteq S^3$.

The Maximum Volume conjecture naturally leads to the question of what is the largest volume that can be attained by proper generalized hyperbolic polyhedra with a fixed 1-skeleton. In the case of the tetrahedron, the answer is v_8 (the volume of the ideal right-angled octahedron) as proved in [51]. As we discuss in Chapter 5, this question is complicated by the fact that the space of polyhedra that we consider is very large: it includes polyhedra with obtuse angles and with any kind (real, ideal, hyperideal) of vertices, which precludes the use of powerful results like Andreev’s theorem [1] and the Bao-Bonahon theorem [2].

In Chapter 5 we prove the following theorem, answering this question.

Theorem 1.6 (The Maximum Volume Theorem). [6] *For any 3-connected planar graph Γ ,*

$$\sup_P \text{Vol}(P) = \text{Vol}(\bar{\Gamma})$$

where P varies among all proper generalized hyperbolic polyhedra with 1-skeleton Γ and $\bar{\Gamma}$ is the rectification of Γ .

The rectification of a graph is defined in Definition 2.25; for now it suffices to say that $\bar{\Gamma}$ is a finite volume polyhedron that can be easily computed (together with its volume) from Γ .

Theorem 1.6 is proven by deforming a polyhedron while increasing its volume, and carefully studying the possible degenerations.

Finally in Chapter 6 we prove the Maximum Volume Conjecture for a large family of graphs.

Theorem 1.7. [5] *The Maximum Volume Conjecture is verified for any planar graph obtained from the tetrahedron by applying any sequence of the following two moves:*

- *blowing up a trivalent vertex (see Figure 1.1) or*
- *triangulating a triangular face (see Figure 1.2).*

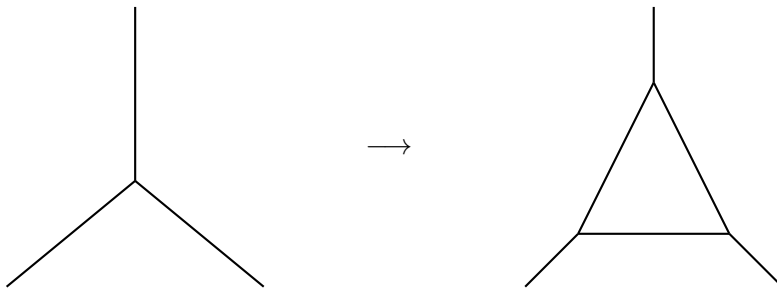


Figure 1.1: Truncating a vertex

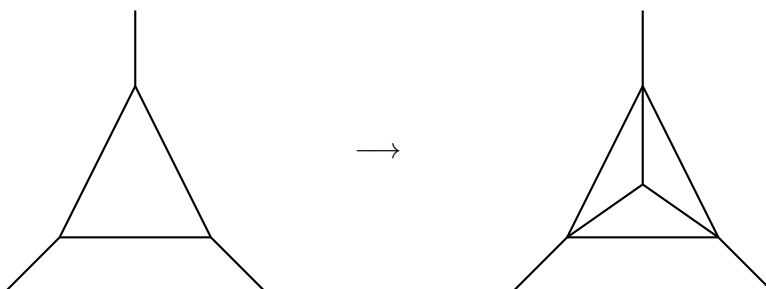


Figure 1.2: Triangulating a face

Theorem 1.6 is instrumental in calculating $\sup_P \text{Vol}(P)$ for the graphs involved.

As a corollary of Theorem 1.7, we prove the volume conjecture for a different family of hyperbolic manifolds (see Theorem 6.18). These manifolds are obtained by gluing ideal right-angled octahedra, but are different from the Fundamental Shadow Link complements.

The main tool in evaluating the growth of the Turaev-Viro invariant (both in Theorem 1.4 and Theorem 1.7) is a sharp upper bound on the asymptotic growth of the $6j$ -symbol.

Theorem 1.8. [7] *For any r , and any r -admissible 6-tuple $n_1, n_2, n_3, n_4, n_5, n_6$, we have*

$$\frac{2\pi}{r} \log \left| \left| \begin{matrix} n_1 & n_2 & n_3 \\ n_4 & n_5 & n_6 \end{matrix} \right|_{q=e^{\frac{2\pi i}{r}}} \right| \leq v_8 + O\left(\frac{\log(r)}{r}\right).$$

Furthermore, the proof of Theorem 1.7 relies on an interesting application of the Fourier transform for the Yokota invariant, first introduced by Barrett [3].

Chapter 2

Three-manifolds and hyperbolic geometry

In this chapter we lay the topological and geometric groundwork for the rest of the thesis. In Section 2.1 we discuss knots, links and 3-manifolds, introducing the combinatorial presentation needed to define the colored Jones polynomials and the Reshetikhin-Turaev invariants. In Section 2.2 we talk about hyperbolic geometry, with a particular emphasis on hyperbolic polyhedra and the tools needed to state and prove the Maximum Volume Theorem 1.6. Finally in Section 2.3 we focus on the topic of hyperbolic 3-manifolds.

The material in Sections 2.1 and 2.3 is standard and is covered for example in [32]. The material in Section 2.2 is partly new; references for known results are given, as appropriate, in the text.

2.1 Dehn surgery and Kirby calculus

Throughout the thesis, M will be a compact, oriented, smooth 3-manifold; it could have boundary. Recall that a *link* $L \subseteq M$ is a closed submanifold of dimension 1 disjoint from ∂M ; topologically it is just a disjoint union of copies of S^1 . If the link is connected we call it a *knot*. Two links are considered equivalent if there is an ambient isotopy of M sending one to the other.

Definition 2.1. A *framing* for a knot L is a trivialization of its normal bundle. A *framed knot* is a knot together with a framing; a *framed link* is a link with a framing for each component.

Once again, two framed links are equivalent if there is an ambient isotopy sending one to the other together with their framings.

In dimension 3 there are a few different points of view to see framed knots and links.

- First of all, if K is a knot and ν is a section of the normal bundle, we can extend it to a trivialization by choosing a Riemannian structure on M and taking the orthogonal to ν . Up to isotopy the choice of Riemannian structure is inconsequential; therefore, a framing of K is the same as a nowhere vanishing vector field normal to K .
- If we push slightly K in the direction of this vector field, we obtain a parallel copy of K ; this parallel copy determines the framing as well, therefore we could view a framed knot as a knot K together with a choice of a parallel copy of K .
- Furthermore, K and its parallel copy co-bound an annulus $S^1 \times [0, \epsilon]$; therefore we could think of framed knots as the image of embeddings of $S^1 \times [0, \epsilon]$ in M .
- Another point of view comes from the fact that a trivialization of the normal bundle of K fixes a diffeomorphism of a regular neighborhood of K with $S^1 \times D^2$; therefore, we could think of a framed knot as an embedding of $S^1 \times D^2 \rightarrow S^3$. It is important to be careful that in this case the framed knot is the whole embedding, and not just its image in S^3 .

If K is a framed knot in S^3 , we define the *self-linking number* $\text{lk}(K)$ to be the linking number of K and its parallel. Notice that we need an orientation on K to define the linking number: we can choose either one as long as we choose the same orientation on the parallel, and the result does not depend on the choice.

Similarly, if $L = L_1 \cup \dots \cup L_k$ is a framed oriented link the symbol $\text{lk}(L)$ stands for the *linking matrix* of L ; this is the matrix whose component i, j is $\text{lk}(L_i, L_j)$ if $i \neq j$ and $\text{lk}(L_i)$ if $i = j$.

It is convenient to encode framed links into diagrams $D \subseteq S^2$, as is usually done for links; in this case by convention we take the normal vector field to be tangent (equivalently, orthogonal) to the plane of the diagram (in other words, the parallel to each component lies on one side of it, without ever crossing it). Notice that a framing which “wraps around” a component of the link, may be described with a “kink” in the diagram (see Figure 2.1).

A framed link can have many different diagrams, however any two such diagrams are related to one another by a finite sequence of isotopies of S^2 and Reidemeister moves of type 2 and 3. This fact can be exploited to define invariants of framed links from diagrams.

Consider now a framed knot K in S^3 , given by an embedding of $H := S^1 \times D^2 \subseteq S^3$. The *exterior* of K is $E_K := S^3 \setminus \overset{\circ}{H}$ which is a compact manifold whose boundary is identified with $S^1 \times S^1$ by the embedding $S^1 \times S^1 = \partial H \subseteq$

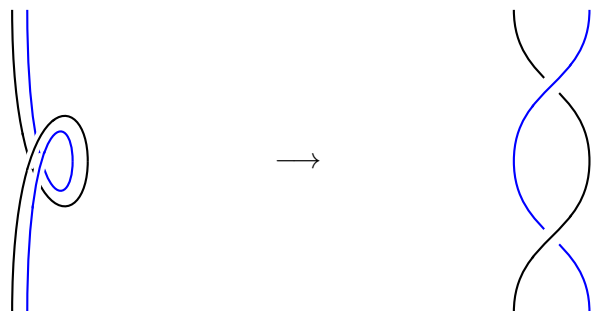


Figure 2.1: The framing (blue) for a knot (black), through an isotopy

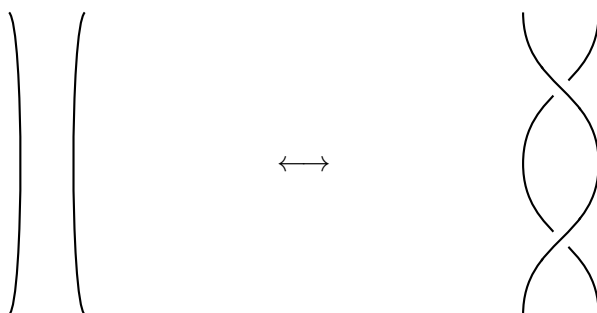


Figure 2.2: Reidemeister 2 move

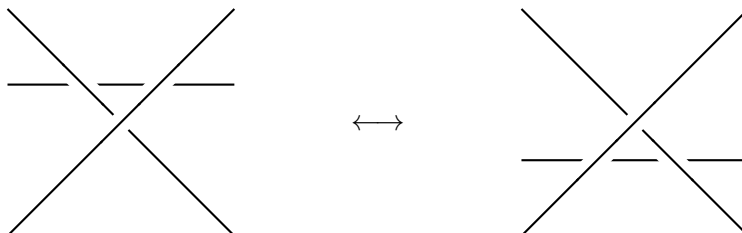


Figure 2.3: Reidemeister 3 move

S^3 . We can now “fill” this boundary component of E_K by gluing in a solid torus $S^1 \times D^2$ via the map $\phi : \partial(S^1 \times D^2) \rightarrow \partial E_K$ that sends $(x, y) \in S^1 \times S^1$ to (y, x) , with the identification of ∂E_K to $S^1 \times S^1$ mentioned above. The result of the gluing is a closed manifold S_K^3 that we call the *Dehn surgery* on K . Gluing component by component we can define the Dehn surgery on a framed link L , denoted with S_L^3 . More in general, given a manifold M with a toric boundary component T and a diffeomorphism $\phi : T \rightarrow S^1 \times S^1$ we can define as above the *Dehn filling* of the component T of ∂M by gluing a solid torus $S^1 \times D^2$ via ϕ .

The following result, due independently to Lickorish and Wallace, states that this construction can be used to obtain any 3-manifold (see for example [32, Theorem 11.3.15]).

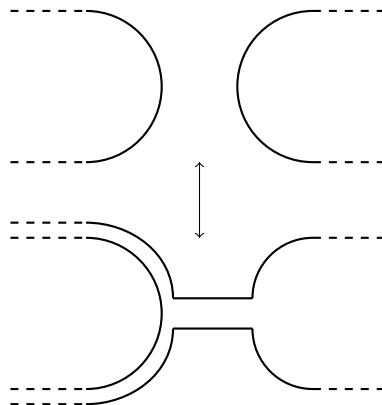


Figure 2.4: Handle slide between two different components of L

Theorem 2.2. *Let M be a closed connected oriented 3-manifold. Then there exists a framed link $L \subseteq S^3$ such that $M \cong S_L^3$.*

There are always many different ways to realize the same manifold M via different (i.e. non isotopic) framed links in S^3 . However it is possible to give, similarly to Reidemeister moves, a complete set of moves (the Kirby moves [27]) relating two links giving the same manifold.

Theorem 2.3. *Let $L_1, L_2 \subseteq S^3$ be two framed links giving the same 3-manifold M under Dehn surgery. Then it is possible to change L_1 into L_2 via a finite sequence of*

- isotopies of framed links;
- adding and removing unknots with framing ± 1 that are unlinked from anything else;
- handle slides (see Figure 2.4);

We are going to use this result in the next chapter to define an invariant of 3-manifolds starting from an invariant of framed links.

2.2 Hyperbolic geometry

In this section we lay the necessary background of hyperbolic geometry needed to state the various volume conjectures and to state and prove the Maximum Volume Theorem 1.6. Although the definition and many of the results hold in any dimension, we are going to concentrate ourselves on the case of dimension 3.

The Beltrami-Klein model of hyperbolic space

Let $\mathbb{R}^{3,1}$ be the 4-dimensional Minkowski space; that is to say, the vector space \mathbb{R}^4 with the scalar product of signature $(3, 1)$ given by $\langle x, y \rangle = -x_0y_0 + x_1y_1 + x_2y_2 + x_3y_3$.

Define the upper hyperboloid as

$$I = \{x \in \mathbb{R}^{3,1} \text{ such that } \langle x, x \rangle = -1 \text{ and } x_0 > 0\}.$$

One can check that I is a smooth simply connected manifold, and the restriction of $\langle \cdot, \cdot \rangle$ to TI gives a Riemannian structure on I that is complete and has sectional curvature constantly equal to -1 . We call any manifold isometric to I the *hyperbolic space* of dimension 3 and we denote it with \mathbb{H}^3 . Furthermore we say that I is the hyperboloid model for \mathbb{H}^3 .

In I , geodesic k -planes correspond to intersections of $k + 1$ -planes in $\mathbb{R}^{3,1}$ with I . Furthermore, if two points $x, y \in I$ have distance d , we have

$$\cosh(d) = -\langle x, y \rangle. \quad (2.1)$$

Consider now the projection $\pi : \mathbb{R}^{3,1} \rightarrow \mathbb{RP}^3$. The image of I under this projection is equal to the image of $\{x \in \mathbb{R}^{3,1} \text{ such that } \langle x, x \rangle < 0\}$, and in the standard affine chart $\mathbb{R}^3 \subseteq \mathbb{RP}^3$ given by $(x_1, x_2, x_3) \rightarrow [1, x_1, x_2, x_3]$ the set $\pi(I)$ is the open unit ball $B = \{(x_1, x_2, x_3) \text{ such that } x_1^2 + x_2^2 + x_3^2 < 1\}$. Of course π induces a diffeomorphism between I and $B \subseteq \mathbb{R}^3 \subseteq \mathbb{RP}^3$; if we push forward the Riemannian metric of I via π , we obtain a Riemannian metric on B that makes it isometric to I , therefore B is a model of hyperbolic space that we call the *Beltrami-Klein model* (sometimes also referred to as the *projective model*). From now on we are going to only consider the Beltrami-Klein model of hyperbolic space, therefore we are simply going to call it \mathbb{H}^3 instead of B .

The Beltrami-Klein model of hyperbolic space is somewhat less employed than other models, like the *disc model* or the *half-space model*. This is mainly because the Beltrami-Klein model is not conformal (i.e. it is not diffeomorphic to the Euclidean space via an angle-preserving map) and because the metric tensor is slightly more complicated. However, it also presents a few useful properties. First of all, geodesic k -planes are intersections of projective planes in \mathbb{RP}^3 with B ; when seen in the standard affine chart described above, this means that hyperbolic lines, planes etc. are the same as Euclidean lines, planes etc. in B .

Furthermore, the embedding $B \subseteq \mathbb{R}^3 \subseteq \mathbb{RP}^3$ allows us to talk about points of \mathbb{H}^3 that are *at infinity* and even *beyond infinity*.

Definition 2.4. We say that a point $p \in \mathbb{H}^3$ is *real*, a point $p \in \partial\mathbb{H}^3 \subseteq \mathbb{RP}^3$ is *ideal*, and a point $q \in \mathbb{RP}^3 \setminus \overline{\mathbb{H}^3}$ is *hyperideal*.

Ideal points correspond to the (positive) light-cone $\{\langle x, x \rangle = 0\} \subseteq \mathbb{R}^{3,1}$, while hyperideal points correspond to points on the quadric $\{\langle x, x \rangle = 1\} \subseteq \mathbb{R}^{3,1}$, which is a Lorentzian manifold called *de Sitter space*.

Finally, for our purpose the most useful property of the Beltrami-Klein model is that we can define a duality in \mathbb{H}^3 from the duality of \mathbb{RP}^3 . Explicitly, let M be a k -dimensional plane (for $0 \leq k \leq 2$) in \mathbb{RP}^3 . Then $\pi^{-1}(M)$ is going to be a $k+1$ dimensional subspace of $\mathbb{R}^{3,1}$. Take its orthogonal $(\pi^{-1}(M))^\perp$ with respect to $\langle \cdot, \cdot \rangle$, and define $M^\perp = \pi(\pi^{-1}(M)^\perp)$ which is a $2 - k$ dimensional plane.

Some property of the duality:

- $(M^\perp)^\perp = M$;
- $M \cap \mathbb{H}^3 \neq \emptyset$ implies $M^\perp \cap \mathbb{H}^3 = \emptyset$;
- if $M \in \mathbb{RP}^3 \setminus \mathbb{H}^3$ is a point, take the cone tangent to $\partial\mathbb{H}^3$ with vertex M . Then M^\perp is the plane in \mathbb{RP}^3 that intersects $\partial\mathbb{H}^3$ at the points of tangency.
- if p_1, p_2 are points connected by a line M , then $M^\perp = p_1^\perp \cap p_2^\perp$;
- if $p \in \partial\mathbb{H}^3$, then p^\perp is the plane tangent to $\partial\mathbb{H}^3$ in p ;
- if p is a point at infinity of $\mathbb{R}^3 \subseteq \mathbb{RP}^3$, then p^\perp is an equatorial plane (i.e. a plane containing $0 \in \mathbb{R}^3$);
- if p_1, p_2 are connected by a line intersecting \mathbb{H}^3 , p_1^\perp and p_2^\perp do not intersect in \mathbb{H}^3 .

Definition 2.5. If $v \in \mathbb{RP}^3 \setminus \overline{\mathbb{H}^3}$ is a hyperideal point, we call $\Pi_v := v^\perp \cap \mathbb{H}^3$ the *polar plane* of v . The hyperbolic half space of \mathbb{H}^3 that is on the other side of v is denoted with H_v .

Hyperbolic polyhedra

Definition 2.6. A *projective polyhedron* in \mathbb{RP}^3 is a non-degenerate convex polyhedron in some affine chart of \mathbb{RP}^3 . Alternatively, it is the closure of a connected component of the complement of finitely many planes in \mathbb{RP}^3 that does not contain any projective line.

Up to isometry of \mathbb{H}^3 we can assume that any given projective polyhedron is contained in the standard affine chart.

Definition 2.7. We introduce the following definitions.

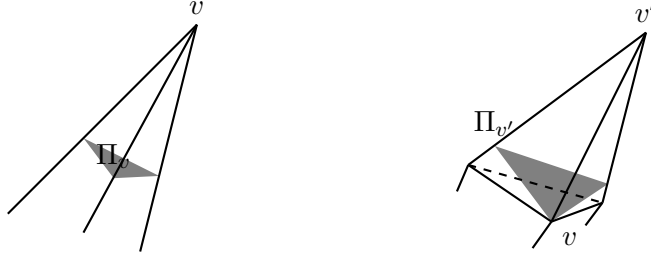


Figure 2.5: A proper (left) and almost proper (right) truncation.

- We say that a projective polyhedron $P \subseteq \mathbb{R}^3 \subseteq \mathbb{RP}^3$ is a *generalized hyperbolic polyhedron* if each edge of P intersects \mathbb{H}^3 ([45, Definition 4.7]).
- A vertex of a generalized hyperbolic polyhedron is *real* if it lies in \mathbb{H}^3 , *ideal* if it lies in $\partial\mathbb{H}^3$ and *hyperideal* otherwise.
- A generalized hyperbolic polyhedron P is *proper* if for each hyperideal vertex v of P the interior of the polar half space H_v contains all the other real vertices of P (see Figure 2.5, left). We say that it is *almost proper* if it is not proper but still for each hyperideal vertex v of P , the polar half space H_v contains all the other real vertices of P ; we call a vertex v belonging to some $\Pi_{v'}$ an *almost proper vertex* (see Figure 2.5, right), and $\overrightarrow{vv'}$ an almost proper edge (by contrast, the other vertices and edges are *proper*).
- We define the *truncation* of a generalized hyperbolic polyhedron P at a hyperideal vertex v to be the intersection of P with H_v ; similarly the *truncation* of P is the truncation at every hyperideal vertex, that is to say $P \cap (\bigcap_{v \text{ hyperideal}} H_v)$. We say that the *volume* of P is the volume of its truncation; in the same spirit, the *length* of an edge of P is the length of its subsegment contained in the truncation. Notice that the volume of a non-empty generalized hyperbolic polyhedron could be 0 if the truncation is empty; likewise the length of some of its edges could be 0.

In the remainder of the paper we simply say *proper polyhedra* (or *almost proper polyhedra*) for proper (respectively, almost proper) generalized hyperbolic polyhedra. We are mostly interested in proper polyhedra; almost proper polyhedra can arise as limits of proper polyhedra, and they will be studied carefully in the proof of Theorem 1.6.

When it has positive volume, the truncation of a generalized hyperbolic polyhedron P is itself a polyhedron; some of its faces are the truncation of

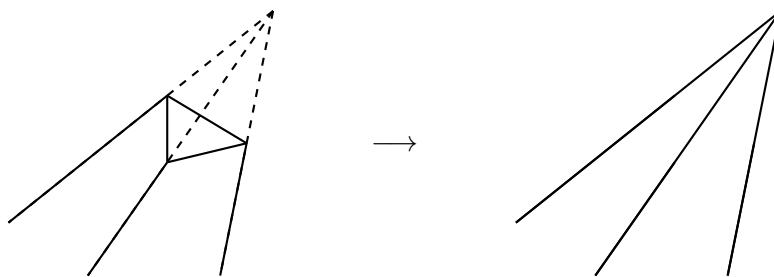


Figure 2.6: Removing the truncation faces recovers the original polyhedron.

the faces of P , while the others are the intersection of P with some truncating plane; we call such faces *truncation faces*. Notice that distinct truncation faces are disjoint (even more, the planes containing them are disjoint) [2, Lemma 4]. If an edge of the truncation of P is not the intersection of an edge of P with the truncating half-spaces, then we say that the edge is arising from the truncation. Every edge that arises from truncation is an edge of a truncation faces. The converse is true for proper polyhedra but not necessarily for almost proper ones: it could happen that an entire edge of P lies in a truncation plane, and we do not consider this to be an edge arising from the truncation.

Remark 2.8. For proper or almost proper polyhedra the dihedral angles at the edges arising from the truncation are $\frac{\pi}{2}$.

Remark 2.9. An important feature of the truncation of a proper polyhedron P is that it determines P (once we know which faces of P are the truncation faces), since it is enough to remove the truncation faces to undo the truncation (see Figure 2.6). This also holds for almost proper polyhedra (see Figure 2.8 in Section 5). In particular this will allow us to use many standard techniques to study them, such as the Schläfli formula (see Theorem 2.36).

We are always going to consider *face marked* polyhedra; this means that each face of a polyhedron is uniquely determined, and therefore they never have any symmetry.

Remark 2.10. If Γ is the 1-skeleton of a projective polyhedron, then it is 3-connected (that is to say, it cannot be disconnected by removing two vertices). Conversely, any 3-connected planar graph is the 1-skeleton of a proper polyhedron [46]. If a planar graph is 3-connected, then it admits a unique embedding in S^2 (up to isotopies of S^2 and reflection) [21, Corollary 3.4]. Hence when in the following we consider a planar graph Γ , it is always going to be 3-connected and embedded in S^2 . In particular, it will make sense to talk about the faces of Γ and the dual of Γ , denoted with Γ^* . The graph Γ^* is the 1-skeleton of the cellular decomposition of S^2 dual to that of Γ . Notice that if Γ is the 1-skeleton of a polyhedron P , then Γ^* is the 1-skeleton of the polyhedron whose vertices are dual to the faces of P , hence Γ is 3-connected

if and only if Γ^* is.

Definition 2.11. Let Γ be a planar 3-connected graph; the space of all the face-marked proper polyhedra with 1-skeleton Γ considered up to isometry (i.e. projective transformations preserving the unit sphere) is denoted with \mathcal{A}_Γ .

Remark 2.12. It is important not to mix up the 1-skeleton of a projective polyhedron with the 1-skeleton of its truncation. In what follows, whenever we refer to 1-skeleta we always refer to those of projective polyhedra (and not their truncation) unless specified.

Whether a vertex of a polyhedron is real, ideal or hyperideal can be read directly from the dihedral angles.

Lemma 2.13. *Let P be a generalized hyperbolic polyhedron, v a vertex of P and $\theta_1, \dots, \theta_k$ the dihedral angles of the edges incident to v . Then v is hyperideal if and only if $\theta_1, \dots, \theta_k$ are the angles of a hyperbolic k -gon; v is ideal if and only if $\theta_1, \dots, \theta_k$ are the angles of a Euclidean k -gon; $v \in \mathbb{H}^3$ if and only if $\theta_1, \dots, \theta_k$ are the angles of a spherical k -gon. Equivalently,*

- v is hyperideal if and only if $\sum_i \theta_i < (k - 2)\pi$;
- v is ideal if and only if $\sum_i \theta_i = (k - 2)\pi$;
- $v \in \mathbb{H}^3$ if and only if $\sum_i \theta_i > (k - 2)\pi$.

For a proof of this Lemma see for example [2, Proposition 5].

Finally in the proof of the main theorem we will need a way to deform a almost proper polyhedron to be proper. We will rely on the following easy lemma.

Lemma 2.14. *Let $v \in \mathbb{R}\mathbb{P}^3 \setminus \overline{\mathbb{H}^3}$ and $w \in H_v$. If Ψ is a translation of \mathbb{R}^3 or a homothety centered in 0 such that $\Psi(v)$ is contained in the tangent cone of v to $\partial\mathbb{H}^3$, then if $\Psi(w) \in \mathbb{H}^3$ it is also contained in the interior of $H_{\Psi(v)}$.*

Notice that in particular this lemma says that if w is an almost proper vertex of a polyhedron P , then $\Psi(w)$ is a proper vertex of $\Psi(P)$.

Proof. The plane $\Pi_{\Psi(v)}$ is disjoint from H_v (see Figure 2.7), and certainly $\Psi(w) \in H_v$. □

The Bao-Bonahon existence and uniqueness theorem

A special class of proper polyhedra is that of the *hyperideal polyhedra*, i.e. generalized hyperbolic polyhedra with no real vertices. Since there are no real vertices, hyperideal polyhedra are automatically proper. In [2], Bao and Bonahon gave a complete description of the space of angles of hyperideal polyhedra.

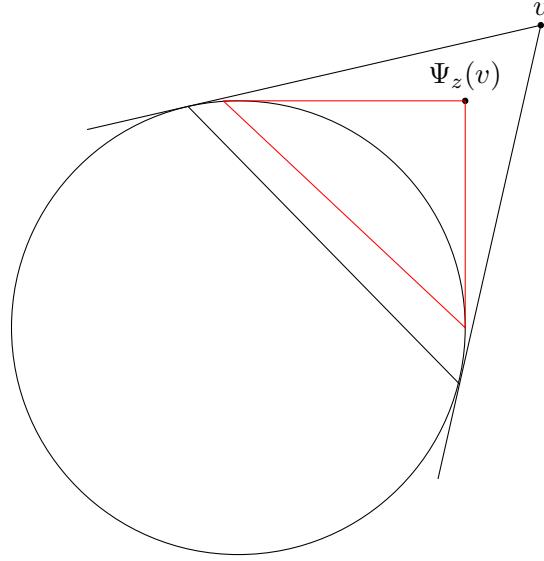


Figure 2.7: Pushing P towards \mathbb{H}^3 pushes its dual plane away from the center

Theorem 2.15. *Let Γ be a 3-connected planar graph with edges e_1, \dots, e_k . There exists a hyperideal polyhedron P with 1-skeleton Γ and dihedral angles $\theta_1, \dots, \theta_k \in (0, \pi)$ at the edges e_1, \dots, e_k if and only if the following conditions are satisfied:*

- for any closed curve $\gamma \subseteq S^2$ passing transversely through distinct edges e_{i_1}, \dots, e_{i_h} of Γ exactly once, we have $\sum_{j=1}^h \theta_{i_j} \leq (h-2)\pi$ with equality possible only if e_{i_1}, \dots, e_{i_h} share a vertex;
- for any arc $\gamma \subseteq S^2$ with endpoints in two different faces sharing a vertex, and passing transversely through the distinct edges e_{i_1}, \dots, e_{i_h} of Γ exactly once, we have $\sum_{j=1}^h \theta_{i_j} < (h-1)\pi$ unless the edges e_{i_1}, \dots, e_{i_h} share a vertex.

Moreover, if P exists it is unique up to isometry.

In particular, this theorem says that dihedral angles uniquely determine a hyperideal polyhedron, and the space of angles of hyperideal polyhedra with fixed 1-skeleton is a convex subset of \mathbb{R}^k .

The space of proper polyhedra \mathcal{A}_Γ

Let Γ be a 3-connected planar graph, and denote with \mathcal{A}_Γ the set of isometry classes of face-marked proper polyhedra with 1-skeleton Γ .

The first result about \mathcal{A}_Γ that we need is an explicit description.

Proposition 2.16. *The set \mathcal{A}_Γ is naturally a smooth manifold.*

Proof. Montcoquiol proved in [35] that face-marked Euclidean polyhedra in \mathbb{R}^3 with 1-skeleton Γ form a smooth submanifold of $((\mathbb{R}\mathbb{P}^3)^*)^F$, with F the number of faces of Γ . Since proper polyhedra are in natural 1-1 correspondence with an open subset of Euclidean polyhedra, they are also a smooth submanifold of $((\mathbb{R}\mathbb{P}^3)^*)^F$. To conclude we notice that the action of the isometries of \mathbb{H}^3 on this space of polyhedra is free and proper, so that the quotient \mathcal{A}_Γ is a manifold as well. \square

Consider the dihedral angle map $\Theta : \mathcal{A}_\Gamma \rightarrow \mathbb{R}^{\#\text{ of edges}}$ assigning to each polyhedron the tuple of dihedral angles of its edges. This is clearly a smooth map; it is also a local diffeomorphism at any polyhedron with no ideal vertices.

Theorem 2.17. [35, Theorem 19],[54, Theorem 1.1] *If P is a compact hyperbolic polyhedron (i.e. P has only real vertices), the dihedral angles are local coordinates for \mathcal{A}_Γ around P .*

Corollary 2.18. *If P is a proper polyhedron with no ideal vertices, the dihedral angles are local coordinates for \mathcal{A}_Γ around P .*

Proof. Take P^0 the truncation of P , and denote with Γ^0 its 1-skeleton. Since P^0 is compact the dihedral angles are local coordinates for \mathcal{A}_{Γ^0} around P^0 ; the dihedral angles of P^0 are either $\frac{\pi}{2}$ (at the edges lying on truncation faces) or those of P (at the remaining edges). Then the dihedral angles of P form a local set of coordinates for the subset of \mathcal{A}_{Γ^0} of polyhedra with right angles at the edges arising from truncation, and any polyhedron in this subset is going to be the truncation of a proper polyhedron in \mathcal{A}_Γ close to P . \square

Definition 2.19. The *closure* of \mathcal{A}_Γ , denoted with $\overline{\mathcal{A}_\Gamma}$, is the topological closure of the space of proper polyhedra with 1-skeleton Γ (as a subset of $((\mathbb{R}\mathbb{P}^3)^*)^F$), quotiented by isometries. As customary the *boundary* of \mathcal{A}_Γ is $\overline{\mathcal{A}_\Gamma} \setminus \mathcal{A}_\Gamma$ and is denoted with $\partial\mathcal{A}_\Gamma$. We make no claim that $\overline{\mathcal{A}_\Gamma}$ is a manifold; even if it were, its boundary as a manifold would not necessarily be $\partial\mathcal{A}_\Gamma$.

We will also need local coordinates for certain parts of $\partial\mathcal{A}_\Gamma$; this is provided by the following corollary.

Corollary 2.20. *If P is an almost proper polyhedron with 1-skeleton Γ and no ideal vertices, it lies in the closure of \mathcal{A}_Γ . Moreover, if $\vec{\theta} = (\theta_1, \dots, \theta_e)$ are the dihedral angles of the proper edges of P , and $\vec{\theta}' = (\theta'_1, \dots, \theta'_e)$ is close enough to $\vec{\theta}$, then there is a unique almost proper polyhedron with 1-skeleton Γ close to P in $\overline{\mathcal{A}_\Gamma}$ with the same almost proper vertices and with angles $\vec{\theta}'$.*

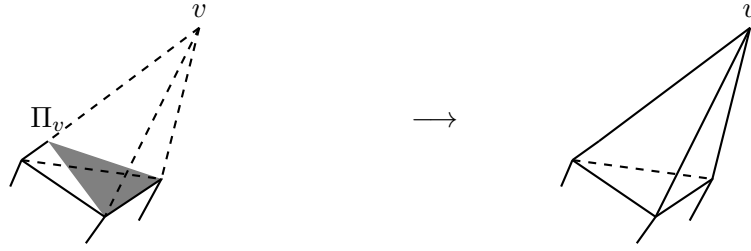


Figure 2.8: Removing a truncation face to recover an almost proper polyhedron

Proof. To show the fact that $P \in \overline{\mathcal{A}_\Gamma}$ we need to exhibit a family of proper polyhedra with 1-skeleton Γ converging to P in $(\mathbb{RP}^3)^{*F}$. To do this apply an isometry so that $0 \in P$, and consider $\Phi_\lambda : \mathbb{R}^3 \rightarrow \mathbb{R}^3$ the multiplication by λ . Then for $\lambda \in (1 - \epsilon, 1]$ the polyhedron $\Phi_\lambda(P)$ is proper by Lemma 2.14, has 1-skeleton Γ and converges to P as $\lambda \rightarrow 1$. To see that $\Phi_\lambda(P)$ is proper notice that for every hyperideal vertex v , $\Phi_\lambda(v)$ is contained in the tangent cone of v to $\partial\mathbb{H}^3$, and we can conclude by applying Lemma 2.14.

To show the second assertion, reorder the indices so that $\theta_1, \dots, \theta_l$ are the angles of the proper edges that are contained in some truncation plane. Then P_0 , the truncation of P , is compact, has 1-skeleton Γ_0 and dihedral angles $\theta_1 - \frac{\pi}{2}, \dots, \theta_l - \frac{\pi}{2}, \theta_{l+1}, \dots, \theta_e, \frac{\pi}{2}, \dots, \frac{\pi}{2}$. By Theorem 2.17, if $\theta'_1, \dots, \theta'_e$ are sufficiently close to $\theta_1, \dots, \theta_e$ there is a unique Q_0 (up to isometry) close to P_0 with 1-skeleton Γ_0 and angles $\theta'_1 - \frac{\pi}{2}, \dots, \theta'_l - \frac{\pi}{2}, \theta'_{l+1}, \dots, \theta'_e, \frac{\pi}{2}, \dots, \frac{\pi}{2}$. Some faces of Q_0 correspond to truncation faces of P_0 ; if we glue to Q_0 the convex hull of a truncation face and its dual point, we undo the truncation (see Figure 2.8). Notice that the angles at the edges that are glued are either $\theta'_i - \frac{\pi}{2} + \frac{\pi}{2} = \theta'_i$ if $i \leq l$, or $\frac{\pi}{2} + \frac{\pi}{2}$ otherwise (hence the edge in this case disappears).

If we undo every truncation in this manner, we obtain an almost proper polyhedron Q with 1-skeleton Γ and angles $\theta'_1, \dots, \theta'_e$. To see that Q is close to P notice that Q_0 is close to P_0 , which means that all the faces of Q_0 are close to the corresponding faces of P_0 ; but the faces of P and Q depend continuously on the faces of P_0 and Q_0 .

□

Convergence of polyhedra

As we have seen in Subsection 2.2, a proper polyhedron P is naturally an element of $((\mathbb{RP}^3)^*)^F$ where F is the number of faces of P . Therefore when we say that a sequence P_n of polyhedra with 1-skeleton Γ converges to $P \in ((\mathbb{RP}^3)^*)^F$ (or has P as an accumulation point) we mean in the topology of $((\mathbb{RP}^3)^*)^F$. Since \mathbb{RP}^3 is compact, any such sequence P_n has an accumulation point $P \in ((\mathbb{RP}^3)^*)^F$. Each component of P_n is a plane in \mathbb{RP}^3 , and P_n selects

one of the two hyperspaces on either side of it. Therefore if $P_n \rightarrow P$ then P can still be interpreted as a convex intersection of half-spaces, however it could stop being a projective polyhedron if it is contained in a plane or not contained in an affine chart.

Analogously, we will consider sequences of k -gons $A_n \subseteq \mathbb{H}^2$, which are naturally elements of $((\mathbb{R}\mathbb{P}^2)^*)^k$; when we say that they converge to a polygon A , we mean in the topology of this space, with the same considerations we made for polyhedra.

If the limit point P is a projective polyhedron, each of its vertices is a limit of some vertices of P_n , similarly every line containing an edge of P is the limit of some lines containing edges of P_n and every plane containing a face of P is the limit of some planes containing a face of P_n respectively. However some vertices of P_n could converge to points of P which are not vertices; similarly some edge of P_n could collapse to a point or converge to a segment which is not an edge, and a face of P_n could collapse to an edge or a point.

Furthermore in some degenerate cases, even though P_n converges to P , some of its vertices do not converge; for example, if v_n lies on three faces of P_n that become coplanar, the sequence v_n could have accumulation points anywhere on the limit face. Throughout the paper we are almost always going to be concerned with sequences of polyhedra with angles which are decreasing and bounded away from 0; in this case the situation is somewhat nicer.

Notation: throughout the rest of the paper we consider sequences of polyhedra P_n with the same 1-skeleton Γ . Their boundary will always be equipped with a fixed isomorphism to the pair (S^2, Γ) ; because of Remark 2.10, there is essentially a unique way to do this, so it will be not explicitly defined. If we consider a sequence of vertices $v_n \in P_n$ we always assume that each v_n is the vertex of P_n corresponding to a fixed vertex v of Γ ; the same with a sequence of edges or faces.

Lemma 2.21. *Let P_n be a sequence of proper or almost proper polyhedra with 1-skeleton Γ and with angles bounded away from 0 and π , and converging to the projective polyhedron P . If $\Pi_n^1 \neq \Pi_n^2$ are planes containing faces of P_n converging to the planes Π^1, Π^2 containing faces F^1, F^2 of P , then $\Pi^1 \neq \Pi^2$.*

Proof. Suppose by contradiction that $\Pi^1 = \Pi^2$. If Π_1^n and Π_2^n share an edge of P_n this would imply that the dihedral angle at this edge would either converge to π or 0 which is a contradiction. If instead Π_1^n and Π_2^n do not share an edge in P_n , still there must be some other Π_3^n containing a face of P_n such that Π_1^n and Π_3^n must share an edge and $\Pi_3^n \rightarrow \Pi_1$; otherwise, if every plane containing a face adjacent to Π_1^n converged to a plane different from Π_1 , then P would not be convex. \square

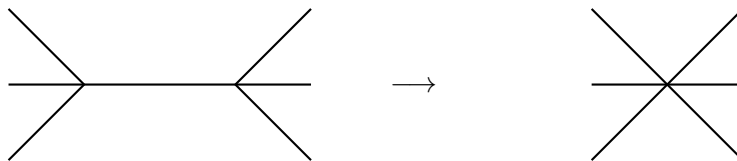


Figure 2.9: An edge collapsing to a vertex.

Corollary 2.22. *With the same hypotheses of Lemma 2.21, if v_n is a sequence of vertices of P_n , then it cannot converge to (or have an accumulation point in) an internal point of a face of P . Similarly, any accumulation point of a sequence of edges e_n of P_n cannot intersect the interior of any face of P .*

Proof. If v_n converged to (or had an accumulation point in) an internal point of a face of P , then all faces of P_n containing v_n would become coplanar in the limit, contradicting Lemma 2.21.

Consider now a sequence of edges e_n : following the same reasoning, if e_n converged (or has an accumulation point) to an edge that intersected the interior of a face of P , the two faces of P_n containing e_n would become coplanar in the limit. \square

Corollary 2.23. *If v_n converges to an internal point of an edge, then the accumulation points of all edges that have v_n as endpoints must be contained in that edge as well.*

Suppose that P_n satisfies all the hypotheses of Lemma 2.21, that $P_n \rightarrow P$ with P a generalized hyperbolic polyhedron with 1-skeleton Γ' and additionally that all vertices of P_n converge. Then the limit induces a simplicial map $\phi : \Gamma \rightarrow \tilde{\Gamma}'$ where $\tilde{\Gamma}'$ is obtained from Γ' by adding bivalent vertices to some of its edges. The map ϕ sends

- each vertex of Γ to its limit in $\tilde{\Gamma}'$;
- each edge of Γ linearly to the convex hull of the image of its endpoints (the convex hull is contained in $\tilde{\Gamma}'$ by Corollary 2.22).

Notice that $\tilde{\Gamma}'$ is not always 3-connected, however it is still 2-connected since it cannot be disconnected by removing a single vertex.

Lemma 2.24. *The map $\phi : \Gamma \rightarrow \tilde{\Gamma}'$ factors through a graph $\hat{\Gamma}$, isomorphic to $\tilde{\Gamma}'$ and obtained from Γ via a finite sequence of the following moves:*

- (i) an edge of Γ collapses to a vertex (see Figure 2.9);
- (ii) a face of Γ collapses to an edge (see Figure 2.10).

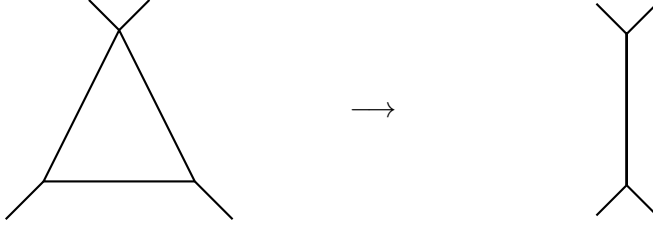


Figure 2.10: A face collapsing to an edge.

Proof. Let $\Lambda_v \subseteq \Gamma$ be the subset $\Lambda_v := \phi^{-1}(v)$ for any v vertex of $\tilde{\Gamma}'$.

The map ϕ satisfies the following properties:

- ϕ is a surjective simplicial map between 2-connected planar graphs;
- for every v vertex of $\tilde{\Gamma}'$, the set Λ_v is connected;
- if a cycle λ is contained in Λ_v , then all vertices in one of the two components of the sphere bounded by λ must be in Λ_v .

The fact that ϕ is surjective, simplicial and between 2-connected planar graphs is obvious; let us prove that Λ_v is connected.

First notice that if $w_1, w_2 \in \Lambda_v$ lie on the same face of Γ , they are in the same connected component of Λ_v (even if they are not vertices of Γ). This is because the face must correspond to a convex face of P_n , and if two different vertices of a sequence of convex polygons coincide in the limit, then by convexity one of the two paths connecting them (on either side of the boundary of the polygon) must coincide in the limit as well.

Take now generic $w_1, w_2 \in \Lambda_v$: they determine points $w_1^n, w_2^n \in P_n$. Pick any converging sequence of planes Π_n containing w_1^n, w_2^n and cut P_n along Π_n ; for n big enough the planes can be chosen so that the 1-skeleta of the resulting polyhedra do not change with n (since they depend on the edges of P_n that are intersected by Π_n). This gives a sequence of polyhedra R_n with w_1^n and w_2^n collapsing to the same point as $n \rightarrow \infty$; moreover now w_1^n and w_2^n share a face $F_n \subseteq \Pi_n$. Then there is a sequence z_1^n, \dots, z_k^n of vertices of R_n that all converge to v ; each z_i^n shares an edge with z_{i-1}^n and z_{i+1}^n . The points z_1^n, \dots, z_k^n can also be naturally viewed as points in the 1-skeleton of P_n : notice that z_i shares a face with z_{i+1} in Γ , therefore they are all in the same connected component of Λ_v . Similarly w_1 lies on the same face of z_1 and w_2 lies on the same face of z_k , and we obtain that w_1 and w_2 are in the same connected component of Λ_v .

Finally, let λ be a cycle contained in Λ_v , and K_1, K_2 the two connected components of S^2 bounded by λ . If $v_1 \in \Gamma \cap K_1$ and $v_2 \in \Gamma \cap K_2$ and neither

of them was in Λ_v , then $\tilde{\Gamma}'$ could be disconnected by removing v . To see this, notice that $\phi(v_1) \neq \phi(v_2)$ and take any path γ connecting $\phi(v_1)$ to $\phi(v_2)$. We wish to prove that γ must contain v , and to do so we show that there is a path from v_1 to v_2 contained in $\phi^{-1}(\gamma)$ (such a path has to cross $\lambda \subseteq \Lambda_v$, hence $v \in \gamma$). Take the edge e of γ containing $\phi(v_1)$, and lift it to any edge \tilde{e} of Γ . If $v_1 \notin \tilde{e}$, it can be connected to one of its endpoints via a path contained in $\Lambda_{\phi(v_1)}$ since this is connected. We can keep lifting the path γ to a path contained in $\phi^{-1}(\gamma)$, one edge at a time, gluing endpoints with a path contained in $\phi^{-1}(\gamma)$ when necessary.

To see this, notice that $\phi(v_1) \neq \phi(v_2)$ and any path γ connecting $\phi(v_1)$ to $\phi(v_2)$ must pass through v , since it would lift to a path contained in $\phi^{-1}(\gamma)$ connecting v_1 to v_2 which has to pass through λ . This contradicts the fact that $\tilde{\Gamma}'$ is 2-connected.

We now prove that any map $\phi : \Gamma_1 \rightarrow \Gamma_2$ satisfying the previous 3 properties must factor through a graph $\tilde{\Gamma}$ obtained via edge or face collapses as in the thesis of the Lemma. Let n be the number of vertices of Γ_1 and m the number of vertices of Γ_2 , and proceed by induction on $n - m$.

If $n - m = 0$ then Γ_1 is isomorphic to Γ_2 and there is nothing to prove.

For the inductive step, we have $n > m$ which implies there is a w such that Λ_w contains more than one vertex; we have by hypothesis that Λ_w is a connected subgraph of Γ_1 .

If Λ_w has a leaf, then ϕ factors through the graph obtained from Γ_1 by contracting the two vertices of this leaf. If Λ_w contains a cycle λ , then all vertices in one of the two components of the plane bounded by λ must be in Λ_w . In particular Λ_w contains a cycle that bounds a face, and ϕ factors through the graph obtained from collapsing this face to an edge.

In either case, the new graph has fewer vertices than Γ_1 and the induced ϕ has the same 3 properties. We can then conclude by induction. \square

The rectification of a polyhedron

Definition 2.25. We say that a projective polyhedron $\bar{\Gamma}$ is a *rectification* of a 3-connected planar graph Γ if the 1-skeleton of $\bar{\Gamma}$ is equal to Γ and all the edges of $\bar{\Gamma}$ are tangent to $\partial\mathbb{H}^3$.

Remark 2.26. Notice that, by definition, $\bar{\Gamma}$ is not a generalized hyperbolic polyhedron, since none of its edges intersect \mathbb{H}^3 . However as we will see it is still possible to give a definition of the volume of $\bar{\Gamma}$ as for any proper polyhedron.

Remark 2.27. A rectification of Γ gives a circle packing in $\partial\mathbb{H}^3 = S^2$ with tangency graph Γ^* . To see this, take the circles arising from the intersection of $\bar{\Gamma}$ with $\partial\mathbb{H}^3$; it is immediate to see that they are a circle packing and that

their tangency graph is Γ^* , since each circle corresponds to a face of $\bar{\Gamma}$ and two circles are tangent if and only if their faces share an edge.

From this we could quickly prove the existence and uniqueness of the rectification by invoking the Koebe-Thurston Theorem [47, Corollary 13.6.2] about the existence and uniqueness of circle packings; however Thurston's proof of this theorem requires implicitly the existence and uniqueness of the rectification. Therefore, we are going to prove this separately in Proposition 2.29, with essentially the same proof given in [47].

Remark 2.28. If two planes of \mathbb{RP}^3 intersect in a line tangent to $\partial\mathbb{H}^3$, then their hyperbolic dihedral angle is 0; furthermore two distinct planes which intersect in $\bar{\mathbb{H}}^3$ have dihedral angle 0 if and only if they intersect in a line tangent to $\partial\mathbb{H}^3$. Therefore, a projective polyhedron is a rectification of Γ if and only if its 1-skeleton is Γ , all its edges intersect $\bar{\mathbb{H}}^3$ and all its dihedral angles are 0.

The polyhedron $\bar{\Gamma}$ is not a generalized hyperbolic polyhedron, since its edges do not intersect \mathbb{H}^3 . However its truncation can be defined in the same way as before, and it can be described very explicitly. Consider two vertices v, v' of $\bar{\Gamma}$ connected by an edge $\overline{vv'}$ tangent to $\partial\mathbb{H}^3$. The planes Π_v and $\Pi_{v'}$ intersect at the point of tangency, and the truncation of $\bar{\Gamma}$ is going to have an ideal, 4-valent vertex with only right angles at that point. This can be repeated for every edge of $\bar{\Gamma}$ to see that its truncation has only right angles, and only ideal 4-valent vertices. Some of its faces come from faces of Γ , while the others from its vertices. Notice that because of this, even though $\bar{\Gamma}$ is not a generalized hyperbolic polyhedron, its truncation is an ideal finite volume right-angled hyperbolic polyhedron and therefore $\bar{\Gamma}$ has a well defined hyperbolic volume.

This explicit description of the truncation of $\bar{\Gamma}$ quickly leads to the existence and uniqueness of the rectification.

Proposition 2.29. *For any 3-connected planar graph Γ , the rectification $\bar{\Gamma}$ exists and is unique up to isometry.*

Proof. Consider the planar graph obtained by taking a vertex for each edge of Γ , where two vertices are joined by an edge if and only if the corresponding edges share an angle (i.e. they share a vertex and they lie on the same face) in Γ . This graph is 4-valent, and by Theorem 2.15 it is the 1-skeleton of a unique (up to isometry) right-angled ideal polyhedron P ; this is going to be the truncation of $\bar{\Gamma}$. Some faces of P correspond to vertices of Γ , while the others correspond to its faces. Then, the faces of P corresponding to faces of Γ bound the rectification $\bar{\Gamma}$ of Γ , and we can reconstruct uniquely $\bar{\Gamma}$ from Γ . \square

Remark 2.30. Notice that from the polyhedron P constructed in the proof of Proposition 2.29 it is immediate to see that the rectification of Γ and of its dual Γ^* have the same truncation (and in particular the same volume): if

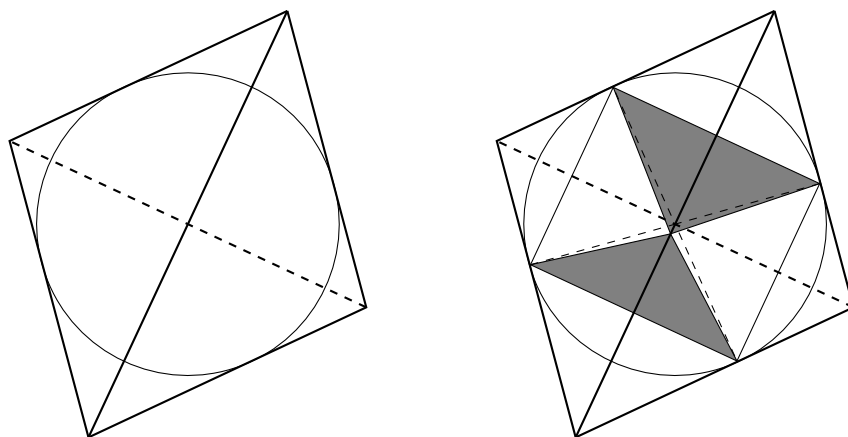


Figure 2.11: The rectification of a tetrahedron (left) and its truncation (right), the ideal right-angled octahedron. The gray faces arise from the truncation of the top and bottom vertices.

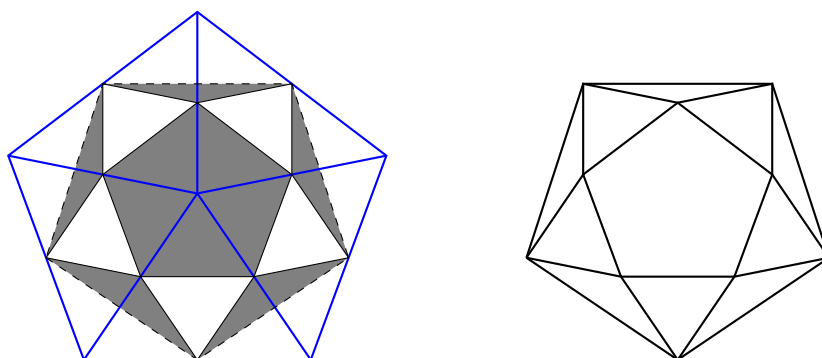


Figure 2.12: The pentagonal pyramid (left, thick blue) with the truncation faces (in gray); on the right, its truncation, the pentagonal antiprism.

we took the faces of P corresponding to vertices of Γ , these would bound the rectification of Γ^* .

Example 2.31. The truncation of the rectification of the tetrahedral graph (Figure 2.11) is the right-angled hyperbolic ideal octahedron, whose volume is $v_8 \cong 3.66$. As we noted in the introduction, it is proven in [51, Theorem 4.2] that indeed the supremum of volumes of proper hyperbolic tetrahedra is equal to v_8 .

Example 2.32. The truncation of the rectification of the n -gonal pyramid is the n -gonal antiprism. Its volume is given by the formula [47]:

$$2n \left(\Lambda \left(\frac{\pi}{4} + \frac{\pi}{2n} \right) + \Lambda \left(\frac{\pi}{4} - \frac{\pi}{2n} \right) \right).$$

Remark 2.33. As we noted the truncation of $\bar{\Gamma}$ is an ideal right-angled hyperbolic polyhedron; its volume can be calculated with a computer (see [53] for a table with many computed volumes).

To finish we prove that even though the rectification of Γ is not a generalized hyperbolic polyhedron, nevertheless it is a limit of hyperideal (hence, proper) hyperbolic polyhedra.

Lemma 2.34. *There exists a continuous family of proper polyhedra P_ϵ with 1-skeleton Γ that converges to (a polyhedron in the isometry class of) $\bar{\Gamma}$ as $\epsilon \rightarrow 0$.*

Proof. Take P_ϵ to be in the unique isometry class of polyhedra with 1-skeleton Γ and all angles equal to ϵ ; this can be done for any $\epsilon < \frac{\pi}{k}$ (where k is the maximum valence among vertices of Γ) by Theorem 2.15.

Since P_ϵ is defined only up to isometry, we need to fix an isometry class to establish the convergence. To do so we need a preliminary lemma of planar hyperbolic geometry.

Lemma 2.35. *If $\theta_1^n, \dots, \theta_k^n$ are angles of a hyperbolic k -gon A_n , for $n \in \mathbb{N}$, and as $n \rightarrow \infty$ we have $\theta_i^n \rightarrow \theta_i$ with $\sum_i \theta_i < (k-2)\pi$ then up to a suitable choice of isometry class of each A_n , every accumulation point of A_n (with the convergence described in Section 2.2) is a hyperbolic polygon (possibly with ideal vertices); furthermore there is always at least one accumulation point.*

Proof. Suppose first that A_n is a triangle and v_1^n, v_2^n, v_3^n are its vertices. Up to isometry we can suppose that for all n the vertices v_1^n and v_2^n lie on the line $(-1, 1) \times \{0\} \subseteq \mathbb{H}^2 \subseteq \mathbb{R}^2$ and v_3^n lies on the line $\{0\} \times \mathbb{R}$. Then as $n \rightarrow \infty$, up to a subsequence if necessary, $v_i^n \rightarrow v_i \in \bar{\mathbb{H}}^2$.

Pass to a subsequence such that v_1^n, v_2^n, v_3^n converge to v_1, v_2, v_3 . If the v_i 's are distinct, then A_n converges to the triangle with vertices v_1, v_2, v_3 . If $v_i = v_j$ we assume $i = 1, j = 2$ and $v_3 \neq v_1$ (all other cases are identical). However this would mean that the internal angle of A_n at v_2^n must have the same limit as the external angle of A_n at v_1^n . This implies that the limit of the sum of angles of A_n is π , contradicting the hypothesis on the angles.

Suppose now that A_n is an n -gon, and triangulate it (with the same combinatorial triangulation for all n). One of the triangles must satisfy the hypotheses of the lemma, and thus we can choose an isometry class for each n so that in any subsequence, this triangle converges to a non degenerate triangle; of course then if A_{n_k} converges to some A , then A must be non-degenerate since it contains a non-degenerate triangle. \square

Now pick a vertex v of Γ ; up to isometry we can make it so that the corresponding vertex $v_\epsilon \in P_\epsilon$ is independent of ϵ . Then any subsequence of

$A_\epsilon := P_\epsilon \cap \Pi_{v_\epsilon}$ satisfies the hypotheses of Lemma 2.35, and we can choose a representative of P_ϵ so that (in this subsequence) A_ϵ converges to some A of positive area.

Each plane containing a face of P_ϵ is naturally an element of $(\mathbb{RP}^3)^*$, hence up to taking a subsequence each face of P_ϵ converges to a subset of a plane: the set of all limit planes will delimit a convex set P^* . To show that P^* is a polyhedron, we need to prove that it is non-degenerate: this is because it must contain the cone from v to A .

As we noted previously every vertex of P^* must be a limit of vertices of P_ϵ ; likewise every edge of P^* is a limit of edges of P_ϵ . However a priori many vertices of P_ϵ could converge to the same vertex, and likewise with the edges. Furthermore, the angles of P^* could be different than the limit of the angles of P_ϵ . We now show however that in this specific case none of this happens.

Notice that each edge e_ϵ of P_ϵ has its dihedral angle converging to 0, hence the faces Π_ϵ^1 and Π_ϵ^2 determining e must either coincide in the limit (which would contradict the fact that P^* is non-degenerate) or must converge to two faces Π_1 and Π_2 intersecting in an edge tangent to $\partial\mathbb{H}^3$. Therefore, every edge of P^* is tangent to $\partial\mathbb{H}^3$ and P^* is the rectification of its 1-skeleton. If there are no two vertices of P_ϵ converging to the same vertex of P^* then of course the 1-skeleton of P^* is Γ and we have concluded. Suppose then that many vertices of P_ϵ converge to a vertex w of P^* : since each vertex of P_ϵ is outside \mathbb{H}^3 and each edge intersects \mathbb{H}^3 , w must lie on the sphere at infinity. Then P^* is a non-degenerate projective polyhedron such that:

- each of its edges is tangent to $\partial\mathbb{H}^3$;
- some of its vertices are in $\partial\mathbb{H}^3$.

However such a polyhedron does not exist. Therefore $P^* = \bar{\Gamma}$.

Suppose now that P_ϵ has a different subsequence converging to some other \tilde{P}^* . The same argument implies that this subsequence converges to $\bar{\Gamma}$, hence $P_\epsilon \rightarrow \bar{\Gamma}$. \square

The Schläfli formula and volume

The fundamental tool to study the volume of proper polyhedra is the Schläfli formula (see for example [33, Chapter: The Schläfli differential equality]). Remember that the volume of a proper polyhedron is equal to the hyperbolic volume of its truncation.

Theorem 2.36. *If P_t is a smooth family of proper or almost proper polyhedra without ideal vertices with the same 1-skeleton, same set of almost proper*

vertices, dihedral angles $\theta_1^t, \dots, \theta_n^t$ and edge lengths l_1^t, \dots, l_n^t , then

$$\frac{\partial \text{Vol}(P_t)}{\partial t} \Big|_{t=t_0} = -\frac{1}{2} \sum_i l_i^{t_0} \frac{\partial \theta_i^t}{\partial t} \Big|_{t=t_0}$$

Remark 2.37. Usually this result is stated for compact hyperbolic polyhedra (i.e. with no hyperideal vertices), however it is straightforward to generalize it to proper or almost proper polyhedra without ideal vertices (it can also be generalized to the case with ideal vertices; however this case carries some technical difficulties and we will not need it). This is because a path of proper or almost proper polyhedra P_t induces a path of truncated polyhedra P_t^0 ; the length of an edge in P_t is the same (by definition) as the length of the corresponding edge in the truncation, and the derivatives of all angles are the same, since an angle of P_t^0 is either the same as the corresponding angle of P_t , differs by a constant, or is constantly $\frac{\pi}{2}$ and thus does not contribute to the sum.

However the Schläfli formula definitely does not hold for generalized hyperbolic polyhedra, as the truncation angles could vary.

In particular, the Schläfli formula implies that if all the angles are *decreasing*, the volume is *increasing*.

We recall a well known fact about the convergence of volumes.

Lemma 2.38. *If $P_n \subseteq \mathbb{H}^3$, $n \in \mathbb{N}$ is a sequence of compact hyperbolic polyhedra, and P_n converges to the compact convex set P as $n \rightarrow +\infty$ (as elements of $((\mathbb{RP}^3)^*)^F$), then $\text{Vol}(P_n) \rightarrow \text{Vol}(P)$.*

Proof. Suppose first that P has non-empty interior (i.e. it is a polyhedron). Up to isometry, we can assume that 0 is in the interior of P (therefore, $0 \in P_n$ for n big enough). Consider the map $\Phi_\lambda^0 : \mathbb{R}^3 \rightarrow \mathbb{R}^3$ given by multiplication by λ . View P_n and P as subsets of $\mathbb{H}^3 \subseteq \mathbb{R}^3$. Since $P_n \rightarrow P$, there exists an ϵ_n such that $\Phi_{1-\epsilon_n}(P_n) \subseteq P$ with $\epsilon_n \rightarrow 0$ as $n \rightarrow \infty$, because P has non-empty interior. By modifying ϵ_i for $i \leq n$ appropriately, we can assume that $\Phi_{1-\epsilon_n}(P_n)$ contains every $\Phi_{1-\epsilon_i}(P_i)$ for $i < n$ (since P_n is convex for every n). Therefore the sequence $\Phi_{1-\epsilon_n}(P_n)$ is an increasing sequence of compact (convex) polyhedra that converges to P ; the monotone convergence theorem then tells us that $\text{Vol}(\Phi_{1-\epsilon_i}(P_i)) \rightarrow \text{Vol}(P)$. Since $\epsilon_i \rightarrow 0$ then $\text{Vol}(\Phi_{1-\epsilon_i}(P_i)) - \text{Vol}(P_i)$ converges to 0 , which concludes the proof.

If instead P has volume 0 , then for any $\epsilon > 0$, there is an \bar{n} big enough that P_n is contained in an ϵ neighborhood of P for any $n > \bar{n}$, which implies that $\text{Vol}(P_n) \rightarrow \text{Vol}(P) = 0$. \square

Notice that in general it is *not true* that if P_n is a sequence of compact hyperbolic polyhedra that converges to a (non-degenerate) *finite-volume* P ,

then $\text{Vol}(P_n) \rightarrow \text{Vol}(P)$. To see a counterexample, take a tetrahedron T_α with 3 real vertices and a hyperideal vertex, with sum of angles at the hyperideal vertex equal to $\alpha < \pi$. Glue two copies of T_α along the truncation face to obtain a compact prism P_α , and let $\alpha \rightarrow \pi$. Then $\text{Vol}(P_\alpha) = 2\text{Vol}(T_\alpha) \rightarrow 2\text{Vol}(T_\pi)$ but P_α converges to a tetrahedron (where one copy of T_α gets pushed to infinity), and thus $\text{Vol}(P_\pi) = \text{Vol}(T_\pi)$.

However, if P_n converges to a finite-volume polyhedron P and the convergence is nice enough, then the result still holds; this is the content of the following lemma.

Lemma 2.39. *Suppose P_n is a sequence of compact polyhedra (i.e. all their vertices are real) with 1-skeleton Γ such that $P_n \rightarrow P$ with P a finite volume (possibly degenerate) convex subset of \mathbb{H}^3 and such that if v_1^n, v_2^n are vertices of P_n that converge to the same point in P , then the distance between v_1^n and v_2^n converges to 0. Then $\text{Vol}(P_n) \rightarrow \text{Vol}(P)$.*

Proof. If P is a point on $\partial\mathbb{H}^3$ then every edge length of P_n goes to 0 by assumption; this implies that P_n is contained in an ϵ -neighborhood of one of its vertices, hence its volume goes to 0. Suppose then that P contains a point $p \in \mathbb{H}^3$.

Take any subsequence P_{n_k} of P_n ; up to a subsequence $P_{n_{k_j}}$ we can assume that every vertex of $P_{n_{k_j}}$ converges. If we prove that $\text{Vol}(P_{n_{k_j}}) \rightarrow \text{Vol}(P)$ we conclude the proof; therefore we can assume that every vertex of P_n converges.

It suffices to prove the lemma for tetrahedra. Indeed we can triangulate P_n by taking the cone over an interior point p_n converging to p , and by further triangulating each pyramid in a fixed combinatorial way. Each tetrahedron in the triangulation converges to a (maybe degenerate) tetrahedron in a triangulation of P , hence if the volume of each tetrahedron converges to the volume of its limit, then the volume of P_n must converge to the volume of P .

So let P_n be a tetrahedron converging to a (possibly degenerate) tetrahedron T . If T is compact we can apply Lemma 2.38 to conclude. If T is non-degenerate and has ideal points, we can for the sake of simplicity further triangulate so that T only has one ideal vertex v . Then if we truncate P_n and T along a horosphere centered in v we obtain a sequence of compact sets with volumes close to those of P_n converging to a compact set with volume close to that of T , which concludes the proof.

If instead T is degenerate and has ideal vertices, we distinguish 2 cases. If no two vertices of P_n converge to the same point, then we can apply the same reasoning as the previous case by cutting along appropriate horospheres. Otherwise, we need to show that $\text{Vol}(P_n) \rightarrow 0$. There are (at least) two vertices of P_n converging to the same vertex of T , and by assumption their distance goes

to 0. This means that for n big enough, P_n is contained in an ϵ -neighborhood of one of its faces. Since P_n has bounded surface area, $\text{Vol}(P_n) \rightarrow 0$. \square

2.3 Hyperbolic 3-manifolds

The material in this section is standard and can be found for example in [32] or [47].

Definition 2.40. A *hyperbolic 3-manifold* is a connected smooth 3-manifold with a complete Riemannian structure with sectional curvature everywhere -1 . In other words, a hyperbolic 3-manifold is a Riemannian manifold isometric to the quotient of \mathbb{H}^3 by a free, discrete group of isometries.

Since the works of Thurston [47], it has been clear that hyperbolic 3-manifolds are central to the study of topology in dimension 3. The result which forms the basis for this interconnectedness between geometry and topology in dimension 3 is the Mostow Rigidity Theorem.

Theorem 2.41 (Mostow Rigidity Theorem). *Let M_1, M_2 be two finite volume hyperbolic 3-manifolds, and $\phi : \pi_1(M_1) \rightarrow \pi_1(M_2)$ be an isomorphism between their fundamental groups. Then there is an isometry $\Phi : M_1 \rightarrow M_2$ such that Φ induces ϕ on fundamental groups.*

The Mostow rigidity theorem has far reaching consequences; for the purpose of this thesis, the most salient is the fact that if M is a 3-manifold with a hyperbolic structure, then $\text{Vol}(M)$ is a well-defined topological invariant of M .

More mundanely, since if a smooth 3-manifold admits a finite volume hyperbolic structure then this is essentially unique, we also say “finite volume hyperbolic 3-manifold” to mean “smooth manifold admitting a finite volume hyperbolic structure”. Likewise, if $L \subseteq M$ is a link, we say that it is *hyperbolic* if $M \setminus L$ admits a finite volume hyperbolic structure.

Theorem 2.42 (Thick-thin decomposition). *Let M be a finite volume orientable hyperbolic 3-manifold; then M is diffeomorphic to the interior of a compact 3-manifold with only toric boundary components.*

Theorem 2.43 (Thurston’s hyperbolic Dehn filling Theorem). *Let M be a finite volume orientable hyperbolic 3-manifold which is the interior of \overline{M} . Let T be a boundary component of \overline{M} ; then for all but a finite number of choices for $\phi : T \rightarrow S^1 \times S^1$, the manifold obtained by Dehn filling T with ϕ is hyperbolic with finite volume.*

There is a plethora of interesting examples of hyperbolic 3-manifolds; indeed, “most” interesting 3-manifolds are hyperbolic, in some sense. Here we describe the family of hyperbolic manifolds which will be featured in Theorem 1.4, the *Fundamental Shadow Links*.

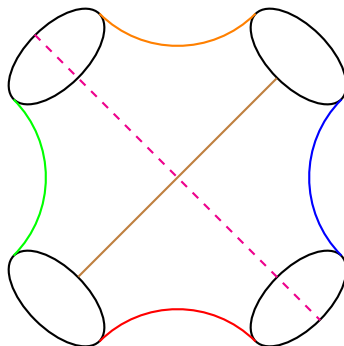


Figure 2.13: The building block

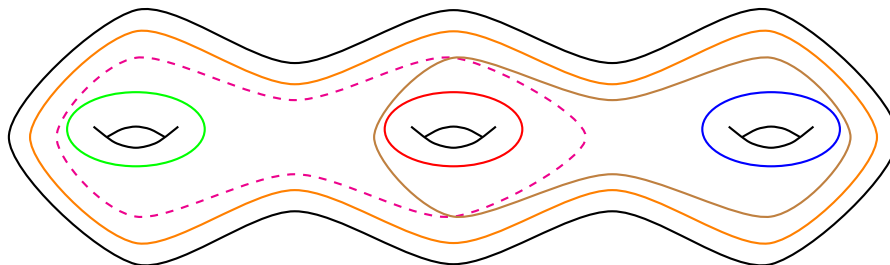


Figure 2.14: The link in the boundary of the handlebody

The building block for these links is a 3-ball with 4 disks on its boundary, and 6 arcs connecting them, as in Figure 2.13. If we take c building blocks B_1, \dots, B_c and glue them together along the disks, in such a way that each endpoint of each arc is glued to some other endpoint (possibly of the same arc), we obtain a (possibly non-orientable) handlebody H of genus $c + 1$ with a link in its boundary, such as in Figure 2.14. By taking the orientable double of this handlebody (by picking the orientable double cover \tilde{H} and quotienting $\partial\tilde{H}$ by the deck involution), we obtain a link inside $M_c := \#^{c+1}(S^1 \times S^2)$. We call a link obtained in such a way a *Fundamental Shadow Link* (FSL for short).

The most important features of these links are that their quantum invariants (see Lemma 3.13) and geometry are well understood:

Lemma 2.44. [17, Proposition 3.33] *If $L \subseteq M_c$ is a fundamental shadow link, then $M_c \setminus L$ is hyperbolic of volume $2cv_8$.*

Chapter 3

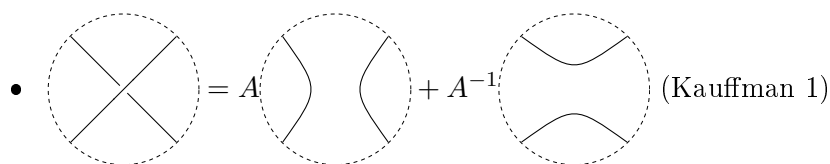
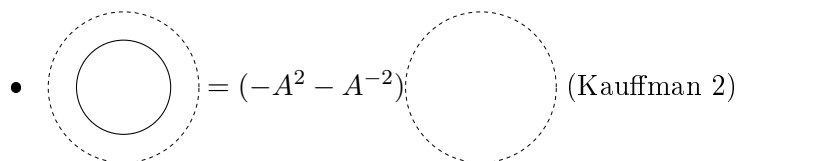
Quantum invariants

In this chapter we introduce the quantum invariants we study: the colored Jones polynomial in Section 3.1, the Kauffman skein bracket for trivalent graphs in 3.2, the Reshetikhin-Turaev invariants in Section 3.3, the Turaev-Viro invariants in Section 3.4 and finally the Yokota invariant in Section 3.5. An introduction to some of these topics can be found in Chapters 3, 13 and 14 of [31] or in [26]. This chapter contains almost no original material; we mostly follow the aforementioned textbooks with only mild generalizations or reformulations.

3.1 The Kauffman skein module

Let M be a compact, oriented 3-dimensional manifold, and take A to be a variable.

Definition 3.1. The *skein module* of M , denoted with $S(M)$, is the $\mathbb{Z}[A, A^{-1}]$ -module spanned by all framed links in M up to isotopy, quotiented by the following two relations:

-  (Kauffman 1)
-  (Kauffman 2)

The skein module of M behaves well with respect to embeddings between manifolds; that is to say, if $f : M \rightarrow N$ is an embedding, then there is an induced map $f_* : S(M) \rightarrow S(N)$.

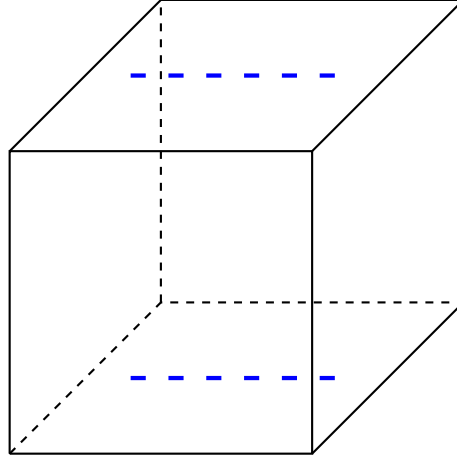


Figure 3.1: The cube $[-1, 1] \times [0, 1] \times [0, 1]$ with 6 marked segments in the top and bottom face.

The study of the skein module of manifolds is a fruitful and interesting field; however for the purpose of this thesis only a few easy examples are needed, starting with $M = S^3$ and $M = S^1 \times D^2$.

Lemma 3.2. 1. *The skein module of S^3 is 1-dimensional and spanned by the empty link;*

2. *The skein module of $S^1 \times D^2$ is isomorphic to the module of polynomials $\mathbb{Z}[A, A^{-1}][x]$, where x^i is the framed link given by i parallel copies of $S^1 \times [-\epsilon, \epsilon] \subseteq S^1 \times D^2$.*

In particular, the fact that S^3 is one dimensional and spanned by the empty set permits to define the *Kauffman bracket* of a link (or even linear combinations thereof), by taking $\langle L \rangle_K$ to be the unique element of $\mathbb{Z}[A, A^{-1}]$ such that $L = \langle L \rangle_K \emptyset$ as elements of $S(S^3)$.

There is also a relative version of the skein module. Let M be a manifold with boundary ∂M containing some disjoint segments I_1, \dots, I_{2n} . We define the skein module of $(M, \partial M, I)$ as the module generated by framed links and framed embedded arcs L such that $L \cap \partial M = I$, quotiented by the Kauffman relations above. Notice that if I contains $2n$ segments, then L must contain exactly n arcs. If ∂M is connected, then the skein module only depends on the number of segments, hence we simply denote it with $S(M, 2n)$.

Consider $M = [-1, 1] \times [-1, 1] \times [-1, 1]$ with n segments contained in $\{-1\} \times \{0\} \times [0, 1]$ and the same n segments contained in $\{1\} \times \{0\} \times [0, 1]$ (i.e. they are the same subset of $[0, 1]$, as in Figure 3.1). We can take M_1, M_2 to be two copies of M and stack them on top of each other, gluing $1 \times [0, 1] \times [0, 1]$ of M_1 to $-1 \times [0, 1] \times [0, 1]$ of M_2 , and rescaling the first coordinate to once again

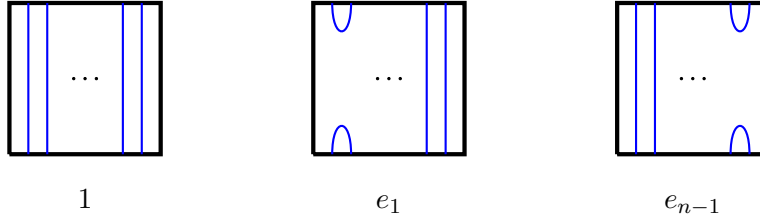


Figure 3.2: The basis of \mathcal{T}_n

obtain $[-1, 1] \times [0, 1] \times [0, 1]$. This gives a smooth map $\phi : M_1 \sqcup M_2 \rightarrow M$ that induces a product in $S(M, 2n)$; it is immediate to see that this turns the skein module in an algebra \mathcal{T}_n usually called the *Temperley-Lieb algebra*. A basis $1, e_1, \dots, e_{n-1}$ for \mathcal{T}_n as an algebra is given by Figure 3.2; the identity element is the first tangle on the left.

Lemma 3.3. *The Jones-Wenzl idempotent $f^{(n)}$, defined inductively by the following formula*

$$\begin{array}{|c|} \hline \square \\ \hline \end{array} \begin{array}{|c|} \hline n \\ \hline \end{array} = \begin{array}{|c|} \hline \square \\ \hline \end{array} \begin{array}{|c|} \hline n-1 \\ \hline \end{array} + \frac{A^{2n-2} - A^{-2n+2}}{A^{2n} - A^{-2n}} \begin{array}{|c|} \hline \begin{array}{c} \square \\ \text{---} \\ \square \end{array} \\ \hline \end{array} \begin{array}{|c|} \hline n-1 \\ \hline \end{array} \quad (3.1)$$

has the following properties:

- $f^{(n)} f^{(n)} = f^{(n)}$;
- $f^{(n)} e_i = e_i f^{(n)} = 0$;
- $f^{(n)} - 1$ is in the algebra generated by e_1, \dots, e_{n-1} .

The Jones-Wenzl idempotent is a linear combination of diagrams; however, in practice it is helpful to think of it as if it was a single diagram. When we do this, we draw it as in the left hand side of (3.1), with a single strand instead of n , and a label next to the square to signify that we are considering $f^{(n)}$.

We can define an additional map on $S(M, 2n)$ by gluing the top of the cylinder to its bottom to obtain $S^1 \times D^2$; a skein element γ of $S(M, 2n)$ is sent to a skein element $\text{tr}(\gamma) \in S(S^1 \times D^2)$ which we call the *trace* of γ .

Definition 3.4. Let $K \subseteq S^3$ be a framed knot, realized by an embedding $i : S^1 \times D^2 \rightarrow S^3$, and take $n \in \mathbb{N}^+$. We define the n -th colored Jones polynomial of K (denoted with J_n^K) to be the Kauffman bracket of the image of $f^{(n)}$ under the composition $i_* \circ \text{tr}$. If L is a link, and each component is colored with $\text{col} = (n_1, \dots, n_k)$ we define J_{col}^L by embedding the corresponding Jones-Wenzl idempotent in each component.

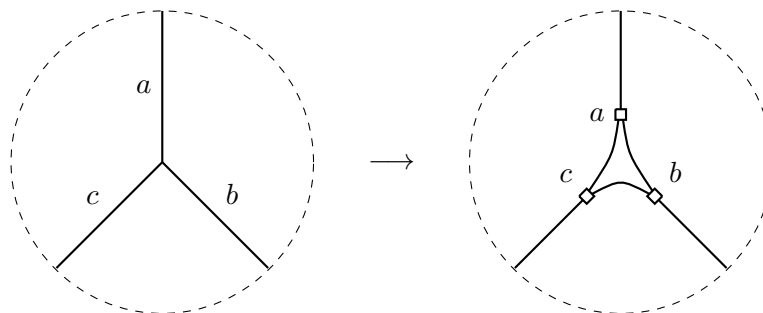


Figure 3.3: Inserting Jones-Wenzl idempotents along a vertex

3.2 The Kauffman bracket of trivalent graphs

The colored Jones polynomial could be calculated, in principle, directly from the definition, expanding the Jones-Wenzl idempotent as a linear combination of diagrams and calculating the Kauffman bracket of the resulting links. However this approach is very cumbersome, and leads to a satisfying result only in a handful of cases. Fortunately there are ways to compute the Jones polynomial exploiting some of the properties of the Jones-Wenzl idempotent; to carry out these calculation however we need a way to extend the definition of the Jones polynomial.

Definition 3.5. A *framed graph* $\Gamma \subseteq S^3$ is a graph in S^3 together with a 2-dimensional oriented thickening, considered up to isotopy. More precisely, a framed graph Γ is a pair G, F with G an embedded graph in S^3 and F an embedded orientable surface containing G as a deformation retract.

In this subsection we only consider *trivalent* framed graphs, that is to say only framed graphs where each vertex lies on exactly 3 edges (notice that circular component are allowed, as they have no vertices). We will study more general graphs in Subsection 3.5.

Definition 3.6. We say that a triple (a, b, c) of non-negative integers is *admissible* if

- $a + b + c$ is even;
- $a \leq b + c$, $b \leq a + c$ and $c \leq a + b$ (the triangular inequality).

We call a map $\{\text{edges of } \Gamma\} \rightarrow \mathbb{N}$ a *coloring* of Γ ; we say that it is admissible if the triple surrounding each vertex is admissible.

Let $\Gamma \subseteq S^3$ be a trivalent framed graph and col an admissible coloring of Γ . We can associate to (Γ, col) a linear combination of framed links in S^3 as follows: every edge e gets replaced by $col(e)$ parallel strands and every

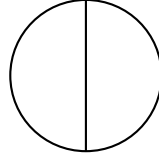


Figure 3.4: A Theta graph

vertex gets replaced as in Figure 3.3 (notice that since col is admissible, this substitution can always be done uniquely). This associates to (Γ, col) a linear combination of links $\mathcal{L} \in \mathcal{S}(S^3)$. Then the Kauffman bracket $\langle \Gamma, col \rangle_K$ is defined as the Kauffman bracket of \mathcal{L} . If col is not admissible, by convention we say that $\langle \Gamma, col \rangle_K = 0$. For the remainder of the thesis we are going to use the variable $q = A^2$, so that $\langle \cdot \rangle_K \in \mathbb{Z}[q^{1/2}, q^{-1/2}]$. If L is a colored framed link, we think of it as a framed graph with no vertices, and of course $J_{col}^L = \langle L, col \rangle_K$.

From now on we are going to be interested only in the Kauffman bracket evaluated at a root of unity; we fix $r \geq 3$ odd and $q \in \mathbb{C}^*$ a primitive r -th root of unity.

The *quantum integer* $\{n\}$ is defined as $q^n - q^{-n}$, and the quantum factorial $\{n\}!$ is $\prod_{i=1}^n \{i\}$. Sometimes we will write $[n]$ for $\frac{\{n\}}{\{1\}}$ for short, and similarly $[n]!$ for $\prod_{i=1}^n [i]$. Furthermore, we denote with I_r the set of even numbers $\{0, 2, \dots, r-3\}$.

Remark 3.7. The choice of even numbers in the definition of I_r corresponds to using the $SO(3)$ Reshetikhin-Turaev invariants rather than the $SU(2)$ version.

We say that a triple (a, b, c) is r -admissible if (a, b, c) is admissible and

- $a, b, c \leq r - 2$;
- $a + b + c \leq 2r - 4$.

We say that a coloring of Γ is r -admissible if the triple at every edge is r -admissible.

We can obtain the following simple formulas for the Kauffman bracket by induction on the colors.

- If U is the trivial knot colored with n , then $\langle \Gamma, n \rangle_K = \Delta_n := (-1)^n [n+1]$.
- If Θ is the Theta graph depicted in Figure 3.4, colored with the r -admissible triple a, b, c , we have

$$\Theta(a, b, c) = (-1)^{\frac{a+b+c}{2}} \frac{[\frac{a+b+c}{2} + 1]! [\frac{a+b-c}{2}]! [\frac{a-b+c}{2}]! [\frac{-a+b+c}{2}]!}{[a]! [b]! [c]!} \quad (3.2)$$

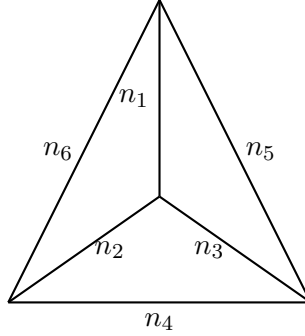


Figure 3.5: An admissible coloring for a tetrahedron

When a vertex v of Γ is colored by an r -admissible triple a, b, c , for convenience we write $\Theta(v)$ instead of $\Theta(a, b, c)$. For convenience we also define $\Delta(a, b, c) = \Theta(a, b, c)^{-1/2}$ and $\Delta(v)$ analogously. Notice that the number inside the square root is real; by convention we take the positive square root of a positive number, and the square root with positive imaginary part of a negative number.

The bracket $\langle \cdot \rangle_K$ we just defined is sometimes called the *Kauffman bracket in the Kauffman normalization*. In the remainder of the thesis we will prefer to deal with the *unitary* normalization instead.

Definition 3.8. The Kauffman bracket with the unitary normalization, denoted simply by $\langle \cdot \rangle$, is defined by

$$\langle \Gamma, col \rangle = \left(\prod_{v \text{ vertex of } \Gamma} \Delta(v) \right) \langle \Gamma, col \rangle_K$$

It is possible to show by induction on the colors that in this normalization the tetrahedron of Figure 3.5 colored with the r -admissible tuple (n_1, \dots, n_6) is equal to the $6j$ -symbol given by

$$\begin{vmatrix} n_1 & n_2 & n_3 \\ n_4 & n_5 & n_6 \end{vmatrix} = \prod_{i=1}^4 \Delta(v_i) \sum_{z=\text{Max}T_i}^{\text{Min}Q_j} \frac{(-1)^z [z+1]!}{\prod_{i=1}^4 [z-T_i]! \prod_{j=1}^3 [Q_j-z]!} \quad (3.3)$$

where:

- $v_1 = (n_1, n_2, n_3)$, $v_2 = (n_1, n_5, n_6)$, $v_3 = (n_2, n_4, n_6)$, $v_4 = (n_3, n_4, n_5)$;
- $T_1 = \frac{n_1+n_2+n_3}{2}$, $T_2 = \frac{n_1+n_5+n_6}{2}$, $T_3 = \frac{n_2+n_4+n_6}{2}$ and $T_4 = \frac{n_3+n_4+n_5}{2}$;
- $Q_1 = \frac{n_1+n_2+n_4+n_5}{2}$, $Q_2 = \frac{n_1+n_3+n_4+n_6}{2}$ and $Q_3 = \frac{n_2+n_3+n_5+n_6}{2}$.

Remark 3.9. Notice that if $z \geq r - 1$, then the summand in (3.3) corresponding to z is equal to 0.

Proposition 3.10. *The Kauffman bracket is the unique map*

$$\langle \cdot \rangle : \{ \text{colored trivalent framed graphs in } S^3 \} \rightarrow \mathbb{C}$$

satisfying the following properties:

1. If Γ is the planar circle with no vertices colored with n , then $\langle \Gamma \rangle = \Delta_n$;
2. If Γ is a Theta graph (see Figure 3.4) colored with the r -admissible triple a, b, c then $\langle \Gamma \rangle = 1$;
3. If Γ is a tetrahedron colored with the r -admissible 6-tuple (n_1, \dots, n_6) then $\langle \Gamma \rangle$ is the 6j-symbol;
4. The fusion rule:

$$\left\langle \begin{array}{c} b \\ \text{---} \\ a \end{array} \right\rangle = \sum_{i \in I_r} \Delta_i \left\langle \begin{array}{c} b \\ \diagup \quad \diagdown \\ a \end{array} \right\rangle \begin{array}{c} i \\ \text{---} \\ i \end{array} \left\langle \begin{array}{c} b \\ \diagdown \quad \diagup \\ a \end{array} \right\rangle \quad (3.4)$$

5. If Γ has a bridge (that is to say, an edge that disconnects the graph if removed) colored with $i \neq 0$, then $\langle \Gamma \rangle = 0$;
6. If at some vertex of Γ the colors do not form an r -admissible triple, then $\langle \Gamma \rangle = 0$;
7. If Γ is colored with an r -admissible coloring such that the color of a non-circular edge e is equal to 0, then $\langle \Gamma \rangle = \frac{1}{\sqrt{\Delta_a \Delta_b}} \langle \Gamma' \rangle$ where Γ' is Γ with e removed, and a, b are the colors of the edges that share a vertex with e (notice that since the coloring is r -admissible, two edges sharing the same vertex with e will have the same color);
8. The framing change:

$$\left\langle \begin{array}{c} \diagup \quad \diagdown \\ b \quad c \\ \diagdown \quad \diagup \\ a \end{array} \right\rangle = (-1)^{\frac{b+c-a}{2}} q^{\frac{b(b+2)+c(c+2)-a(a+2)}{4}} \left\langle \begin{array}{c} c \quad b \\ \diagdown \quad \diagup \\ a \end{array} \right\rangle$$

9. If Γ is the distant union of Γ_1 and Γ_2 , then $\langle \Gamma \rangle = \langle \Gamma_1 \rangle \langle \Gamma_2 \rangle$.

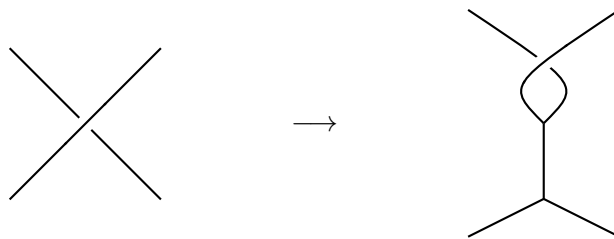


Figure 3.6: Adding two vertices to remove a crossing

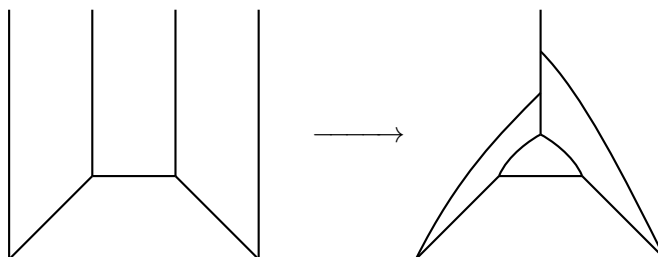
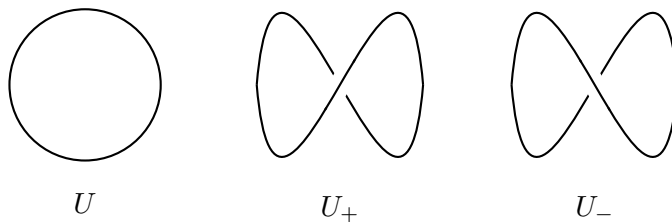


Figure 3.7: Applying the fusion rule to all edges incident to a face to obtain a bridge

Proof. The fact that the Kauffman bracket satisfies the listed properties can be found in [26, Summarized in Chapter 9] (notice that [26] uses the Kauffman normalization; however going from one to the other is immediate). The fact that these properties determine the bracket uniquely comes from the fact that they are enough to calculate the bracket of any colored framed graph. To see this, take a framed colored graph (Γ, col) in S^3 , and take a diagram for it. First we show that $\langle \Gamma, col \rangle$ can be calculated as a linear combination of colored planar graphs. Then we show that the bracket of colored planar graphs can be computed from the trivial knot, the Theta graph and the tetrahedron.

To see this consider a crossing of Γ ; apply a fusion rule to the two strands to obtain a picture as in Figure 3.6; then the crossing can be undone using rule 8.

Consider now Γ, col a planar colored graph with n vertices, and fix a planar diagram for it. By Property 9 we can assume that Γ is connected. Let k be the minimum number of edges of a face of Γ . We show that Γ, col can be calculated by induction on n . If $n = 0$ then Γ is a trivial knot and Property 1 gives its value. Suppose now that we can calculate $\langle \Gamma, col \rangle$ using Properties 1-9 for any $i < n$. If $k = 1$ there is a bridge; if it is colored with $a \neq 0$ then $\langle \Gamma, col \rangle = 0$, otherwise the bridge can be eliminated to remove two vertices, and $\langle \Gamma, col \rangle$ can be computed as the bracket of a graph with $n - 2$ vertices. If $k > 1$ we can take a minimal face and apply the fusion rule iteratively to all edges incident to the face (see Figure 3.7 for the case of $k = 4$). This creates a bridge which is removed as before, and Γ is split into two disjoint graphs;

Figure 3.8: The framed trivial knots U, U_+, U_- .

the first has $n - k$ vertices and the second (the one that contains the minimal face) has $2k - 2$ vertices. However since k is the minimal number of edges on a face of Γ we must have either $n \geq 2k$, $n = 4, k = 3$ or $n = 2, k = 2$, and the latter two cases are the tetrahedron and theta graph respectively. \square

In what follows sometimes we will color edges of Γ with linear combinations of colors; the Kauffman bracket can be extended linearly to this context. In particular, we will use Kirby's color $\Omega := \sum_{i \in I_r} \Delta_i i$.

3.3 The Reshetikhin-Turaev invariants

Let M be a closed oriented connected 3-manifold, and choose $L \subseteq S^3$ a framed link that gives M by Dehn surgery. Let U, U_+ and U_- be the framed knots given by Figure 3.8; each is a trivial knot but with different framing. Let $\text{lk}(L)$ be the linking matrix of L , and σ_+ and σ_- be the numbers of positive and negative eigenvalues of $\text{lk}(L)$ respectively. Finally we still denote with Ω the coloring of any link with Kirby's color Ω on each component of the link. Recall that r is odd and greater than 2, and q is a primitive r -th root of unity.

Define the *Reshetikhin-Turaev invariant* as

$$RT_r(M) := \langle U, \Omega \rangle^{\frac{-1-b_1(M)}{2}} \frac{\langle L, \Omega \rangle}{\langle U_+, \Omega \rangle^{\sigma_+} \langle U_-, \Omega \rangle^{\sigma_-}}$$

Theorem 3.11. *The Reshetikhin-Turaev invariant does not depend on the choice of L .*

This invariant can also be extended to an invariant of links in 3-manifolds as follows.

Let $L \subseteq M$ be a framed link in a 3-manifold, and let col be a coloring of the components of L with elements of $I_r = \{0, 2, \dots, r - 3\}$. Find a link $L' \subseteq M$ such that $M \setminus L'$ is diffeomorphic to a link complement in S^3 (by an abuse of notation we still call this second link L'); this is just saying that M is obtained via Dehn surgery on $L' \subseteq S^3$. If L and L' intersect (in M), do a

small isotopy of one of them to have them disjoint. Since $M \setminus L' \cong S^3 \setminus L'$ the link L can be seen as a (colored) link in S^3 (which, once again, we still denote with L) disjoint from L' . Let $\Omega \cup col$ be the coloring of the link $L' \cup L$ given by coloring each component of L' by Ω and each component of L by its color in col . As before σ_{\pm} are the number of \pm -signed eigenvalues of $\text{lk}(L')$. Then

$$RT_r(M, L) := \langle U, \Omega \rangle^{\frac{-1-b_1(M)}{2}} \frac{\langle L' \cup L, \Omega \cup col \rangle}{\langle U_+, \Omega \rangle^{\sigma_+} \langle U_-, \Omega \rangle^{\sigma_-}}$$

is an invariant of the link $L \subseteq M$ with coloring col . Notice that we picked an arbitrary perturbation of either L or L' to make them disjoint; however it can be shown that RT_r is independent of this choice.

Example 3.12. The invariants of the following links/manifolds are trivial to calculate:

- The manifold $S^1 \times S^2$ is obtained as surgery from U ; it is immediate to check that $RT_r(S^1 \times S^2) = 1$ for all r ;
- The manifold S^3 is obtained as surgery from either U_+ or U_- ; therefore $RT_r(S^3) = \langle U, \Omega \rangle^{-1/2} = \frac{q-q^{-1}}{\sqrt{-r}}$;
- For any colored framed link $L \subseteq S^3$, $RT_r(S^3, L, col) = RT_r(S^3) \langle L, col \rangle$.

While it is technically possible to compute the Reshetikhin-Turaev invariants for any manifold directly from the definition, it is almost always unwieldy. There is an alternative point of view which allows for much cleaner computation: shadows. The shadow reformulation of the Reshetikhin-Turaev invariants can be found in [48, 49]; we are not going into details, as we only need the calculation of the Reshetikhin-Turaev invariants for the case of the Fundamental Shadow Links.

Lemma 3.13. *[[13, Proposition 4.1] following [14]] If $L = L_1 \sqcup \dots \sqcup L_k \subseteq M_c$ is a fundamental shadow link and $col \in I_r^k$ is a coloring of its components, then*

$$RT_r(M_c, L, col) = \left(2\sqrt{\frac{\sin\left(\frac{2\pi}{r}\right)}{r}} \right)^{-c} \prod_{i=1}^c \begin{vmatrix} col(i_1) & col(i_2) & col(i_3) \\ col(i_4) & col(i_5) & col(i_6) \end{vmatrix} \quad (3.5)$$

where i_j is the component of the link L passing through the j -th strand of block i .

3.4 The Turaev-Viro invariants

Let M be an orientable compact 3-manifold with a partially ideal triangulation τ . By this we mean that

- some vertices of some tetrahedra are truncated;
- the intersection of any tetrahedron T with ∂M is exactly the faces corresponding to the truncated vertices of T ;
- the faces corresponding to truncated vertices give a triangulation for ∂M .

Denote with $A_r(\tau)$ the set of r -admissible colorings of τ , with V the set of interior vertices of τ (exactly those that are not truncated) and with E the set of interior edges (by which we mean edges that are not contained in the boundary). If $col \in A_r(\tau)$ assigns to $T \in \tau$ the colors $n_1, n_2, n_3, n_4, n_5, n_6$ as in Figure 3.5, then we denote with $|T|_{col}$ the $6j$ -symbol

$$\begin{vmatrix} n_4 & n_5 & n_6 \\ n_1 & n_2 & n_3 \end{vmatrix}.$$

Similarly, if $e \in E$ we define

$$|e|_{col} = (-1)^{col(e)} \frac{\{col(e) + 1\}}{q - q^{-1}}.$$

Define the Turaev-Viro invariant of M at level r in the root q as

$$TV_r(M, \tau, q) := \left(\frac{2 \sin\left(\frac{2\pi}{r}\right)}{\sqrt{r}} \right)^{2|V|} \sum_{col \in A_r(\tau)} \prod_{e \in E} |e|_{col} \prod_{T \in \tau} |T|_{col}.$$

If τ and τ' are two partially ideal triangulations of M , then $TV_r(M, \tau, q) = TV_r(M, \tau', q)$ [50]. Hence we have a topological invariant of M , denoted by $TV_r(M, q)$, depending on r and q .

Proposition 3.14. [7, Proposition 5.3] *For any link $L = L_1 \sqcup \cdots \sqcup L_k$ in a closed oriented 3-manifold M ,*

$$TV_r(M \setminus U(L)) = \sum_{col \in I_r^k} |RT_r(M, L, col)|^2 \quad (3.6)$$

where $U(L)$ is an open regular neighborhood of L .

Proof. For a compact, oriented 3-manifold X with toroidal boundary,

$$TV_r(X) = RT_r(|DX|)$$

where DX is the double of X along its boundary ([8, Theorem 3.2] for the case $q = e^{\frac{\pi i}{r}}$, adapted to other roots of unity in [19, Theorem 3.1]). Now let $X = M \setminus U(L)$. Because of the axioms of the TQFT associated to the

Reshetikhin-Turaev invariants, we have $RT_r(DX) = \langle Z_r(X), Z_r(X) \rangle$, where $Z_r(X)$ is the vector in the TQFT hermitian vector space $V_r(\partial X)$.

The boundary of X is a union of connected toroidal components $T_1 \sqcup \cdots \sqcup T_k$, and $V_r(\partial X) = V_r(T_1) \otimes \cdots \otimes V_r(T_k)$. An orthogonal basis for the vector space $V_r(T_i)$ is $(e_j)_{j \in I_r}$ where e_j is the solid torus with boundary T_i and whose core is colored with color j . Therefore, an orthogonal basis for $V_r(\partial X)$ is $(e_{j_1} \otimes \cdots \otimes e_{j_k})_{j \in I_r^k}$. By the gluing axioms of the TQFT, $RT_r(M, L, col) = Z_r(M, L, col) = \langle Z_r(X), e_{col_1} \otimes \cdots \otimes e_{col_k} \rangle$. Since the basis is orthogonal, we have

$$Z_r(X) = \sum_{col \in I_r^k} RT_r(M, L, col) e_{col_1} \otimes \cdots \otimes e_{col_k}$$

hence

$$\langle Z_r(X), Z_r(X) \rangle = \sum_{col \in I_r^k} |RT_r(M, L, col)|^2$$

concluding the proposition. \square

3.5 The Yokota invariant

In this subsection we give an overview of the Yokota invariant, which generalizes the Kauffman bracket invariant of trivalent graphs to graphs with vertices of any valence; it was first introduced in [56].

Suppose $\Gamma \subseteq S^3$ is a framed graph with vertices of valence ≥ 3 ; as before $r > 2$ is odd and $q = e^{2\pi i/r}$.

For a vertex v of Γ , we can take a small ball B containing v , and replace $\Gamma \cap B$ with a trivalent planar tree in B having the same endpoints in $\partial B \cap \Gamma$ (see figure 3.9). We call this procedure a *desingularization* of Γ at v . Notice that if v has valence greater than 3, then this procedure is not unique; however, any desingularization is related to any other via a sequence of Whitehead moves (see figure 3.10).

We say that the trivalent graph Γ' is a desingularization of Γ if it is obtained from Γ by desingularization of each vertex of valence > 3 .

Definition 3.15. Let (Γ, col) be a framed graph in S^3 colored with elements of I_r . Let Γ' be a desingularization of Γ . Call e'_1, \dots, e'_k the edges of Γ' that were added by the desingularization. If $k > 0$, the *Yokota invariant* of (Γ, col) is

$$Y_r(\Gamma, col) := \sum_{col' \in I_r^k} \left(\prod_{i=1}^k \Delta_{col'(e'_i)} \right) |\langle \Gamma', col \cup col' \rangle|^2$$

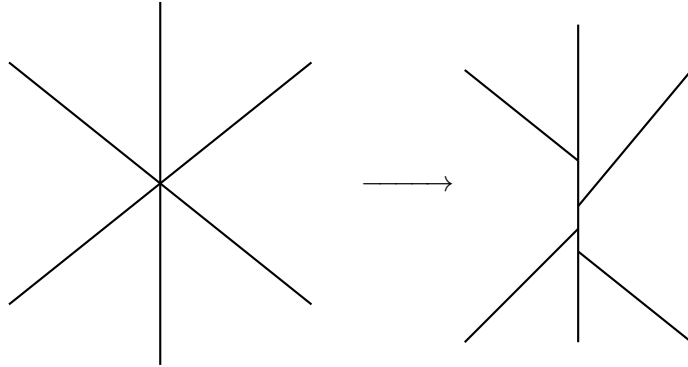


Figure 3.9: Desingularization of a vertex of valence 6

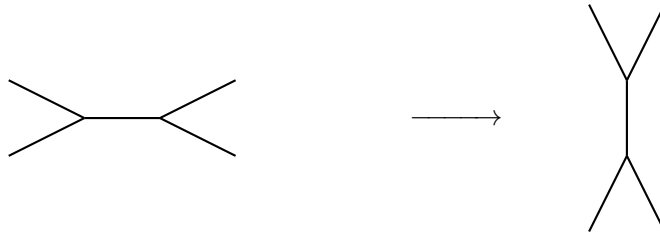


Figure 3.10: A Whitehead move

with col' coloring the edges e'_1, \dots, e'_k . If instead $k = 0$ (i.e. $\Gamma = \Gamma'$ i.e. Γ is trivalent) then $Y_r(\Gamma, col) = |\langle \Gamma, col \rangle|^2$.

As we did with the Kauffman bracket, we extend linearly the Yokota invariant to linear combinations of colors. Notice that in this case, even if Γ is trivalent, we may get $Y_r(\Gamma, col) \neq |\langle \Gamma, col \rangle|^2$.

Remark 3.16. We stress the fact that we are using the unitary normalization for the Kauffman bracket. If we instead used the Kauffman normalization $\langle \cdot \rangle_K$ of [26], the definition of the Yokota invariant of Γ, col would be

$$Y_r(\Gamma, col) := \sum_{col' \in I_r^k} \frac{\prod_{i=1}^k \Delta_{col'(e'_i)}}{\prod_{v \text{ vertex of } \Gamma} \Theta(v)} |\langle \Gamma', col \cup col' \rangle_K|^2$$

Proposition 3.17. [56] *The Yokota invariant does not depend on the choice of desingularization.*

We can easily extend the Yokota invariant to graphs with 1-valent and 2-valent vertices as well via the following definition and formulas.

The Yokota invariant of a graph with a single edge and two distinct endpoints colored with i is $\delta_{i,0}$;

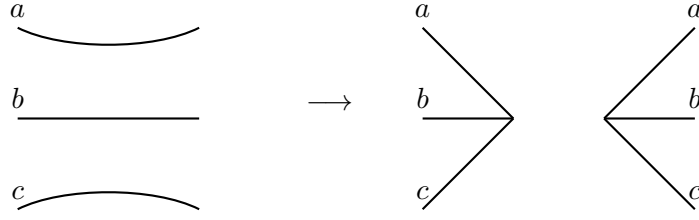


Figure 3.11: A vertex sum of two trivalent vertices

$$Y \left(\begin{array}{c} i \quad j \\ \bullet \\ \hline \end{array} \right) = \frac{\delta_{i,j}}{\Delta_i} Y \left(\begin{array}{c} i \\ \hline \end{array} \right);$$

$$Y \left(\begin{array}{c} \triangleright \\ \bullet \\ \hline \end{array} \right) = \delta_{i,0} Y \left(\begin{array}{c} \triangleright \\ \hline \end{array} \right).$$

Now we give four important properties of the Yokota invariant.

Proposition 3.18. *The following hold:*

1. *The Yokota invariant does not depend on the framing of Γ .*
2. *If an edge e of Γ is colored with the Kirby color Ω , and Γ' is obtained from Γ via a Whitehead move on the edge e (keeping every color the same) then $Y_r(\Gamma, \text{col}) = Y_r(\Gamma', \text{col})$.*
3. *If Γ is a vertex sum of Γ_1, Γ_2 along trivalent vertices $v_1 \in \Gamma_1$ and $v_2 \in \Gamma_2$ (see Figure 3.11), then $Y_r(\Gamma, \text{col}) = Y_r(\Gamma_1, \text{col}_1)Y_r(\Gamma_2, \text{col}_2)$ where $\text{col}_1, \text{col}_2$ are the restrictions of col to Γ_1, Γ_2 respectively.*
4. *If a link $L \subseteq S^3$ is colored with $\text{col} \in I_r^{|L|}$, then $Y_r(L, \text{col}) = |J_{\text{col}}^L(q)|^2$ where J_{col}^L is the colored Jones polynomial of L colored with col .*

Proof. Part 1 holds because $\langle \Gamma \rangle$ depends on the framing of Γ only up to a factor of q^a , thus when taking squared norms this becomes 1. Part 2 is essentially the well definition of the Yokota invariant: both sides of the equality are equal to the Yokota invariant of the graph obtained by collapsing e to a point.

Part 3 follows from the analogous property for the Kauffman bracket; this is obtained via two applications of the fusion rule and one application of the bridge rule 5 (see Figure 3.12). Part 4 is just the fact that in the case of L , seen as a trivalent graph with no vertices, $Y_r(L, \text{col}) = |\langle L, \text{col} \rangle|^2 = J_{\text{col}}^L(q)$. \square

It is very important that the vertex sum in Proposition 3.18.3 is done between trivalent vertices; the assertion is false in general. However, a particular case still holds.

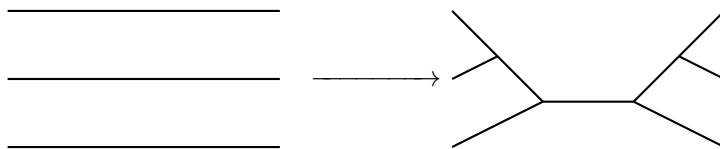


Figure 3.12: Applying the fusion rule to three edges arising from a vertex sum.

Definition 3.19. Let Γ, col be a colored planar graph and v one of its vertices. We define the *double* of Γ at the vertex v to be the graph Γ^2, col^2 obtained from a vertex sum of two copies, both colored with col , of Γ at the vertex v .

Lemma 3.20.

$$Y_r(\Gamma^2, col^2) = Y_r(\Gamma, col)^2$$

Proof. We give the proof in the case of v having valence 4; the general case is identical, except that the notation is heavier.

By linearity, we can assume that Γ^2 only has trivalent vertices.

Apply the fusion rule to the edges arising from the vertex sum until you obtain a bridge which is eliminated.

We have

$$\begin{aligned} Y_r \left(\text{triple lines} \right) &= \left(\sum_{i,j,k \in I_r} \Delta_i \Delta_j \Delta_k \left\langle \begin{array}{c} i \\ \diagdown \quad \diagup \\ j \end{array} \right\rangle \right)^2 = \\ &= \left(\sum_{i \in I_r} \Delta_i \left\langle \begin{array}{c} i \\ \diagdown \quad \diagup \\ i \end{array} \right\rangle \right)^2 = \sum_{i,j \in I_r} \Delta_i \Delta_j \left\langle \begin{array}{c} i \\ \diagdown \quad \diagup \\ i \end{array} \right\rangle \left\langle \begin{array}{c} i \\ \diagdown \quad \diagup \\ i \end{array} \right\rangle \left\langle \begin{array}{c} j \\ \diagdown \quad \diagup \\ j \end{array} \right\rangle \left\langle \begin{array}{c} j \\ \diagdown \quad \diagup \\ j \end{array} \right\rangle \\ &= \sum_{i,j \in I_r} \Delta_i \Delta_j \left\langle \begin{array}{c} i \\ \diagdown \quad \diagup \\ i \end{array} \right\rangle \left\langle \begin{array}{c} j \\ \diagdown \quad \diagup \\ j \end{array} \right\rangle^2 = Y_r(\Gamma, col)^2 \end{aligned}$$

□

Remark 3.21. The Kauffman bracket (hence, the Yokota invariant) can also be defined in the much larger setting of framed trivalent graphs in closed oriented 3-manifolds; since we will not need such a generality that carries some more technical details, we will restrict ourselves to the S^3 case.

Chapter 4

The upper bound of the $6j$ -symbol

In this chapter we prove Theorem 1.8 and use it to prove the Turaev-Viro volume conjecture for the complements of FSLs.

The material presented here was obtained through a joint work with R. Detcherry, E. Kalfagianni and T. Yang in [7].

4.1 Proof of the upper bound

We now give the proof of Theorem 1.8; the proofs of the technical lemmas used can be found in Section 4.2.

Denote with $\Lambda(x)$ the Lobachevski function, defined as

$$\Lambda(x) := - \int_0^x \log|2 \sin(t)| dt.$$

It is π -periodic, odd, and real analytic outside of $\{k\pi, k \in \mathbb{Z}\}$.

The tool used to estimate the quantum $6j$ -symbol is the following lemma, first appeared in [22, Proposition 8.2] for $q = e^{\frac{i\pi}{r}}$, and then in the other roots of unity in [18, Proposition 4.1]:

Lemma 4.1. *For any integer $0 < n < r$*

$$\log \left| \{n\}!_{|q=\exp(2\pi i/r)} \right| = -\frac{r}{2\pi} \Lambda \left(\frac{2n\pi}{r} \right) + O(\log(r))$$

where the term $O(\log(r))$ is such that there exist constants C, r_0 independent of n and r such that $O(\log(r)) \leq C \log(r)$ whenever $r > r_0$.

Remark 4.2. If $0 < n < r - 1$, we can equally well use the estimate

$$\log \left| \{n+1\}_{|q=\exp(2\pi i/r)} \right| = -\frac{r}{2\pi} \Lambda \left(\frac{2n\pi}{r} \right) + O(\log(r)),$$

since by applying a Taylor expansion to Λ we find

$$\begin{aligned} \Lambda \left(\frac{2n\pi}{r} + \frac{2\pi}{r} \right) - \Lambda \left(\frac{2n\pi}{r} \right) &= \frac{2\pi}{r} \Lambda' \left(\frac{2n\pi}{r} \right) + o \left(\frac{1}{r} \right) = \\ &= -\frac{2\pi}{r} \log \left| 2 \sin \frac{2n\pi}{r} \right| + o \left(\frac{1}{r} \right) = O \left(\frac{\log(r)}{r} \right) \end{aligned}$$

since $|\sin(\frac{2\pi n}{r})| \geq \frac{\pi}{r}$ (because $2n \neq r$), and thus $-\frac{2\pi}{r} \log(|2 \sin \frac{2n\pi}{r}|) \leq \frac{\log(r)}{r}$, since $\log(ax) \leq a \log(x)$. Notice again that the constants involved in the $O(\frac{\log(r)}{r})$ are independent of n and r .

Theorem 1.8. For any r , and any admissible 6-tuple $(n_1, n_2, n_3, n_4, n_5, n_6)$, we have

$$\frac{2\pi}{r} \log \left| \begin{vmatrix} n_1 & n_2 & n_3 \\ n_4 & n_5 & n_6 \end{vmatrix}_{q=e^{\frac{2\pi i}{r}}} \right| \leq v_8 + O \left(\frac{\log(r)}{r} \right)$$

where $v_8 \cong 3.66$ is the volume of the regular ideal hyperbolic octahedron.

Proof. Applying Lemma 4.1 (together with the subsequent remark) to the formula for the quantum $6j$ -symbol (3.3) we obtain the estimate

$$\frac{2\pi}{r} \log \left| \begin{vmatrix} n_1 & n_2 & n_3 \\ n_4 & n_5 & n_6 \end{vmatrix}_{q=e^{\frac{2\pi i}{r}}} \right| \leq V(\theta_1, \theta_2, \theta_3, \theta_4, \theta_5, \theta_6) + O \left(\frac{\log(r)}{r} \right) \quad (4.1)$$

where

$$\begin{aligned} V(\theta_1, \theta_2, \theta_3, \theta_4, \theta_5, \theta_6) &:= \max_{\max U_i \leq Z \leq \min V_j, 2\pi} F(Z, \theta_1, \theta_2, \theta_3, \theta_4, \theta_5, \theta_6) + \\ &\nu(\theta_1, \theta_2, \theta_3) + \nu(\theta_1, \theta_5, \theta_6) + \nu(\theta_2, \theta_4, \theta_6) + \nu(\theta_3, \theta_4, \theta_5) \end{aligned} \quad (4.2)$$

and:

- $\theta_i = \frac{2\pi n_i}{r}$ and $Z = \frac{2\pi z}{r}$;
- $U_i = \frac{2\pi T_i}{r}$ and similarly $V_i = \frac{2\pi Q_i}{r}$;
- $\nu(\alpha, \beta, \gamma) = \frac{1}{2}(\Lambda(\frac{\alpha+\beta+\gamma}{2}) - \Lambda(\frac{\alpha+\beta-\gamma}{2}) - \Lambda(\frac{\alpha-\beta+\gamma}{2}) - \Lambda(\frac{-\alpha+\beta+\gamma}{2}))$;

$$\bullet F(Z, \theta_1, \theta_2, \theta_3, \theta_4, \theta_5, \theta_6) = \sum_{i=1}^4 \Lambda(Z - U_i) + \sum_{j=1}^3 \Lambda(V_j - Z) - \Lambda(Z)$$

and all variables involved are between 0 and 2π , thanks to the admissibility conditions. Notice that the θ_i s satisfy similar triangular inequalities and admissibility conditions as the n_i s. In particular $\theta_1 + \theta_2 + \theta_3 \leq 4\pi$, $\theta_1 + \theta_5 + \theta_6 \leq 4\pi$, $\theta_2 + \theta_4 + \theta_6 \leq 4\pi$ and $\theta_3 + \theta_4 + \theta_5 \leq 4\pi$.

We now want to maximize V subject to the admissibility conditions of the θ_i s. This is broken down in the following two technical lemmas, whose proofs are postponed to Section 4.2.

Lemma 4.3. *If $0 \leq \alpha, \beta, \gamma \leq \pi$ then $\nu(\alpha, \beta, \gamma) \leq 0$.*

Corollary 4.4. *If $0 \leq \gamma \leq \pi$ and $\pi \leq \alpha, \beta \leq 2\pi$, then $\nu(\alpha, \beta, \gamma) \leq 0$.*

Proof. It is immediate to check that $\nu(\pi - \alpha, \pi - \beta, \gamma) = \nu(\alpha, \beta, \gamma)$. \square

Lemma 4.5. *If $0 \leq \theta_1, \dots, \theta_6 \leq 2\pi$ and*

$$\max(U_1, U_2, U_3, U_4) \leq Z \leq \min(V_1, V_2, V_3, 2\pi),$$

then

$$F(Z, \theta_1, \theta_2, \theta_3, \theta_4, \theta_5, \theta_6) + 2\nu(\theta_1, \theta_2, \theta_3) \leq 8\Lambda\left(\frac{\pi}{4}\right) = v_8$$

We obtain the following corollary.

Corollary 4.6. *We have*

$$\max_{\max U_i \leq Z \leq \min V_j} F(Z, \theta_1, \theta_2, \theta_3, \theta_4, \theta_5, \theta_6) + \nu(\theta_1, \theta_2, \theta_3) + \nu(\theta_1, \theta_5, \theta_6) \leq v_8.$$

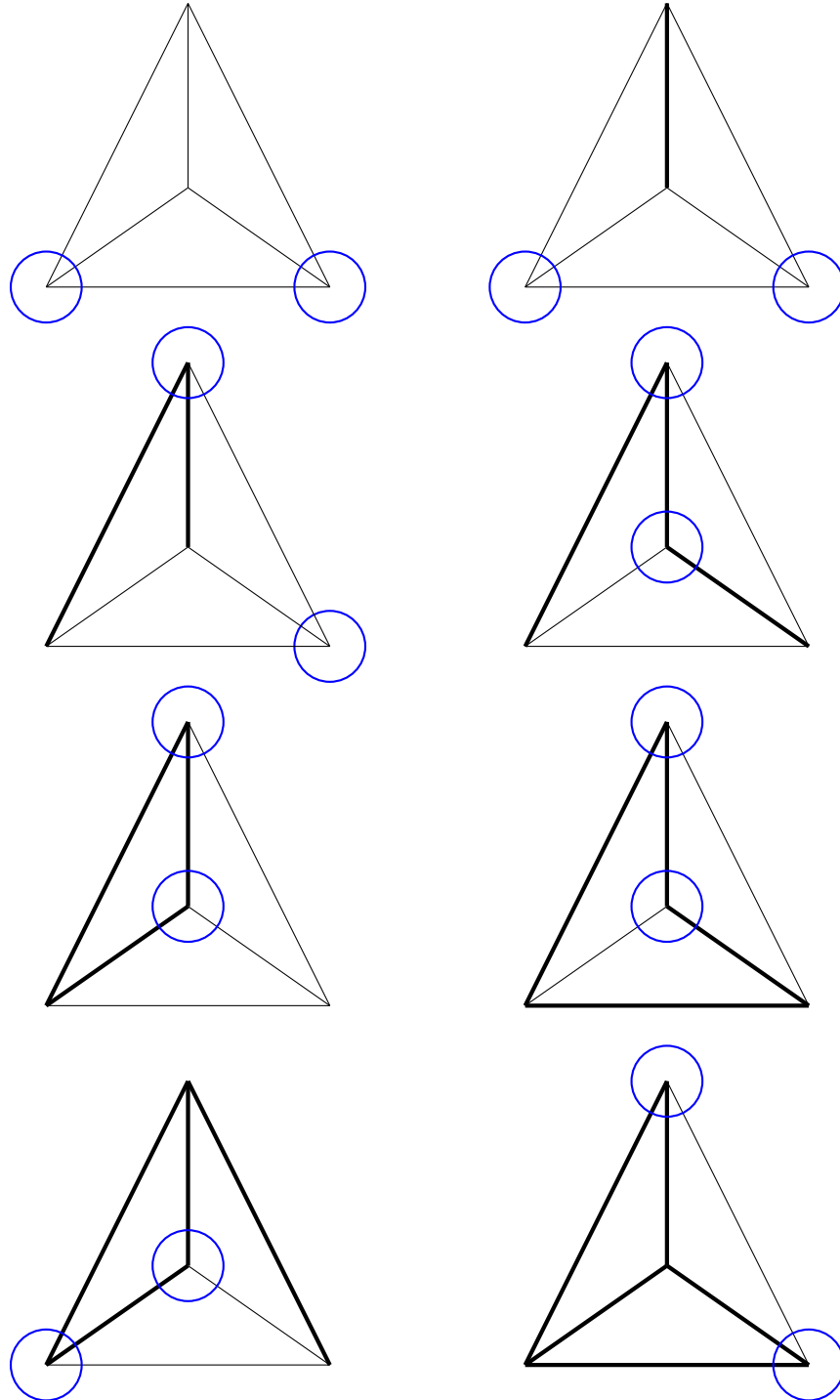
Proof. Follows immediately by using Lemma 4.5 twice and taking averages. \square

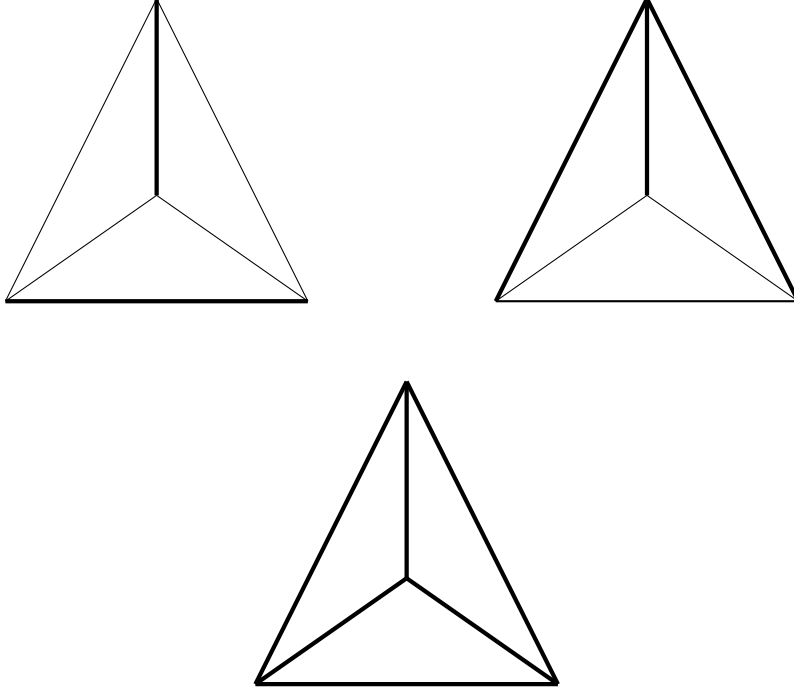
Consider now an admissible 6-tuple $(\theta_1, \theta_2, \theta_3, \theta_4, \theta_5, \theta_6)$. If $\theta_i \leq \pi$ for all i , then Lemmas 4.3, 4.5 and Corollary 4.6 imply that

$$V(\theta_1, \theta_2, \theta_3, \theta_4, \theta_5, \theta_6) \leq \max_{\max U_i \leq Z \leq \min V_j} F(Z, \theta_1, \theta_2, \theta_3, \theta_4, \theta_5, \theta_6) + \nu(\theta_1, \theta_2, \theta_3) + \nu(\theta_1, \theta_5, \theta_6) \leq v_8$$

Similarly, as soon as Lemma 4.3 or Corollary 4.4 imply that $\nu \leq 0$ for two vertices of the tetrahedron, we obtain that $V \leq v_8$. Figures 4.1 and 4.2 show all the possibilities (up to symmetry) with regards to the relationship between the θ_i s and π : a thick line indicates that the corresponding $\theta_i \geq \pi$, and a thin line that $\theta_i \leq \pi$. In Figure 4.1, two circles mark the vertices where Lemma 4.3 or 4.4 implies $\nu \leq 0$.

Thus, we only need to examine the cases of figure 4.2; notice that in each of those cases, either 1 or 3 θ s are greater than π .

Figure 4.1: Two vertices satisfy $\nu \leq 0$

Figure 4.2: All vertices have $\nu \geq 0$.

Lemma 4.7. *Suppose $(\theta_1, \dots, \theta_6)$ are as shown in figure 4.2. Then the 6-tuple $(\tilde{\theta}_1, \dots, \tilde{\theta}_6)$ defined as $\tilde{\theta}_i = \theta_i$ if $\theta_i \leq \pi$ and $\tilde{\theta}_i = 2\pi - \theta_i$ if $\theta_i \geq \pi$ is the 6-tuple of external dihedral angles of a unique hyperbolic truncated tetrahedron.*

Proof. By [2, Theorem 1], $(\tilde{\theta}_1, \dots, \tilde{\theta}_6)$ are the external dihedral angles of a hyperbolic truncated tetrahedron if and only if $\tilde{\theta}_1 + \tilde{\theta}_2 + \tilde{\theta}_3 \geq 2\pi$, $\tilde{\theta}_1 + \tilde{\theta}_5 + \tilde{\theta}_6 \geq 2\pi$, $\tilde{\theta}_2 + \tilde{\theta}_4 + \tilde{\theta}_6 \geq 2\pi$, $\tilde{\theta}_3 + \tilde{\theta}_4 + \tilde{\theta}_5 \geq 2\pi$.

If $\theta_1 \geq \pi$ while $\theta_2, \theta_3 \leq \pi$, then $\tilde{\theta}_1 + \tilde{\theta}_2 + \tilde{\theta}_3 = 2\pi - \theta_1 + \theta_2 + \theta_3 \geq 2\pi$ since $-\theta_1 + \theta_2 + \theta_3 \geq 0$. If instead $\theta_1, \theta_2, \theta_3 \geq \pi$, then $\tilde{\theta}_1 + \tilde{\theta}_2 + \tilde{\theta}_3 = 6\pi - \theta_1 - \theta_2 - \theta_3 \geq 2\pi$ since $\theta_1 + \theta_2 + \theta_3 \leq 4\pi$. The inequalities around the other vertices are dealt by symmetry. \square

Lemma 4.8. *If $(\theta_1, \dots, \theta_6)$ are as in figure 4.2, then*

$$V(\theta_1, \dots, \theta_6) = V(\tilde{\theta}_1, \dots, \tilde{\theta}_6).$$

The proof of this lemma is also postponed to Section 5.3.

Combining Lemmas 4.3, 4.4, 4.5 and 4.8, we finally obtain

$$\frac{2\pi}{r} \log \left| \left\{ \begin{matrix} n_1 & n_2 & n_3 \\ n_4 & n_5 & n_6 \end{matrix} \right\} \right|_{q=\exp(2\pi i/r)} \leq v_8 + O\left(\frac{\log(r)}{r}\right).$$

□

Remark 4.9. In [18] a less sharp upper bound on the growth rate of the quantum $6j$ -symbol was given, to prove that if a compact 3-manifold M admits a triangulation with t tetrahedra, then

$$\limsup_{r \rightarrow \infty} \frac{2\pi}{r} \log |TV_r(M)| \leq 2.08v_8t.$$

The improvement of the upper bound allows us to state a better estimate.

Corollary 4.10. *If M is a compact manifold that admits a triangulation with t tetrahedra, then*

$$\limsup_{r \rightarrow \infty} \frac{2\pi}{r} \log |TV_r(M)| \leq v_8t.$$

Remark 4.11. There is a concept of *complexity* of a manifold that is related to quantum invariants, the so called *shadow complexity*. For an overview of shadows and shadow complexity, see for example [49, Part 2] or [17]. Shadow complexity easily gives a bound on the growth of the Turaev-Viro invariants:

Corollary 4.12. *If M has shadow complexity c , then*

$$\limsup_{r \rightarrow \infty} \frac{2\pi}{r} \log |TV_r(M)| \leq 2cv_8.$$

Furthermore we have equalities for fundamental shadow links.

Proof. The inequality is an immediate consequence of Theorem 1.8 and the shadow formula for the Reshetikhin-Turaev invariants [49, Theorem X.3.3]. By [17], for fundamental shadow link in $\#^{c+1}(S^2 \times S^1)$ the shadow complexity is c . Hence sharpness follows from Theorem 1.8. □

Moreover, shadow complexity also gives an upper bound on the simplicial volume:

Theorem ([17], Theorem 3.37). *Let M be a manifold with (possibly empty) toroidal boundary, simplicial volume $\text{Vol}(M)$ and shadow complexity c ; then, $\text{Vol}(M) \leq 2cv_8$. Furthermore this bound is sharp for complements of fundamental shadow links.*

Remark 4.13. The bound in Corollary 4.10 is likely not sharp. However in [18] it is used to show that for 3-manifolds M with toroidal or empty boundary the exponential growth of $TV_r(M)$ is bounded above linearly by the Gromov norm of M . On the other hand, the Gromov norm upper bound of the shadow complexity obtained in [17] is quadratic.

Before we move on to prove the volume conjecture for fundamental shadow links, we need to show that the bound of Theorem 1.8 is sharp.

Lemma 4.14. *If the sign is chosen such that $\frac{r\pm 1}{2}$ is even, then*

$$\lim_{r \rightarrow \infty} \frac{2\pi}{r} \log \left| \left| \frac{\frac{r\pm 1}{2}}{\frac{r\pm 1}{2}} \quad \frac{\frac{r\pm 1}{2}}{\frac{r\pm 1}{2}} \quad \frac{\frac{r\pm 1}{2}}{\frac{r\pm 1}{2}} \right|_{q=e^{\frac{2\pi i}{r}}} \right| = v_8.$$

Proof. Because of the color choice, then $\max T_i > \frac{r}{2}$, hence in the sum defining the $6j$ -symbol $\frac{r}{2} < z < r$, and $\{z\} = 2i \sin(2\pi iz/r)$ is an imaginary number with negative sign. Moreover, $0 \leq z - T_i < \frac{r}{2}$ and $0 \leq Q_j - z < \frac{r}{2}$ for all i, j . Therefore,

$$\frac{(-1)^z \{z+1\}!}{\prod_{i=1}^4 \{z - T_i\}! \prod_{j=1}^3 \{Q_j - z\}!}$$

is an imaginary number, and passing from z to $z+1$ in the sum does not change its sign, since all terms in the denominator do not change sign, and there is a change of sign due to $\{z+2\}$ that gets corrected by $(-1)^{z+1}$. Since there is no change in sign among the summands, the estimate given by (4.1) is actually an equality. We have $\Delta(\pi, \pi, \pi) = 0$, and

$$F\left(\frac{7\pi}{4}, \pi, \pi, \pi, \pi, \pi, \pi\right) = 8\Lambda\left(\frac{\pi}{4}\right) = v_8.$$

Thus, using Theorem 1.8,

$$\frac{2\pi}{r} \log \left| \left| \frac{\frac{r\pm 1}{2}}{\frac{r\pm 1}{2}} \quad \frac{\frac{r\pm 1}{2}}{\frac{r\pm 1}{2}} \quad \frac{\frac{r\pm 1}{2}}{\frac{r\pm 1}{2}} \right|_{q=e^{\frac{2\pi i}{r}}} \right| = v_8 + O\left(\frac{\log r}{r}\right)$$

which concludes the proof. \square

4.2 Proofs of the technical lemmas

We now turn to the proofs of Lemmas 4.3 and 4.5.

Lemma 4.3. If $0 \leq \alpha, \beta, \gamma \leq \pi$ then $\nu(\alpha, \beta, \gamma) \leq 0$.

Proof. Put $x = \frac{\alpha+\beta-\gamma}{2}$, $y = \frac{\alpha-\beta+\gamma}{2}$, $z = \frac{-\alpha+\beta+\gamma}{2}$. Then we need to maximize

$$\nu(\alpha, \beta, \gamma) = \vartheta(x, y, z) = \frac{1}{2}(\Lambda(x+y+z) - \Lambda(x) - \Lambda(y) - \Lambda(z))$$

with the constraints $0 \leq x + y \leq \pi$, $0 \leq x + z \leq \pi$ and $0 \leq y + z \leq \pi$.

To do this, we check first its stationary points in the interior of the domain, then we explore the boundary, and finally the points where ϑ is not smooth.

$$\frac{\partial \vartheta(x, y, z)}{\partial x} = \frac{1}{2}(\log(2|\sin(x + y + z)|) - \log(2|\sin(x)|)); \quad (4.3)$$

$$\frac{\partial \vartheta(x, y, z)}{\partial y} = \frac{1}{2}(\log(2|\sin(x + y + z)|) - \log(2|\sin(y)|)); \quad (4.4)$$

$$\frac{\partial \vartheta(x, y, z)}{\partial z} = \frac{1}{2}(\log(2|\sin(x + y + z)|) - \log(2|\sin(z)|)) \quad (4.5)$$

So by putting them all equal to 0, we first see that $\sin(x) = \pm \sin(y) = \pm \sin(z)$, so either $x = y = z$ modulo π or one of $x + y$, $y + z$ or $x + z$ is equal $k\pi$ for some $k \in \mathbb{Z}$. Suppose $x + y = k\pi$. Then

$$\vartheta(x, y, z) = \Lambda(k\pi + z) - \Lambda(k\pi - y) - \Lambda(y) - \Lambda(z) = 0;$$

because Λ is odd and π -periodic; $y + z = k\pi$ and $x + z = k\pi$ are the same by symmetry.

If instead $x = y = z$ modulo π , substituting $x = y = z$ in (4.3), we get $\sin(3x) = \pm \sin(x)$. This means that $x = y = z = \frac{k\pi}{4}$ modulo π . In the interior of the domain this implies $x = y = z = \frac{\pi}{4}$; all other possibilities lie outside the domain or on its boundary. In this point $\vartheta = -2\Lambda\left(\frac{\pi}{4}\right) \cong -1.83 < 0$.

The boundary cases $x + y = k\pi$ and permutations were already checked, finding $\vartheta = 0$.

Finally we check the points where ϑ is not smooth. This happens when one of the following holds:

- $x = k\pi$, or $y = k\pi$, or $z = k\pi$; or
- $x + y + z = k\pi$.

Remark 4.15. If P is a point and γ is a direction such that the derivative of ϑ in that direction is $+\infty$, then P cannot be a local maximum of ϑ .

If $x = k\pi$, then $\frac{\partial \vartheta(x, y, z)}{\partial x} = +\infty$ unless $x + y + z = h\pi$, and (x, y, z) cannot be a maximum. If instead $x = k\pi$ and $x + y + z = h\pi$, we have $y + z = (h - k)\pi$ and we are in a case we already checked. $y = k\pi$ and $z = k\pi$ are symmetric.

If instead $x + y + z = k\pi$, we find once again an infinite derivative unless $x = h\pi$, and we reason as before. So in conclusion ϑ is equal to 0 on the boundary of the set $\{0 \leq x + y \leq \pi, 0 \leq x + z \leq \pi, 0 \leq y + z \leq \pi\}$, cannot have a maximum in a non-smooth point and has a unique stationary point in the interior, where it is negative. This concludes the proof. \square

Lemma 4.16. *If $0 \leq a, b$ and $a + b \leq 2\pi$, then*

$$-v_3 \leq \Lambda(a + b) - \Lambda(a) - \Lambda(b) \leq v_3$$

where $v_3 = \Lambda\left(\frac{\pi}{3}\right) \cong 1.01$ is the volume of the regular ideal tetrahedron.

Proof. First notice that if $a + b = k\pi$, then because Λ is odd and π -periodic, we have $\Gamma(a, b) = \Lambda(a + b) - \Lambda(a) - \Lambda(b) = 0$. Similarly if $a = 0$ or $b = 0$ then $\Gamma(a, b) = 0$. By calculating the derivatives of Γ and putting them to 0 we obtain, reasoning as before, $a = \pm b$ modulo π . If $a = -b$ modulo π then we have seen that $\Gamma = 0$. Then $a = b$ implies $\sin(2a) = \pm \sin(a)$, and either $a = k\pi$ (in which case $\Gamma = 0$) or $3a = k\pi$. If $a = \frac{\pi}{3}$ we obtain $\Gamma\left(\frac{\pi}{3}, \frac{\pi}{3}\right) = -3\Lambda\left(\frac{\pi}{3}\right) = -v_3$, while $a = \frac{2\pi}{3}$ implies $\Gamma\left(\frac{2\pi}{3}, \frac{2\pi}{3}\right) = 3\Lambda\left(\frac{\pi}{3}\right) = v_3$. \square

Lemma 4.5. *If $0 \leq \theta_1, \dots, \theta_6 \leq 2\pi$ and $\max(T_i) \leq Z \leq \min(Q_j, 2\pi)$, then*

$$F(Z, \theta_1, \theta_2, \theta_3, \theta_4, \theta_5, \theta_6) + 2\nu(\theta_1, \theta_2, \theta_3) \leq 8\Lambda\left(\frac{\pi}{4}\right) = v_8$$

Proof. Put $a_i = Z - U_i$, and $b_j = V_j - Z$. The inverse of this change of variable is:

- $\theta_1 = a_3 + a_4 + b_1 + b_2$;
- $\theta_2 = a_2 + a_4 + b_1 + b_3$;
- $\theta_3 = a_2 + a_3 + b_2 + b_3$;
- $\theta_4 = a_1 + a_2 + b_1 + b_2$;
- $\theta_5 = a_1 + a_3 + b_1 + b_3$;
- $\theta_6 = a_1 + a_4 + b_2 + b_3$ and
- $Z = a_1 + a_2 + a_3 + a_4 + b_1 + b_2 + b_3$.

In these new variables,

$$\begin{aligned} F(Z, \theta_1, \theta_2, \theta_3, \theta_4, \theta_5, \theta_6) &= \tilde{F}(a_1, a_2, a_3, a_4, b_1, b_2, b_3) = \\ &= -\Lambda\left(\sum_{i=1}^4 a_i + \sum_{j=1}^3 b_j\right) + \sum_{i=1}^4 \Lambda(a_i) + \sum_{j=1}^3 \Lambda(b_j) \end{aligned}$$

while

$$\begin{aligned} 2\nu(\theta_1, \theta_2, \theta_3, \theta_4, \theta_5, \theta_6) &= 2\tilde{\nu}(a_1, a_2, a_3, a_4, b_1, b_2, b_3) = \\ &= \left(\Lambda\left(\sum_{i=1}^3 (a_i + b_i)\right) - \sum_{i=1}^3 \Lambda(a_i + b_i)\right). \end{aligned}$$

Notice that $L := \tilde{F} + 2\tilde{\nu}$ is periodic of period π in each variable, hence we can assume $0 \leq a_i \leq \pi$ and $0 \leq b_i \leq \pi$. Moreover, because of the constraints on the θ s and on Z , we have that $0 \leq \sum a_i + \sum b_j \leq 2\pi$. Denote with Ω the region of \mathbb{R}^7 defined by all these inequalities.

Notice furthermore that $\tilde{\nu}$ is independent of a_4 , and that L is symmetric under the exchange of a_i with b_i for any $i \neq 4$, and under

$$(a_1, a_2, a_3, a_4, b_1, b_2, b_3) \rightarrow (a_{\sigma_1}, a_{\sigma_2}, a_{\sigma_3}, a_4, b_{\sigma_1}, b_{\sigma_2}, b_{\sigma_3})$$

where σ is any permutation of 3 elements.

We now proceed by first dealing with the points in the boundary of Ω , then with the points where the function L is not differentiable, and finally by finding the stationary points in the interior of Ω . Start by calculating the partial derivatives of L :

$$\frac{\partial L}{\partial a_4} = \log \left| \frac{\sin(a_1 + a_2 + a_3 + a_4 + b_1 + b_2 + b_3)}{\sin(a_4)} \right| \quad (4.6)$$

$$\frac{\partial L}{\partial a_1} = \log \left| \frac{\sin(a_1 + a_2 + a_3 + a_4 + b_1 + b_2 + b_3) \sin(a_1 + b_1)}{\sin(a_1) \sin(a_1 + a_2 + a_3 + b_1 + b_2 + b_3)} \right| \quad (4.7)$$

$$\frac{\partial L}{\partial a_2} = \log \left| \frac{\sin(a_1 + a_2 + a_3 + a_4 + b_1 + b_2 + b_3) \sin(a_2 + b_2)}{\sin(a_2) \sin(a_1 + a_2 + a_3 + b_1 + b_2 + b_3)} \right| \quad (4.8)$$

$$\frac{\partial L}{\partial a_3} = \log \left| \frac{\sin(a_1 + a_2 + a_3 + a_4 + b_1 + b_2 + b_3) \sin(a_3 + b_3)}{\sin(a_3) \sin(a_1 + a_2 + a_3 + b_1 + b_2 + b_3)} \right| \quad (4.9)$$

$$\frac{\partial L}{\partial b_1} = \log \left| \frac{\sin(a_1 + a_2 + a_3 + a_4 + b_1 + b_2 + b_3) \sin(a_1 + b_1)}{\sin(b_1) \sin(a_1 + a_2 + a_3 + b_1 + b_2 + b_3)} \right| \quad (4.10)$$

$$\frac{\partial L}{\partial b_2} = \log \left| \frac{\sin(a_1 + a_2 + a_3 + a_4 + b_1 + b_2 + b_3) \sin(a_2 + b_2)}{\sin(b_2) \sin(a_1 + a_2 + a_3 + b_1 + b_2 + b_3)} \right| \quad (4.11)$$

$$\frac{\partial L}{\partial b_3} = \log \left| \frac{\sin(a_1 + a_2 + a_3 + a_4 + b_1 + b_2 + b_3) \sin(a_3 + b_3)}{\sin(b_3) \sin(a_1 + a_2 + a_3 + b_1 + b_2 + b_3)} \right|. \quad (4.12)$$

Step 1: the boundary points

Suppose we have a maximum for L in a point P in the boundary of Ω . If $a_1 = \pi$, then by periodicity we would have a maximum with $a_1 = 0$, so we study this case instead. The derivative of L (4.7) with respect to a_1 is $+\infty$ if $a_1 + b_1 \neq k\pi$ and $a_1 + a_2 + a_3 + a_4 + b_1 + b_2 + b_3 \neq k\pi$, and we would not get a maximum. Hence, either $a_1 + a_2 + a_3 + a_4 + b_1 + b_2 + b_3 = k\pi$ or $b_1 = k\pi$. In the first case, we have that

$$L = \Lambda(a_2) + \Lambda(b_2) - \Lambda(a_2 + b_2) + \Lambda(a_3) + \Lambda(b_3) - \Lambda(a_3 + b_3)$$

and using Lemma 4.16 we find $L \leq 2v_3$. In the second case,

$$\begin{aligned} L = & \Lambda(a_2) + \Lambda(b_2) - \Lambda(a_2 + b_2) + \Lambda(a_3) + \Lambda(b_3) - \Lambda(a_3 + b_3) \\ & + \Lambda(b_2 + b_3 + a_2 + a_3) + \Lambda(a_4) - \Lambda(b_2 + b_3 + a_4 + a_2 + a_3) \end{aligned}$$

and again Lemma 4.16 implies $L \leq 3v_3$. If $a_4 = 0$, the same reasoning implies that P cannot be a maximum unless $a_1 + a_2 + a_3 + a_4 + b_1 + b_2 + b_3 = k\pi$, and in this case

$$L = \Lambda(a_1) + \Lambda(b_1) - \Lambda(a_1 + b_1) + \Lambda(a_2) + \Lambda(b_2) + \\ - \Lambda(a_2 + b_2) + \Lambda(a_3) + \Lambda(b_3) - \Lambda(a_3 + b_3) \leq 3v_3.$$

If $a_1 + a_2 + a_3 + a_4 + b_1 + b_2 + b_3 = k\pi$ once again we would have $\frac{\partial L}{\partial(-a_4)} = +\infty$ unless $a_4 = 0$ and we would be in the same case as before. The remaining cases are dealt by symmetry.

Step 2: the non-smooth points

First off, notice that L is differentiable at $P = (a_1, a_2, a_3, a_4, b_1, b_2, b_3)$ unless one (or more) of the following equalities (considered modulo π) holds:

1. $a_i = 0$ for some i ;
2. $b_j = 0$ for some j ;
3. $a_i + b_i = 0$ for some i ;
4. $a_1 + a_2 + a_3 + a_4 + b_1 + b_2 + b_3 = 0$;
5. $a_1 + a_2 + a_3 + b_1 + b_2 + b_3 = 0$.

These cases are dealt in a similar fashion as the boundary cases.

Suppose we have a maximum for L in a point P such that $a_1 + a_2 + a_3 + b_1 + b_2 + b_3 = k\pi$. Then, unless $a_1 + b_1 = k\pi$ or $a_1 + a_2 + a_3 + a_4 + b_1 + b_2 + b_3 = k\pi$ the derivative of L with respect to a_1 is $+\infty$, hence P could not be a maximum. Using Lemma 4.16 we obtain that in the first case,

$$L = \Lambda(a_2) + \Lambda(b_2) - \Lambda(a_2 + b_2) + \Lambda(a_3) + \Lambda(b_3) - \Lambda(a_3 + b_3) \leq 2v_3 \quad (4.13)$$

and in the second

$$L = \Lambda(a_2) + \Lambda(b_2) - \Lambda(a_2 + b_2) + \Lambda(a_3) + \Lambda(b_3) - \Lambda(a_3 + b_3) + \\ \Lambda(b_2 + b_3 + a_2 + a_3) + \Lambda(a_4) - \Lambda(b_2 + b_3 + a_4 + a_2 + a_3) \leq 3v_3.$$

The cases $a_i = k\pi$, $b_j = k\pi$, or $a_1 + a_2 + a_3 + a_4 + b_1 + b_2 + b_3 = k\pi$ were already addressed before. If $a_1 + b_1 = 0$, then $a_1 = b_1 = 0$ and it was already addressed. If $a_1 + b_1 = k\pi > 0$, then the derivative of L in the direction $-a_1$ is $+\infty$ unless $a_1 = 0$ or $a_1 + a_2 + a_3 + b_1 + b_2 + b_3 = k\pi$, which are both cases we have dealt with already. The remaining cases are done by the symmetries of L .

Step 3: the interior smooth points

Now we turn to the smooth points in the interior of Ω . By equating (4.7) and (4.10) to 0, we find $\sin(a_1) = \pm \sin(b_1)$. Similarly $\sin(a_i) = \pm \sin(b_i)$ for $i = 2, 3$ by equating (4.8) to (4.11) and (4.9) to (4.12) respectively. Because of the boundary and smoothness conditions, we have that in the interior of the domain this implies $a_i = b_i$ for $i = 1, 2, 3$. By putting equations (4.7) and (4.8) to 0, we find

$$\frac{\sin(2a_1)}{\sin a_1} = \pm \frac{\sin(2a_2)}{\sin a_2}. \quad (4.14)$$

Which implies that $\cos(a_1) = \pm \cos(a_2)$ and either $a_1 = a_2$ or $a_1 + a_2 = \pi$. However, if $a_1 + a_2 = \pi$, we would have $a_1 + a_2 + a_3 + a_4 + b_1 + b_2 + b_3 = 2a_1 + 2a_2 + 2a_3 + a_4 \geq 2\pi$; hence, this is not possible in the interior of Ω . Similarly $a_1 = a_3$.

Now by putting equation (4.6) equal to 0 we obtain

$$\sin(6a_1 + a_4) = \pm \sin(a_4) \quad (4.15)$$

This implies either $6a_1 = k\pi$ or $6a_1 + 2a_4 = k\pi$, but in the first case we would not be in a smooth point (case 5 of the previous step). By plugging everything we obtained in equation (4.7) we finally find

$$\frac{\sin(a_4) \sin(2a_1)}{\sin(a_1) \sin(2a_4)} = \pm 1 \quad (4.16)$$

Hence $a_4 = a_1$ or $a_4 = \pi - a_1$. Both cases imply that the stationary points of L must be of the form $(\frac{k\pi}{8}, \frac{k\pi}{8}, \frac{k\pi}{8}, \frac{k\pi}{8}, \frac{k\pi}{8}, \frac{k\pi}{8})$, for $k = 1, 2$. In the first case $L \cong 3.01 < v_8$, while in the second $L = 8\Lambda(\frac{\pi}{4}) = v_8$. \square

Lemma 4.8. *If $(\theta_1, \dots, \theta_6)$ are as in figure 4.2, then*

$$V(\theta_1, \dots, \theta_6) = V(\tilde{\theta}_1, \dots, \tilde{\theta}_6).$$

Proof. The value of $V(\tilde{\theta}_1, \dots, \tilde{\theta}_6)$ is equal, by the Murakami-Yano-Ushijima formula [36, Theorems 1 and 2], [51, Theorem 1.1], to the volume of the hyperbolic truncated tetrahedron with external dihedral angles $\tilde{\theta}_1, \dots, \tilde{\theta}_6$. Thus we need to show that this formula is symmetric under the change $(\theta_1, \dots, \theta_6) \leftrightarrow (\tilde{\theta}_1, \dots, \tilde{\theta}_6)$ in all three cases. We now pass to the internal dihedral angles (ξ_1, \dots, ξ_6) with $\xi_i = \pi - \tilde{\theta}_i$, as these are more natural for the MYU formula. In these variables, the formula reads

$$\mathcal{V}(a_1, \dots, a_6) := \frac{1}{2} \text{Im}(U(z_1, \vec{a}) - U(z_2, \vec{a})) \quad (4.17)$$

where:

- $a_i = e^{\sqrt{-1}\xi_i}$;

•

$$\begin{aligned}
U(z, \vec{a}) = & \frac{1}{2}(\text{Li}_2(z) + \text{Li}_2(z a_1 a_2 a_4 a_5) + \text{Li}_2(z a_1 a_3 a_4 a_6) + \\
& + \text{Li}_2(z a_2 a_3 a_5 a_6) - \text{Li}_2(-z a_1 a_2 a_3) - \text{Li}_2(-z a_1 a_5 a_6) + \\
& - \text{Li}_2(-z a_2 a_4 a_6) - \text{Li}_2(-z a_3 a_4 a_5)); \quad (4.18)
\end{aligned}$$

- z_1 and z_2 are the solutions of the equation $\alpha + \beta z + \gamma z^2 = 0$, labeled in such a way as to obtain a positive value for \mathcal{V} ;

•

$$\begin{aligned}
\alpha = & 1 + a_1 a_2 a_4 a_5 + a_1 a_3 a_4 a_6 + a_2 a_3 a_5 a_6 + a_1 a_2 a_3 + a_1 a_5 a_6 + \\
& a_2 a_4 a_6 + a_3 a_4 a_5; \quad (4.19)
\end{aligned}$$

•

$$\begin{aligned}
\beta = & -a_1 a_2 a_3 a_4 a_5 a_6 ((a_1 - a_1^{-1})(a_4 - a_4^{-1}) + \\
& + (a_2 - a_2^{-1})(a_5 - a_5^{-1}) + (a_3 + a_3^{-1})(a_6 - a_6^{-1})); \quad (4.20)
\end{aligned}$$

•

$$\begin{aligned}
\gamma = & a_1 a_2 a_3 a_4 a_5 a_6 (a_1 a_2 a_3 a_4 a_5 a_6 + a_1 a_4 + a_2 a_5 + a_3 a_6 + \\
& + a_1 a_2 a_6 + a_1 a_3 a_5 + a_2 a_3 a_4 + a_4 a_5 a_6). \quad (4.21)
\end{aligned}$$

Notice that in these variables, the symmetries we need to explore are

1. $(a_1, a_2, a_3, a_4, a_5, a_6) \leftrightarrow (a_1^{-1}, a_2, a_3, a_4^{-1}, a_5, a_6)$,
2. $(a_1, a_2, a_3, a_4, a_5, a_6) \leftrightarrow (a_1^{-1}, a_2^{-1}, a_3^{-1}, a_4, a_5, a_6)$ and
3. $(a_1, a_2, a_3, a_4, a_5, a_6) \leftrightarrow (a_1^{-1}, a_2^{-1}, a_3^{-1}, a_4^{-1}, a_5^{-1}, a_6^{-1})$.

Case 1: Call α , β and γ as in formulas (4.19)-(4.21), and α' , β' , γ' the same formulas with $a_1 \rightarrow a_1^{-1}$ and $a_4 \rightarrow a_4^{-1}$. Let z_1 and z_2 be solutions of $\alpha + \beta z + \gamma z^2 = 0$. Now it is immediate to check that $\alpha' = \frac{\gamma}{a_1^2 a_2 a_3 a_4^2 a_5 a_6}$, $\beta' = \frac{\beta}{a_1^2 a_4^2}$ and $\gamma' = \frac{a_2 a_3 a_5 a_6 \alpha}{a_1^2 a_4^2}$. Hence, we need to solve the equation

$$\frac{\gamma}{a_2 a_3 a_5 a_6} + \beta z + \alpha a_2 a_3 a_5 a_6 z^2 = 0;$$

call the solutions \hat{z}_1 and \hat{z}_2 . Then, \hat{z}_1^{-1} and \hat{z}_2^{-1} are solutions of

$$\frac{\gamma}{a_2 a_3 a_5 a_6} z^2 + \beta z + \alpha a_2 a_3 a_5 a_6 = 0;$$

therefore $\hat{z}_1^{-1} = z_1 a_2 a_3 a_5 a_6$ and $\hat{z}_2^{-1} = z_2 a_2 a_3 a_5 a_6$ (after perhaps a relabeling). Since it was shown in [36, Page 384] that z_1 and z_2 must be complex numbers with absolute value 1, we have that $\hat{z}_1 = \overline{z_1 a_2 a_3 a_5 a_6}$ and $\hat{z}_2 = \overline{z_2 a_2 a_3 a_5 a_6}$. Now we can compute

$$\begin{aligned} U(\hat{z}_1, a_1^{-1}, a_2, a_3, a_4^{-1}, a_5, a_6) &= \frac{1}{2} (\text{Li}_2(\overline{z_1 a_2 a_3 a_5 a_6}) + \text{Li}_2(\overline{z_1 a_1 a_3 a_4 a_6}) + \\ &+ \text{Li}_2(\overline{z_1 a_1 a_2 a_4 a_5}) + \text{Li}_2(\overline{z_1}) - \text{Li}_2(-\overline{z_1 a_1 a_5 a_6}) - \text{Li}_2(-\overline{z_1 a_1 a_2 a_3}) + \\ &- \text{Li}_2(-\overline{z_1 a_3 a_4 a_5}) - \text{Li}_2(-\overline{z_1 a_2 a_4 a_6})). \end{aligned}$$

Because $\text{Li}_2(\bar{a}) = \overline{\text{Li}_2(a)}$, we see that

$$U(\hat{z}_1, a_1^{-1}, a_2, a_3, a_4^{-1}, a_5, a_6) = \overline{U(z_1, a_1, a_2, a_3, a_4, a_5, a_6)};$$

the exact same computation shows that

$$U(\hat{z}_2, a_1^{-1}, a_2, a_3, a_4^{-1}, a_5, a_6) = \overline{U(z_2, a_1, a_2, a_3, a_4, a_5, a_6)}.$$

Because we have to switch the labels as to obtain a positive value of \mathcal{V} , we finally obtain $\mathcal{V}(a_1^{-1}, a_2, a_3, a_4^{-1}, a_5, a_6) = \mathcal{V}(a_1, a_2, a_3, a_4, a_5, a_6)$.

The other cases follow the same steps.

Case 2

In this case using the same notations, we find $\alpha' = \frac{\alpha}{a_1 a_2 a_3}$, $\beta' = -\frac{\beta}{a_1^2 a_2^2 a_3^2}$ and $\gamma = \frac{\gamma}{a_1^3 a_2^3 a_3^3}$. Therefore, \hat{z}_1 and \hat{z}_2 are solutions of

$$a_1 a_2 a_3 \alpha - \beta z + \frac{\gamma}{a_1 a_2 a_3} z^2 = 0;$$

this shows that $\hat{z}_1 = -z_1 a_1 a_2 a_3$ and $\hat{z}_2 = -z_2 a_1 a_2 a_3$, once again up to relabeling. We find

$$\begin{aligned} U(\hat{z}_1, a_1^{-1}, a_2^{-1}, a_3^{-1}, a_4, a_5, a_6) &= \frac{1}{2} (\text{Li}_2(-z_1 a_1 a_2 a_3) + \text{Li}_2(-z_1 a_3 a_4 a_5) + \\ &\text{Li}_2(-z_1 a_2 a_4 a_6) + \text{Li}_2(-z_1 a_1 a_5 a_6) - \text{Li}_2(z_1) - \text{Li}_2(z_1 a_2 a_3 a_5 a_6) + \\ &- \text{Li}_2(z_1 a_1 a_3 a_4 a_6) - \text{Li}_2(z_1 a_1 a_2 a_4 a_5)); \end{aligned}$$

therefore, $U(\hat{z}_1, a_1^{-1}, a_2^{-1}, a_3^{-1}, a_4, a_5, a_6) = -U(z_1, a_1, a_2, a_3, a_4, a_5, a_6)$, and $U(\hat{z}_2, a_1^{-1}, a_2^{-1}, a_3^{-1}, a_4, a_5, a_6) = -U(z_2, a_1, a_2, a_3, a_4, a_5, a_6)$ by the same calculation. Then we also get $\mathcal{V}(a_1^{-1}, a_2^{-1}, a_3^{-1}, a_4, a_5, a_6) = \mathcal{V}(a_1, a_2, a_3, a_4, a_5, a_6)$ via the same reasoning as before.

Case 3

In this case, $\alpha' = \frac{\gamma}{a_1^2 a_2^2 a_3^2 a_4^2 a_5^2 a_6^2}$, $\beta' = \frac{\beta}{a_1^2 a_2^2 a_3^2 a_4^2 a_5^2 a_6^2}$, $\gamma' = \frac{\alpha}{a_1^2 a_2^2 a_3^2 a_4^2 a_5^2 a_6^2}$. Hence, \hat{z}_1 and \hat{z}_2 are solutions of

$$\gamma + \beta z + \alpha z^2 = 0$$

which implies $\hat{z}_1 = \bar{z}_1$ and $\hat{z}_2 = \bar{z}_2$, since $|z_{1/2}| = 1$. From this we can easily compute

$$\begin{aligned} U(\hat{z}_1, a_1^{-1}, a_2^{-1}, a_3^{-1}, a_4^{-1}, a_5^{-1}, a_6^{-1}) &= \frac{1}{2}(\text{Li}_2(\bar{z}_1) + \text{Li}_2(\overline{\bar{z}_1 a_1 a_2 a_4 a_5})) + \\ &+ \text{Li}_2(\overline{\bar{z}_1 a_1 a_3 a_4 a_6}) + \text{Li}_2(\overline{\bar{z}_1 a_2 a_3 a_5 a_6}) - \text{Li}_2(-\bar{z}_1 a_1 a_2 a_3) - \text{Li}_2(-\bar{z}_1 a_1 a_5 a_6) + \\ &- \text{Li}_2(-\bar{z}_1 a_2 a_4 a_6) - \text{Li}_2(-\bar{z}_1 a_3 a_4 a_5). \end{aligned}$$

Now the conclusion is the same as in case 1. \square

4.3 The Volume Conjecture for FSLS

We are ready to prove the Turaev-Viro Volume Conjecture for the complements of the fundamental shadow links.

Theorem 1.4. For any fundamental shadow link $L = L_1 \sqcup \cdots \sqcup L_k$ built from c blocks,

$$\lim_{r \rightarrow \infty} \frac{2\pi}{r} \log |TV_r(M_c \setminus L)| = \text{Vol}(M_c \setminus L) = 2cv_8. \quad (4.22)$$

Proof. If $L = L_1 \sqcup \cdots \sqcup L_k$ we have by Proposition 3.14,

$$TV_r(M_c \setminus L) = \sum_{col \in I_r^k} |RT(M_c, L, col)|^2.$$

Because the possible colorings are polynomial in r ,

$$\frac{2\pi}{r} \log(TV_r(M_c \setminus L)) \leq \max_{col \in I_r^k} \frac{2\pi}{r} \log |RT(M_c, L, col)|^2 + O\left(\frac{\log(r)}{r}\right).$$

By Lemma 3.13, we have that $RT(M_c, L, col)$, up to a factor that grows polynomially in r , is equal to

$$\prod_{i=1}^g \begin{vmatrix} col(i_1) & col(i_2) & col(i_3) \\ col(i_4) & col(i_5) & col(i_6) \end{vmatrix}$$

where i_j is the component of the link L passing through the j -th strand of block i . Hence, because of Theorem 1.8,

$$\lim_{r \rightarrow \infty} \frac{2\pi}{r} \log(TV_r(M_c \setminus L)) \leq 2cv_8$$

On the other hand, if we take $col = (\frac{r\pm 1}{2}, \dots, \frac{r\pm 1}{2})$ to be even colors, we have

$$\lim_{r \rightarrow \infty} \frac{2\pi}{r} TV_r(M_c \setminus L) \geq \lim_{r \rightarrow \infty} \frac{2\pi}{r} \log \left| \begin{array}{ccc} \frac{r\pm 1}{2} & \frac{r\pm 1}{2} & \frac{r\pm 1}{2} \\ \frac{r\pm 1}{2} & \frac{r\pm 1}{2} & \frac{r\pm 1}{2} \end{array} \right|_{q=e^{\frac{2\pi i}{r}}}^{2c} = 2cv_8$$

by Lemma 4.14. □

Chapter 5

The Maximum Volume Theorem

This chapter is devoted to the proof of Theorem 1.6.

5.1 Related results

Before we delve into the proof of Theorem 1.6, a few words are necessary on what makes this result particularly complicated.

\mathcal{A}_Γ contains polyhedra with obtuse angles.

Often when hyperbolic polyhedra are considered, they are restricted to have acute angles (especially when studying their relationship to orbifolds and cone-manifolds). This limitation greatly simplifies matters, mainly because of two properties of acute-angled polyhedra, both consequences of Andreev's Theorem [1]:

- Dihedral angles are global coordinates for acute-angle polyhedra;
- The space of dihedral angles of acute-angle polyhedra is a convex subset of \mathbb{R}^N (except when the polyhedron has 4 vertices).

Using these properties, it is just a matter of applying the Schläfli identity 2.36 to prove that the maximum volume of acute-angled polyhedra is the volume of the rectification.

By contrast, if we allow obtuse angles things are considerably more difficult. It is unknown whether dihedral angles determine a polyhedron; furthermore the space of dihedral angles is never convex [20].

On the other hand, requiring that a polyhedron be acute-angled is very restricting; in particular, there are no non-simple acute-angle compact polyhedra. Therefore allowing obtuse angles greatly increases the scope of Theorem 1.6.

\mathcal{A}_Γ contains polyhedra with any combination of real, ideal or hyperideal vertices.

The case of polyhedra with only ideal vertices has been known for a long time.

Theorem 5.1. *[43, Theorem 14.3] There is a unique (up to isometry) hyperbolic ideal polyhedron with fixed 1-skeleton of maximal volume; furthermore this polyhedron is maximally symmetric.*

Notice that even though the maximal volume polyhedron is unique, the symmetry property does not always determine it uniquely.

Theorem 5.1 relies on the fact that ideal polyhedra share the two above properties of acute-angled polyhedra: they are determined by their angles, and the space of dihedral angles is a convex polytope. Moreover, this result relies on the concavity of the volume function for ideal polyhedra; this result once again does not hold for compact polyhedra.

We might wish to extend Theorem 5.1 to polyhedra with both real and ideal vertices; a pleasant result would be the following:

“Theorem”: For any polyhedron P with real and ideal vertices, there is a polyhedron Q with only ideal vertices, with the same 1-skeleton as P and such that $\text{Vol}(P) \leq \text{Vol}(Q)$.

This would imply that the maximal volume ideal polyhedron is also of maximal volume among polyhedra with both real and ideal vertices. Unfortunately, this “Theorem” has no chance of being true: there are some graphs which are the 1-skeleton of hyperbolic polyhedra but are not the 1-skeleton of any ideal polyhedron (a complete characterization of inscribable graphs, i.e. those that are the 1-skeleton of an ideal polyhedron, can be found in [44]). In such a case, the maximal volume polyhedron (if it even existed) would have some ideal vertices and some real vertices, would possibly not be unique and would certainly be very difficult to determine.

Therefore, admitting vertices of all 3 types allows us to obtain a satisfying result, where the maximal volume is obtained at a very concrete polyhedron whose volume can be explicitly computed. However it comes at the cost of increased complications in the proofs, mainly having to deal with almost proper polyhedra.

It is not a simple application of the Schläfli identity.

Looking at the Schläfli identity might suggest that it immediately implies the Maximum Volume Theorem. An argument might go like this:

A local maximum must have every length of an edge (not arising from truncation) equal to 0; therefore it must be the rectification.

This does not work for two reasons:

- Simply putting derivatives equal to 0 would give local maxima in the interior of \mathcal{A}_Γ ; to truly find a supremum we would have to analyze the behavior at its boundary.
- Dihedral angles do not give local coordinates on all of $\overline{\mathcal{A}_\Gamma}$; in particular it is unknown whether they would give local coordinates at the boundary $\partial\mathcal{A}_\Gamma$ (if, for example, some angles are equal to 0).

5.2 Proof of the Maximum Volume Theorem

The following is the main result of the chapter.

Theorem 1.6. [6] *For any planar 3-connected graph Γ ,*

$$\text{Vol}(\overline{\Gamma}) = \sup_{P \in \mathcal{A}_\Gamma} \text{Vol}(P).$$

Proof. For the sake of understanding, the proof of the key Proposition 5.2 is postponed in Subsection 5.3.

It is easy to see that $\text{Vol}(\overline{\Gamma}) \leq \sup_{P \in \mathcal{A}_\Gamma} \text{Vol}(P)$; the family P_ϵ defined in the statement of Lemma 2.34 is a family in \mathcal{A}_Γ , has decreasing angles (hence increasing volume) and it converges to $\overline{\Gamma}$. Since the length of every edge of P_ϵ converges to 0 (because it is equal to the distance between two planes who converge to be asymptotic), we can apply Lemma 2.39 to the truncation of P_ϵ to obtain that $\text{Vol}(P_\epsilon) \rightarrow \text{Vol}(\overline{\Gamma})$.

Now we prove that $\text{Vol}(P) \leq \text{Vol}(\overline{\Gamma})$ for any $P \in \mathcal{A}_\Gamma$. We first assume that P only has hyperideal vertices.

Let $(\theta_1, \dots, \theta_k)$ be the dihedral angles of P . Since the space of dihedral angles of hyperideal polyhedra is convex by Theorem 2.15, there is a continuous family of polyhedra with decreasing angles connecting P to P_ϵ (for a small enough ϵ), which implies that $\text{Vol}(P) < \text{Vol}(P_\epsilon)$. But we have already seen that $\text{Vol}(P_\epsilon)$ increases to $\text{Vol}(\overline{\Gamma})$ as $\epsilon \rightarrow 0$, which implies that $\text{Vol}(P) < \text{Vol}(\overline{\Gamma})$.

Let now P be any polyhedron in \mathcal{A}_Γ . We wish to define inductively a (possibly empty) sequence of polyhedra $P^{(1)}, \dots, P^{(m)}$ without ideal vertices such that

$$\text{Vol}(P) < \text{Vol}(P^{(1)}) < \dots < \text{Vol}(P^{(m)}) < \text{Vol}(\overline{\Gamma}). \quad (5.1)$$

The key proposition in building this chain is the following.

Proposition 5.2. *Let P be either a proper or an almost proper polyhedron with 1-skeleton Γ with no ideal vertices and at least one real vertex. Then there exists a generalized hyperbolic polyhedron P^* with the following properties:*

- $\text{Vol}(P^*) > \text{Vol}(P)$;
- P^* is either proper or almost proper;
- P^* has at most the same number of real vertices as P ;
- P^* either has fewer vertices, fewer real vertices or fewer proper vertices than P ;
- if P^* has ideal vertices, then it has exactly one;
- if P^* has ideal vertices, then it is proper.
- the 1-skeleton of P^* can be obtained from Γ via a finite sequence of the following moves:

(i) an edge of Γ collapses to a vertex (see Figure 2.9);

(ii) a face of Γ collapses to an edge (see Figure 2.10).

The proof of this proposition is postponed to Section 5.3.

Let now P be a proper polyhedron with 1-skeleton Γ .

If P only has hyperideal vertices, then we have already seen that $\text{Vol}(P) < \text{Vol}(\bar{\Gamma})$.

If P has some ideal vertices, then take the polyhedron $P' := \Phi_\lambda^v(P)$ for λ slightly larger than 1 and $v \in P$ where Φ_λ^v is the homothety of center v and factor λ . For any $\epsilon > 0$ there is a $\lambda > 1$ and close enough to 1 such that P' is proper, it has no ideal vertices and its volume is larger than $\text{Vol}(P) - \epsilon$. To see this, notice that as $\lambda \rightarrow 1$, the truncation face of a hyperideal vertex that becomes ideal is a hyperbolic polygon that becomes Euclidean (hence, the length of its sides goes to 0) and thus we can apply Lemma 2.39) to obtain that the volume changes continuously. If we prove that $\text{Vol}(\Phi_\lambda^v(P)) < \text{Vol}(\bar{\Gamma})$ for any λ , then we also prove that $\text{Vol}(P) \leq \text{Vol}(\bar{\Gamma})$ which implies the theorem. Therefore we can assume that P has no ideal vertices.

If P has no ideal vertices and at least one real vertices, take P^* given by Proposition 5.2. If P^* does not have ideal vertices, take $P^{(1)} := P^*$, if it does then take $P^{(1)} := \Phi_\lambda^v(P^*)$ with $v \in P^*$ and $\lambda > 1$ small enough to ensure that $\text{Vol}(P^{(1)}) > \text{Vol}(P)$.

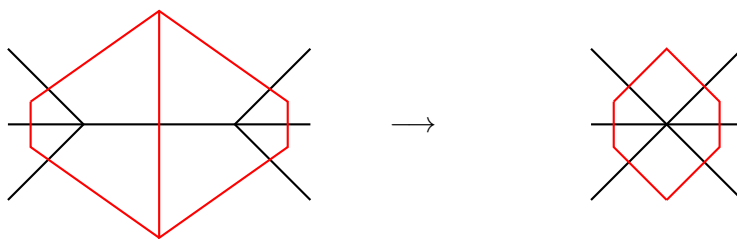


Figure 5.1: If an edge collapses, dually an edge gets deleted.

Suppose now that we have defined the sequence $P^{(1)}, \dots, P^{(j)}$ satisfying the inequalities of (5.1), and define inductively $P^{(j+1)}$.

By hypothesis $P^{(j)}$ cannot have ideal vertices. If $P^{(j)}$ has no real vertices, we stop. If $P^{(j)}$ has some real vertices, then we can apply Proposition 5.2 to it and we define $P^{(j+1)}$ to be the resulting polyhedron (once again applying a small expansion if it has ideal vertices).

Notice that when passing from $P^{(i)}$ to $P^{(i+1)}$ the tuple

$$(\# \text{ of vertices, } \# \text{ of real vertices, } \# \text{ of proper vertices})$$

decreases in the lexicographic order, since we applied Proposition 5.2 to go from $P^{(i)}$ to $P^{(i+1)}$. Therefore at some point we have to arrive at a $P^{(m)}$ with only hyperideal vertices: we have seen at the beginning of the proof that this implies $\text{Vol}(P^{(m)}) < \text{Vol}(\overline{\Gamma'})$ where Γ' is the 1-skeleton of $P^{(m)}$.

The conclusion of the proof comes from the following proposition, which could be of independent interest.

Proposition 5.3. *If Γ' is obtained from Γ either via a single edge collapsing to a vertex (see Figure 2.9) or a single face collapsing to an edge (see Figure 2.10), then $\text{Vol}(\overline{\Gamma'}) \leq \text{Vol}(\overline{\Gamma})$.*

Proof. The proof works exactly the same for either the edge collapse or the face collapse; we carry it out for the edge collapse.

The key observation (see Remark 2.30) is that $\text{Vol}(\overline{\Gamma}) = \text{Vol}(\overline{\Gamma^*})$, and if Γ' is obtained from Γ by an edge collapse, then Γ'^* is obtained from Γ^* by deleting an edge e (see Figure 5.1).

Let now $P_{\epsilon, \alpha}$, be the polyhedron with 1-skeleton Γ^* , dihedral angle α at the edge e and every other dihedral angle equal to ϵ . Because of Theorem 2.15, for any ϵ sufficiently close to 0, $P_{\epsilon, \alpha}$ exists for $\alpha \in (0, \pi - k\epsilon)$ where k depends only on the valence of Γ^* at the endpoints of e . Because of the Schläfli formula, $\text{Vol}(P_{\epsilon, \alpha})$ is decreasing in α , and in particular $\text{Vol}(P_{\epsilon, \pi - k\epsilon}) < \text{Vol}(P_{\epsilon, \epsilon})$. But $\text{Vol}(P_{\epsilon, \epsilon}) \rightarrow \text{Vol}(\overline{\Gamma})$ and $\text{Vol}(P_{\epsilon, \pi - k\epsilon}) \rightarrow \text{Vol}(\overline{\Gamma'})$. The first convergence comes from Lemmas 2.34 and 2.39; the second convergence comes with the same

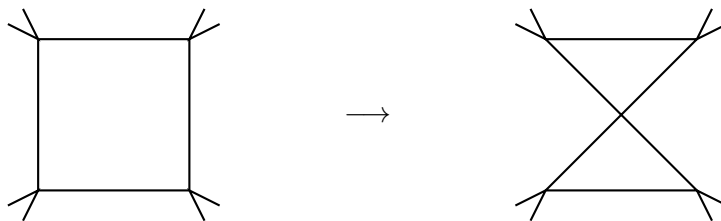


Figure 5.2: Two edges on the same face getting “switched”.

argument as in the proof of Lemma 2.34 after we notice that if two faces have an angle converging to π , then they must converge to the same plane. \square

Remark 5.4. Proposition 5.3 could be translated into a statement about ideal right-angled polyhedra. Specifically, it says that if P_1 and P_2 are two ideal right-angled polyhedra with 1-skeleta Γ_1 and Γ_2 related as in Figure 5.2, then $\text{Vol}(P_1) \geq \text{Vol}(P_2)$. \square

Corollary 5.5.

$$\sup_{P \in \mathcal{A}_\Gamma} \text{Vol}(P) = \sup_{P' \in \mathcal{A}_{\Gamma^*}} \text{Vol}(P')$$

Proof. As we noted before, the rectification of Γ and the rectification of Γ^* have isometric truncations. \square

5.3 Proof of Proposition 5.2

We are going to prove Proposition 5.2 by deforming the polyhedron P until it collapses to a limit polyhedron. First we need two lemmas describing what happens when the limit polyhedron has ideal vertices. Both follow the same general reasoning (and similar notation) of Proposition 5 and Lemma 22 of [2].

Lemma 5.6. *Let P_n be a sequence of proper or almost proper polyhedra with 1-skeleton Γ and with angles bounded away from 0 and π , and suppose P_n converges as $n \rightarrow +\infty$ to the projective polyhedron P^* . Further suppose that all the vertices of P_n also converge, and a sequence of vertices $v_n \in P_n$ converges to $v \in \partial\mathbb{H}^3$. Let e_1, \dots, e_k be the edges of Γ with exactly one endpoint converging to v , and let $e_1, \dots, e_{k'}$ be the subset of those edges converging to a segment intersecting \mathbb{H}^3 . Then the sum of external dihedral angles of $e_1, \dots, e_{k'}$ converges to either 2π (if and only if $k = k'$) or π otherwise.*

Proof. First notice that all edges of a limit of proper or almost proper polyhedra must either intersect \mathbb{H}^3 or be tangent to its boundary.

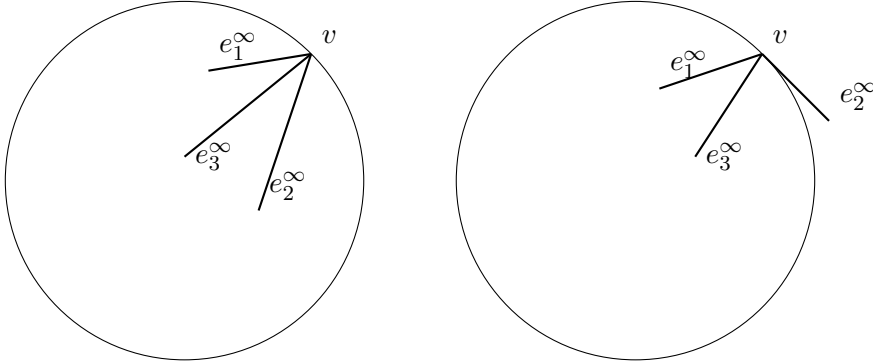


Figure 5.3: Cases 1 and 2

Let e_1^n, \dots, e_k^n be the edges of P^n corresponding to e_1, \dots, e_k respectively, each converging to $e_1^\infty, \dots, e_k^\infty$ (many different e_i^∞ 's could be in the same edge of P^*). We distinguish several cases.

Case 1. The segment e_i^∞ intersects \mathbb{H}^3 for every i .

In this case clearly $k = k'$. Let F_1^n, \dots, F_k^n be the faces of P_n containing e_1^n, \dots, e_k^n . Let Π_j^n be the plane containing F_j^n and denote with Π_j^∞ their limit. Finally let $\tilde{\theta}_1^n, \dots, \tilde{\theta}_k^n$ be the external dihedral angles of e_1^n, \dots, e_k^n respectively.

Since dihedral angles between two planes vary continuously (as long as their intersection is contained in \mathbb{H}^3), $\lim_{n \rightarrow \infty} \tilde{\theta}_j^n = \tilde{\theta}_j^\infty$ where $\tilde{\theta}_j^\infty$ is the angle between planes Π_j^∞ and Π_{j+1}^∞ . Then the second part of [2, Proposition 5] shows that

$$\sum_i \tilde{\theta}_i^\infty = 2\pi$$

which concludes the proof in this case.

Case 2. Some edges e_i^∞ intersect \mathbb{H}^3 , while at least some other e_j^∞ is tangent to $\partial\mathbb{H}^3$; however, every limit edge tangent to $\partial\mathbb{H}^3$ is in the same edge of P^* .

Let v_j^n be the endpoint of e_j^n converging to $v_j^\infty \neq v$; v_j^∞ is necessarily hyperideal; we may suppose also that each v_j^n is hyperideal. Truncate P_n along $\Pi_{v_j^n}$ and double it along the truncation face. This gives a sequence \tilde{P}_n converging to the polyhedron obtained from P^* by truncating along $\Pi_{v_j^\infty}$ and doubling. This sequence falls under Case 1, and the sum of the external dihedral angles of \tilde{P}_n at the edges converging to v must be equal to $2 \sum_{j=1}^{k'} \tilde{\theta}_j$, and it must converge to 2π which gives the thesis.

Case 3. Some edges e_i^∞ intersect \mathbb{H}^3 , while at least some other e_j^∞ is tangent to $\partial\mathbb{H}^3$; moreover, there are at least two distinct edges of P^* tangent to $\partial\mathbb{H}^3$.

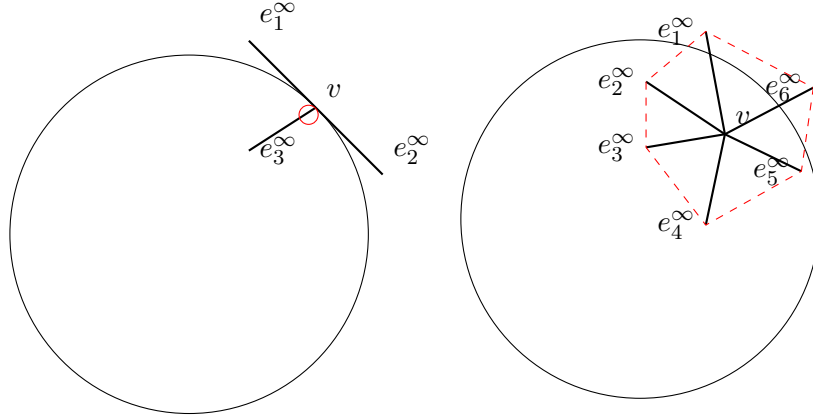


Figure 5.4: Cases 3 and 4

This case (like the following one) is essentially the same as the corresponding case of Lemma 22 of [2]. This means that P^* has two (or more) edges tangent to $\partial\mathbb{H}^3$ in v and some other edge with endpoint v which intersects \mathbb{H}^3 . Then let S be a horosphere centered in v and consider $A := S \cap P^*$. The polygon A is not compact, has at least two ends (one in the direction of each edge tangent to $\partial\mathbb{H}^3$) and at least one vertex with positive angle, but this is impossible, hence this case never happens.

Case 4. Every edge e_i^∞ is tangent to $\partial\mathbb{H}^3$.

This case is impossible as well: each e_i^n has one endpoint v_i^n that does not converge to v . Since Γ is 3-connected, there are three indices a, b, c such that e_a, e_b, e_c have the endpoints v_a, v_b, v_c (the one not converging to v) which are all different. Then the lines connecting v_a^n, v_b^n and v_b^n, v_c^n must intersect \mathbb{H}^3 , but this is impossible since they converge to points each lying on a different line tangent to $\partial\mathbb{H}^3$ in the same point v . This contradicts the fact that P_n is a generalized hyperbolic polyhedron. □

Corollary 5.7. *With the same hypotheses of Lemma 5.6, if a vertex of P_n converges to a point on $\partial\mathbb{H}^3$, then it converges to a vertex of the limit polyhedron.*

Proof. Suppose v_n is a sequence of vertices converging to $v \in P^*$ and v is not a vertex of P^* ; then it is either contained in the interior of an edge or the interior of a face. If it is contained in the interior of an edge, the analysis of Case 3 of Lemma 5.6 show that there is a contradiction; likewise if it is contained in the interior of a face there is a contradiction because of the reasoning in Case 4 of Lemma 5.6. □

Further notice that from the hypotheses of Lemma 5.6 we can drop the assumption that the vertices of P_n converge, since we can always pass to a subsequence such that this holds (and using the easy fact that if every subsequence of a sequence has a subsequence converging to x , the whole sequence converges to x).

Lemma 5.8. *Take a sequence of proper or almost proper polyhedra P_n with 1-skeleton Γ and decreasing angles bounded away from 0, such that P_n converges to the projective polyhedron P^* as $n \rightarrow +\infty$. If there is a vertex v_n of P_n converging to an ideal vertex v of P^* , then v_n is a real vertex of P_n for all n .*

Proof. We proceed by contradiction, supposing that v_n is hyperideal (notice that if $v_{\bar{n}}$ is ideal or hyperideal for some \bar{n} then it is strictly hyperideal for all $n > \bar{n}$ by Lemma 2.13).

Let $K_v \subseteq \Gamma \subseteq S^2$ be the union of all vertices and edges converging to v , and consider as we did before the edges e_1, \dots, e_k of Γ with exactly one endpoint in K_v . Denote with e_1^n, \dots, e_k^n the corresponding edges of P_n and call $e_1^\infty, \dots, e_k^\infty$ the limit edges. As before the external dihedral angle of e_i^n is denoted θ_i^n . Let F_1^n, \dots, F_k^n be the faces containing these edges. Each F_i^n lies on a plane $\Pi_i^n \subseteq \mathbb{R}^3$ and determines a half space $H_i^n \subseteq \mathbb{R}^3$ bounded by Π_i^n (the one that contains P_n). Pick n big enough so that the triple intersections of the various Π_i^n 's are very close to v .

We distinguish the same 4 cases as in Lemma 5.6; we showed that Case 3 and Case 4 are impossible (under more lax assumptions) hence we skip them.

Case 1. Every limit edge e_i^∞ intersects \mathbb{H}^3 .

We show that $\sum_i \tilde{\theta}_i^n > 2\pi$. Since the internal dihedral angles are decreasing, the external dihedral angles are increasing in n , which would contradict Lemma 5.6.

Let Q_n be the intersection of all H_i^n 's; this is a convex non-compact subset of \mathbb{R}^3 . By assumption Q_n has some hyperideal vertices (since certainly $P_n \subseteq Q_n$ and P_n has a hyperideal vertex close to v).

Let $\Upsilon \subseteq \mathbb{R}^2$ be the 1-skeleton of Q_n . It must have (unbounded) edges e_1, \dots, e_k and additional edges e'_1, \dots, e'_l , however it cannot have any cycle since an innermost cycle would bound some face of Q_n not contained in Π_1, \dots, Π_k .

If $\gamma \subseteq \mathbb{R}^2$ is an embedded 1-manifold intersecting transversely distinct edges e_{i_1}, \dots, e_{i_j} exactly once, we write $\sum_\gamma \tilde{\theta}_e$ for the sum $\sum_{m=1}^j \tilde{\theta}_{e_{i_m}}$.

Let Υ_∞ be the subgraph of Υ whose vertices are exactly the hyperideal vertices of Q_n , and whose edges are exactly the edges of Q_n lying completely outside of \mathbb{H}^3 . By assumption Υ_∞ is not empty; choose one of its connected components and consider γ the boundary of its regular neighborhood in \mathbb{R}^2 . Since

Υ contains no cycles, γ must be connected (otherwise the regular neighborhood of Υ_∞ would contain a cycle). Proposition 5 of [2] implies that $\sum_\gamma \tilde{\theta}_e > 2\pi$. If γ only intersects the old edges e_1, \dots, e_k , then we have concluded. Suppose then that instead γ intersects e'_i . We distinguish two cases, based on whether both endpoints of e'_i are in Υ_∞ or not.

If both endpoints of e'_i are in Υ_∞ , still e'_i cannot be contained in Υ_∞ by construction; moreover its endpoints cannot be contained in the same connected component because Υ contains no cycles. One endpoint of e'_i is contained in a connected component U of Υ_∞ whose regular neighborhood is bounded by γ , the other in a component U' whose regular neighborhood is bounded by γ' . Let γ'' be the boundary of the regular neighborhood of $U \cup U' \cup e'_i$. Then

$$\sum_{\gamma''} \tilde{\theta}_e = \sum_{\gamma'} \tilde{\theta}_e + \sum_{\gamma} \tilde{\theta}_e - 2\tilde{\theta}_{e'_i} > 4\pi - 2\tilde{\theta}_{e'_i} > 2\pi.$$

If instead one endpoint v of e'_i is not in Υ_∞ , denote with γ' the boundary of a regular neighborhood U' of v in \mathbb{R}^2 , and with γ'' the boundary of a regular neighborhood of $U \cup U' \cup e'_i$. Then

$$\sum_{\gamma''} \tilde{\theta}_e = \sum_{\gamma} \tilde{\theta}_e + \sum_{\gamma'} \tilde{\theta}_e - 2\tilde{\theta}_{e'_i} > \sum_{\gamma} \tilde{\theta}_e > 2\pi.$$

where the first inequality is because the external angles of hyperbolic polyhedra must satisfy the triangular inequality, thus $\sum_{\gamma'} \tilde{\theta}_e - 2\tilde{\theta}_{e'_i} > 0$.

We can repeat this process, modifying γ while keeping $\sum_\gamma \tilde{\theta}_e > 2\pi$, until γ intersects only e_1, \dots, e_k , obtaining the desired inequality. Figure 5.5 exemplifies this process in a particular case.

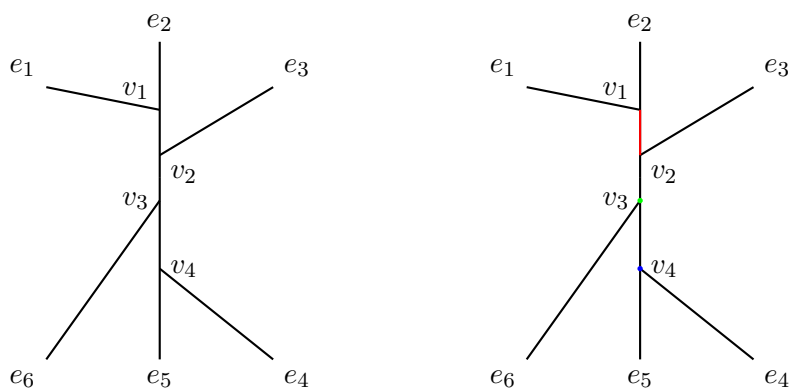
Case 2. Some edges e_i^∞ intersect \mathbb{H}^3 , while at least some other e_j^∞ is tangent to $\partial\mathbb{H}^3$; however every edge tangent to $\partial\mathbb{H}^3$ is in the same edge of P^* .

By renumbering if necessary suppose that $e_1^n, \dots, e_{k'}^n$ converge to edges intersecting \mathbb{H}^3 and the remainder do not.

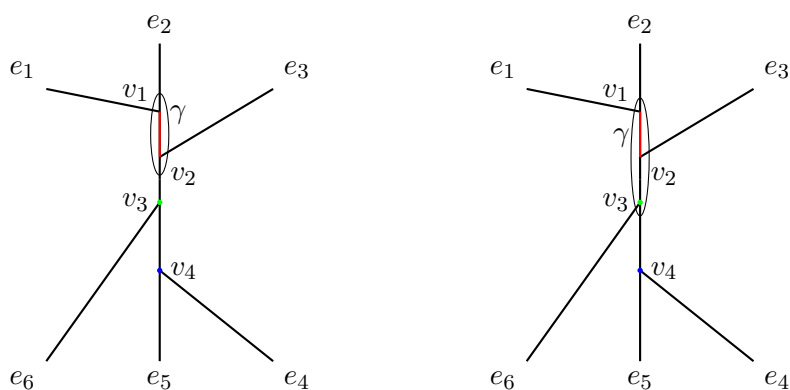
In this case we employ the same trick of Lemma 5.6: we truncate Q_n and we double along the truncation face to fall back into Case 1. This way we show that $\sum_i^{k'} \tilde{\theta}_i^n > \pi$ which once again contradicts Lemma 5.6 since the angles are decreasing. \square

Proposition 5.2. *Let P be either a proper or almost proper polyhedron with 1-skeleton Γ with no ideal vertices and some real vertices. Then there exists a generalized hyperbolic polyhedron P^* with the following properties:*

- $\text{Vol}(P^*) > \text{Vol}(P)$;



The 1-skeleton Υ . The subgraph Υ_∞ is comprised of edge v_1v_2 and vertex v_4 . The edge v_1v_2 in Q_n will lie outside \mathbb{H}^3 , the vertex v_4 will be hyperideal and v_3 will be real.



We start with γ encircling v_1v_2 . We extend Γ to encircle v_3 : doing so increases $\sum_\gamma \tilde{\theta}_e$ because of the triangular inequality.

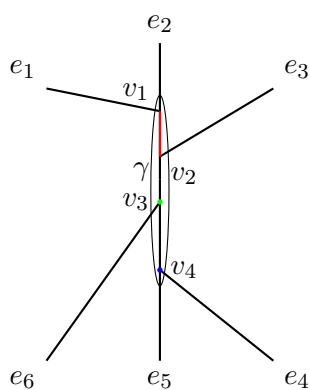


Figure 5.5: We finish by extending γ to encircle v_4 as well. This way γ intersects e_1 through e_6 and $\sum_\gamma \tilde{\theta}_e > 2\pi$ as requested.

- P^* is either proper or almost proper;
- P^* has at most the same number of real vertices as P ;
- P^* either has fewer vertices, fewer real vertices or fewer proper vertices than P ;
- if P^* has ideal vertices, then it is proper.

Furthermore, the 1-skeleton of P^* can be obtained from Γ via a finite sequence of the following moves:

- (i) an edge of Γ collapses to a vertex;
- (ii) a face of Γ collapses to an edge.

Proof. The strategy to obtain the polyhedron P^* is to deform P by decreasing all angles (hence, increasing the volume) until it is no longer possible.

If P has only real vertices, then for an appropriate $\lambda > 1$ the polyhedron $\Phi_\lambda^v(P)$ (for $v \in P$) is a proper polyhedron with 1-skeleton Γ , at least an ideal vertex and larger volume (since it clearly contains P), hence it satisfies the conditions in the thesis.

Suppose now that P has a hyperideal vertex v , and let $\vec{\theta} = (\theta_1, \dots, \theta_k)$ be the dihedral angles of all proper edges of P (if P is proper, all its edges are proper). Then Corollary 2.18 or Corollary 2.20 tell us that for t in a neighborhood of 1 there is a continuous family of polyhedra P_t (defined up to isometry) with $P_1 = P$, 1-skeleton Γ , dihedral angles of proper edges equal to $t\vec{\theta}$ and the same almost proper vertices of P . By the Schläfli identity, the volume of P_t increases as t decreases. Up to a small perturbation of $\vec{\theta}$ that decreases all angles, we can assume that the path $t\vec{\theta}$ intersects the hyperplanes $\sum_{i \in I} \theta_i = k\pi$ one at a time, where I is any possible subset of $\{1, \dots, k\}$. Let t_* the infimum of all t 's such that P_t is defined.

If $t_* = 0$, then for t very close to 0 the polyhedron P_t is hyperideal; since P has some real vertices then P_t has more hyperideal vertices than P and thus satisfies all the conditions of the thesis. Suppose then $t_* > 0$. We prove that in this case P_t has an accumulation point as $t \rightarrow t_*$.

Lemma 5.9. *The family P_t just defined has an accumulation point Q which is a non-degenerate projective polyhedron.*

Proof. We need to prove that, up to a suitable choice of isometry class for P_t , there is a converging subsequence, and its limit is a non-degenerate polyhedron contained in an affine chart (i.e. it does not contain any line). Choose any subsequence $P_n := P_{t_n}$ with $t_n \rightarrow t_*$. Consider representatives in $((\mathbb{RP}^3)^*)^F$

of P_n ; by an abuse of notation we still call them P_n . Up to isometries we can keep a hyperideal vertex v of P_n fixed (we assume there is one because of the remark at the beginning of the proof).

Consider now $A_n := P_n \cap \Pi_v$: it is a sequence of polygons satisfying the hypotheses of Lemma 2.35 (when viewed as subsets of $\Pi_v \cong \mathbb{H}^2$); then up to isometry of \mathbb{H}^2 and subsequence they converge to a non-degenerate polygon A . This shows that we can choose the representatives of P_n so that A_n converges to A .

By compactness of $(\mathbb{R}\mathbb{P}^3)^*$ the polyhedra P_n are going to have a subsequence converging to some convex set $Q \subseteq \mathbb{R}\mathbb{P}^3$.

Then Q must contain the pyramid with base A and vertex v , hence it is non-degenerate.

We need to show that Q is contained in an affine chart. Suppose by contradiction that Q contains a projective line l . If $v \in l$ then there must be $w_n \in P_n$ different from v but converging to v , and then the distance between Π_v and Π_{w_n} must converge to 0. This implies that the thickness of P_n (i.e. the radius of the largest ball contained in P_n) must also converge to 0; this implies that $\text{Vol}(P_n) \rightarrow 0$ by [34, Proposition 4.2] which is a contradiction. If instead $v \notin l$ then we can find a vertex w_n in P_n arbitrarily far (in the Euclidean sense) from $\overline{\mathbb{H}^3}$, and then $\overrightarrow{vw_n}$ does not intersect $\overline{\mathbb{H}^3}$ which is absurd. \square

We pass to a further subsequence, if needed, so that all vertices of P_n converge.

We now distinguish 3 cases.

Case 1. If Q is a generalized hyperbolic polyhedron without ideal vertices, then we define $P^* := Q$.

We need to check several properties of P^* : we do so in the same order we listed them in the statement.

- Since P^* has compact truncation, Lemma 2.38 implies that $\text{Vol}(P_t) \rightarrow \text{Vol}(P^*)$ increasingly, hence $\text{Vol}(P^*) > \text{Vol}(P)$.
- Since P^* is a limit of proper or almost proper polyhedra, it must be proper or almost proper itself, as being proper or almost proper is a closed condition.
- By Lemma 5.8 an ideal or hyperideal vertex of P_n cannot become ideal or real in P^* , hence P^* has at most the same number of real vertices as P .

- If P^* had the same number of vertices (hence the same 1-skeleton), no ideal vertices and the same almost proper vertices, then the dihedral angles of proper edges would be local coordinates around P^* ; this would imply that actually $P_t \rightarrow P^*$ (since all limit points of P_t must have the same angles, hence be locally the same) and we could extend the path P_t . This would contradict the fact that t_* is minimal.

We need to show then that the 1-skeleton of P^* can be obtained by a sequence of edge or face collapses. This is done by applying Lemma 2.24.

This concludes the proof in the case where Q is a generalized hyperbolic polyhedron without ideal vertices.

Case 2. If Q is a projective polyhedron without ideal vertices (i.e. all its vertices are not on the sphere at infinity $\partial\mathbb{H}^3$), then it is a generalized hyperbolic polyhedron.

To see this, remember that we only need to show that every edge of Q intersects \mathbb{H}^3 . Suppose that an edge e of Q is instead tangent to $\partial\mathbb{H}^3$. By assumption neither of the endpoints of e can lie on $\partial\mathbb{H}^3$, hence they must lie outside of \mathbb{H}^3 . First we prove that there is only one sequence of edges e_n converging to e (or even a subset of e). If there was another sequence of edges e'_n of P_n converging to a subset of e , then by the discussion following Lemma 5.6 both of its endpoints would have to converge to points outside $\overline{\mathbb{H}^3}$. Then the lines connecting these endpoints to the endpoints of e_n must, for n big enough, lie outside \mathbb{H}^3 which is a contradiction. Therefore there is only one edge e_n of P_n converging to e , and let F_n, G_n be the two faces containing e_n and converging to F, G faces of Q containing e . If one of F or G was tangent to $\partial\mathbb{H}^3$ then we would have another contradiction as some other edge would lie outside $\overline{\mathbb{H}^3}$. Therefore F, G must be contained in two hyperbolic planes intersecting with dihedral angle 0, and the angle between F_n and G_n would converge to 0 which contradicts the way we chose the angles of P_n .

Therefore, we can once again define $P^* := Q$. The fact that P^* satisfies the thesis is exactly the same as before.

Case 3: Q is a projective polyhedron with some ideal vertices.

The problem in this case is that it could happen that $\text{Vol}(P_n)$ does not converge to $\text{Vol}(Q)$. In this case we need to modify the sequence P_n to arrive at some other polyhedron Q' .

For any v ideal vertex of Q let (as in the proof of Lemma 5.6) $K_v \subseteq \Gamma$ be the union of all edges and vertices collapsing to v . Let e_1, \dots, e_k be the edges of Γ with exactly one endpoint in K_v (notice that since Q is non-degenerate there are at least 3 such edges), let e_1^n, \dots, e_k^n be the corresponding edges of P_n , and $e_1^\infty, \dots, e_k^\infty$ their limit in Q .

Let \bar{n} be big enough that all the vertices of $P_{\bar{n}}$ converging to v are very close to $\partial\mathbb{H}^3$ (in the Euclidean distance), while every other vertex is farther.

We further distinguish two cases.

Case 3a. The ideal vertex of Q is proper (i.e. it is not contained in the dual plane of any hyperideal vertex of Q).

Notice that in this case we can apply the same reasoning of Case 2 to get that Q is a generalized hyperbolic polyhedron.

We have shown Lemma 5.6 that in this case $\lim_{n \rightarrow \infty} \sum_i \theta_{e_i^n}$ is a multiple of π , therefore Q has exactly one ideal vertex because of the way we perturbed θ .

Then there is a hyperbolic plane Π delimiting the half-spaces H_1 and H_2 such that H_1 contains, for every $n \geq \bar{n}$, exactly the vertices of P_n converging to v , while H_2 contains every other vertex of P_n and every truncation plane (notice: not just truncation faces). For simplicity we can assume that Π is the dual plane to some hyperideal point close to v (so that Π is almost orthogonal to e_1^n, \dots, e_k^n). Up to an isometry we can make it so that Π is an equatorial plane (i.e. one containing $0 \in \mathbb{H}^3 \subseteq \mathbb{R}^3$). Let \vec{a} be the unit normal vector to Π pointing toward H_1 . Recall that $\Psi_{\vec{b}}$ is the translation of \mathbb{R}^3 in the direction \vec{b} .

For n big enough, $Q \cap H_2$ is compact and close to $P_n \cap H_2$, hence their volumes are also close. Then for any $\delta > 0$ there is a λ small enough that $\text{Vol}(\Psi_{\lambda\vec{a}}(Q) \cap H_2) > \text{Vol}(Q \cap H_2) - \frac{1}{2}\delta$, which implies that

$$\text{Vol}(\Psi_{\lambda\vec{a}}(P_n) \cap H_2) > \text{Vol}(P_n \cap H_2) - \delta$$

for every n big enough. It is important to notice that λ does not depend on n , only on δ .

Then we define P^* to be $\Psi_{\lambda'\vec{a}}(P_n)$ for some n and $\lambda' < \lambda$. For n sufficiently large and an appropriate λ' , there is some vertex of P_n that becomes ideal. Moreover since every vertex that is close to v is real by Lemma 5.8, this must happen before any edge of P_n gets pushed out of $\overline{\mathbb{H}^3}$. This implies that P^* is a generalized hyperbolic polyhedron.

We prove that P^* satisfies all the conditions of the thesis, in the same order.

- Clearly $\text{Vol}(P^* \cap H_1) > \text{Vol}(P_n \cap H_1)$, since $P_n \cap H_1 \subseteq P^* \cap H_1$. Furthermore we chose $\lambda' < \lambda$ such that $\text{Vol}(P^* \cap H_2) > \text{Vol}(P_n \cap H_2) - \delta$. Therefore $\text{Vol}(P^*) > \text{Vol}(P_n) - \delta$, which implies that $\text{Vol}(P^*) > \text{Vol}(P)$ for δ small enough.
- The translation vector \vec{a} is contained in the tangent cones of all hyperideal vertices of P_n (see Figure 5.6), therefore P^* is proper by Lemma 2.14.

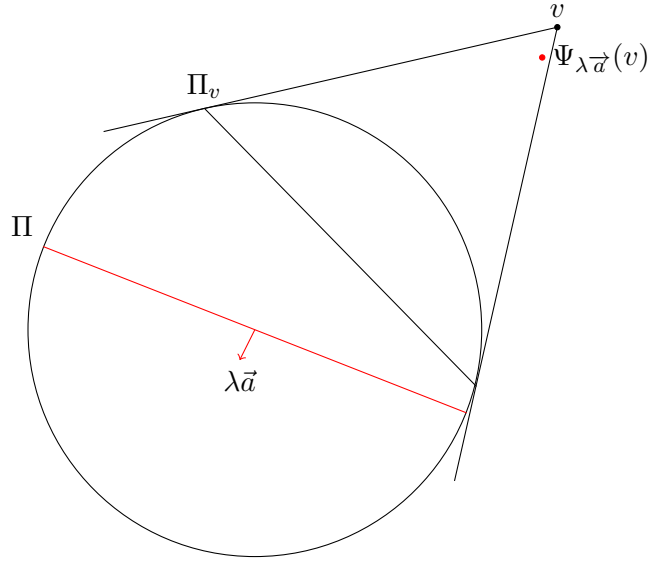


Figure 5.6: Because Π_v is completely contained in H_2 , the translation by $\lambda\vec{a}$ sends v into its tangent cone.

- P_n has at most the same number of real vertices of P by Lemma 5.8; then P^* has some more ideal vertices, hence fewer real vertices.
- P^* has exactly the same number of vertices of P but at least one fewer real vertices, as we noted in the preceding point.
- we have noted that P^* is proper.

Furthermore P^* has the same 1-skeleton as P_n hence the same 1-skeleton as P .

Case 3b. The ideal vertex of Q is almost proper.

This case is almost the same as case 3a; we just need to be careful about the truncating plane containing the almost proper vertex.

Once again by Lemma 5.6 we have that $\lim_{n \rightarrow \infty} \sum_{i=1}^{k'} \theta_{e_i^n}$ is a multiple of π , therefore Q has exactly one ideal vertex.

Let v be the almost proper vertex of Q and let w be the vertex of Q such that $v \in \Pi_w$. Since w must be hyperideal, there is a unique vertex $w_n \in P_n$ converging to it. Now fix n big enough. As before we can find a plane Π that divides \mathbb{H}^3 in H_1, H_2 with H_1 containing every vertex that converges to v and H_2 containing every other vertex and the dual plane to every hyperideal vertex of P_n other than w_n . Furthermore we can choose Π passing through w_n , so that Π and Π_{w_n} are orthogonal.

With an isometry we fix Π_{w_n} to be an equatorial plane and Π_v is an equatorial plane orthogonal to it (notice that in this particular case of equatorial planes, being orthogonal in \mathbb{H}^3 is the same as being orthogonal in \mathbb{R}^3). Having Π_{w_n} being equatorial means that w_n is a point at infinity in \mathbb{RP}^3 .

Let \vec{a} be the unit normal vector to Π pointing towards H_1 and \vec{b}_n be the unit normal vector to Π_{w_n} pointing towards the truncation of P_n .

Then the polyhedron $\Psi_{\lambda(\vec{a}+\epsilon\vec{b}_n)}(P_n)$, for n big enough and λ and ϵ small enough, satisfies all the conditions required for P^* . The proof is almost the same as in case 3a: the only additional detail to check is that any almost proper vertex lying on Π_{w_n} becomes proper. To see this, notice that $\Psi_{\lambda(\vec{a}+\epsilon\vec{b})}$ does not move w_n since it is a point at infinity (hence, leaves Π_{w_n} fixed) and pushes every vertex away from w_n .

□

Chapter 6

Volume conjecture for polyhedra

In this chapter we introduce the Maximum Volume Conjecture for polyhedra. The proof for a large family of examples is in Section 6.2 and relies on Barrett's Fourier transform. Finally in Section 6.3 we use these results to prove the Turaev-Viro Volume Conjecture in a new family of examples.

6.1 The volume conjecture for polyhedra

A Volume Conjecture for trivalent graphs (and their Kauffman bracket invariant) was first proposed in [52] and later refined in [16] to the case of planar trivalent graphs and simple hyperbolic polyhedra. The conjecture of [16] evaluates the invariant at the first root of unity $q = e^{\pi i/r}$; the downside of this choice is that they have to consider poles of the Kauffman bracket, instead of its values directly. Recently, Murakami and Kolpakov [29] proposed a volume conjecture for polyhedra at the second root of unity $q = e^{2\pi i/r}$, but only stated it for simple polyhedra without hyperideal vertices; remarkably this conjecture directly involves the value of the Kauffman bracket. Here we propose an extension of Kolpakov-Murakami's volume conjecture to a very general setting, and then propose a volume conjecture for polyhedra that is similar in spirit to the Turaev-Viro Volume Conjecture.

We propose the following formulation of the volume conjecture, generalizing the aforementioned versions.

Conjecture 1.3 (The volume conjecture for polyhedra). *Let P be a proper polyhedron with dihedral angles $\alpha_1, \dots, \alpha_m$ at the edges e_1, \dots, e_m , and 1-skeleton Γ . Let col_r be a sequence of r -admissible colorings of the edges e_1, \dots, e_m of Γ such that*

$$2\pi \lim_{r \rightarrow +\infty} \frac{col_r(e_i)}{r} = \pi - \alpha_i.$$

Then

$$\lim_{r \rightarrow +\infty} \frac{\pi}{r} \log |Y_r(\Gamma, col_r)| = \text{Vol}(P).$$

Remark 6.1. In the case where P is a simple polyhedron in \mathbb{H}^3 (i.e. a compact polyhedron with only trivalent vertices) this conjecture is the same as the volume conjecture of Kolpakov-Murakami [29].

Conjecture 1.3 was verified in [11] for tetrahedra with at least one hyperideal vertex; we provide some further supporting numerical evidence for Conjecture 1.3 for some pyramids in the Appendix, and prove it for a large family of examples in Proposition 6.12 and the subsequent remark (however, only for a single sequence of colors).

The Maximum Volume Conjecture

As we noted in Proposition 3.14, the Turaev-Viro invariant of the complement of a link $L \subseteq S^3$ is related to the Reshetikhin-Turaev invariants of L via a simple formula. This motivates us to give the following definition of the Turaev-Viro invariant of a graph.

Definition 6.2. Let $\Gamma \subseteq S^3$ be a planar graph with e edges. We define the Turaev-Viro invariant of Γ , in analogy with Propositions 3.14 and 3.18.4, as

$$TV_r(\Gamma) := \sum_{col \in I_r^e} |Y_r(\Gamma, col)|.$$

We now state a volume conjecture for polyhedra in the vein of the Turaev-Viro Volume Conjecture of Chen-Yang.

Conjecture 6.3 (The Maximum Volume Conjecture). *Let $\Gamma \subseteq S^3$ be a 3-connected planar graph. Then*

$$\lim_{r \rightarrow +\infty} \frac{\pi}{r} \log (TV_r(\Gamma)) = \sup_{P \in \mathcal{A}_\Gamma} \text{Vol}(P)$$

where r ranges across all odd natural numbers.

Remark 6.4. If Conjecture 1.3 is true, then of course

$$\lim_{r \rightarrow +\infty} \frac{\pi}{r} \log (TV_r(\Gamma)) \geq \sup_{P \in \mathcal{A}_\Gamma} \text{Vol}(P).$$

However, there could be a sequence of colorings col_r such that $Y_r(\Gamma, col_r)$ grows faster than for any sequence satisfying the hypotheses of Conjecture 1.3; therefore Conjecture 1.3 does not imply the Maximum Volume Conjecture. Nevertheless we believe the Maximum Volume Conjecture to be easier to prove than Conjecture 1.3, as it only concerns the largest values for the volume and the Turaev-Viro invariants, and not those of any particular geometric structure.

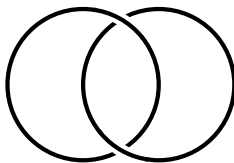


Figure 6.1: The 0-framed Hopf link

We also propose a slightly stronger version of the Maximum Volume Conjecture; the stronger statement can be seen as the natural generalization of Theorem 1.8 to the case of general graphs.

Conjecture 6.5. *If Γ is a planar 3-connected graph and col is any r -admissible coloring of its edges, then*

$$\frac{\pi}{r} \log |Y_r(\Gamma, col)| \leq \text{Vol}(\bar{\Gamma}) + O\left(\frac{\log(r)}{r}\right)$$

Moreover, the inequality is sharp, with equality attained by the sequence of colorings giving the color $\frac{r-2\pm 1}{2}$ to each edge (the sign is chosen so that the colors are even).

It is straightforward to show that Conjecture 6.5 implies the Maximum volume conjecture, since TV_r is a sum of polynomially many terms of the type $Y_r(\Gamma, col)$. However it is slightly more precise since it specifies which colorings give the maximum growth.

6.2 The Fourier Transform

In this section we prove Theorem 1.7. The first main tool used is Theorem 1.8, giving an upper bound on the growth of the $6j$ -symbol.

The second main tool used to prove Theorem 1.7 is the Fourier Transform introduced in [3] by Barrett. We introduce it here in a slightly different context and notation.

Let $H \subseteq S^3$ be the 0-framed Hopf link as in Figure 6.1. If $i, j \in I_r$ we denote with $H(i, j) \in \mathbb{C}$ the value of the Kauffman bracket of the Hopf link colored with i, j ; an easy induction on j shows that

$$H(i, j) = (-1)^{i+j} [(i+1)(j+1)] = (-1)^{i+j} \frac{\sin\left(\frac{2\pi}{r}(i+1)(j+1)\right)}{\sin\left(\frac{2\pi}{r}\right)}.$$

Furthermore denote with

$$N := \frac{r}{4 \sin^2 \left(\frac{2\pi}{r} \right)} = \langle U, \Omega \rangle^2 = \left(\sum_{i \in I_r} \Delta_i^2 \right)^2$$

where U is the 0-framed unknot in S^3 colored with the color $\Omega := \sum_{i \in I_r} \Delta_i i$.

Remark 6.6. Once again we remark that we are using the $SO(3)$ version of the invariants evaluated at $q = e^{2\pi i/r}$. However, the Fourier transform and its properties hold with any choice of primitive $2r$ -th root of unity, or any choice of primitive $4r$ -th root of unity for the $SU(2)$ case; the proofs work verbatim in every other case.

The following proposition was first noticed by Barrett in [3]; a concise proof was later given in [4]. For the sake of completeness, we include a detailed proof of this result.

Proposition 6.7. *If Γ is a planar framed graph and Γ^* is its planar dual, then*

$$Y_r(\Gamma^*, col') = N^{-g} \sum_{col \text{ coloring of } \Gamma} Y_r(\Gamma, col) H(col, col')$$

where

$$H(col, col') := \prod_{e \text{ edge of } \Gamma} H(col(e), col'(e^*)),$$

and g is the genus of a regular neighborhood of Γ .

Proof. The proof is entirely diagrammatic; when we display an equality between (linear combinations of) diagrams, we mean that they have the same Kauffman bracket. Throughout the proof we will liberally add Ω -colored, 0-framed unknots that are unlinked from anything else; this will generate an ambiguity of a power of N that we will account for at the end.

First we show that $Y_r(\Gamma, col)$ is equal to the Kauffman bracket of the link L obtained from Γ as in Figure 6.2. Every vertex is replaced by a circle colored with Ω , and every edge is replaced by a circle colored with the same color as the edge, wrapping around once each of the two circles corresponding to its vertices.

This can be shown by using the definition of Y after applying the following identity to L :

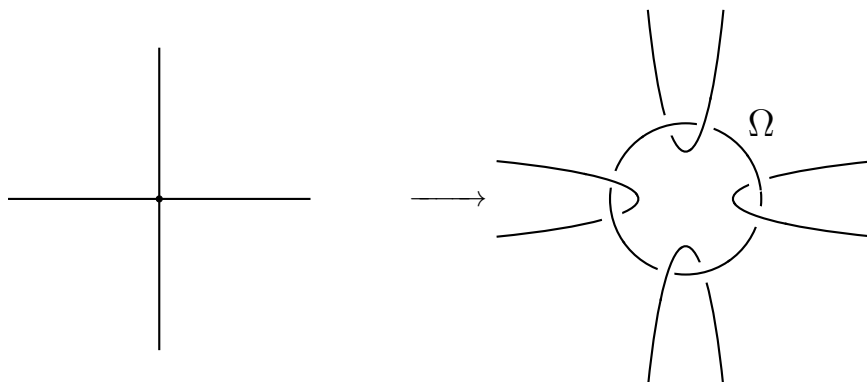


Figure 6.2: The *Chainmail Rule*. Each circle has the same color as its corresponding edge.

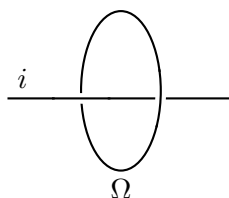


Figure 6.3

$$\begin{array}{c} \text{Diagram of } \Omega \text{ with } r \text{ strands} \end{array} = \sum_{i \in I_r} \Delta_i \begin{array}{c} \text{Diagram of } \Omega \text{ with } i \text{ strands} \end{array} \quad (6.1)$$

This holds for any number of strands; it is obtained by repeated application of the fusion rule followed by the well known fact (see [30, Lemma 6] that if a diagram contains the skein element in Figure 6.3 it is equal to 0 unless $i = 0$).

When passing from Γ to L we still speak of edges and vertices of L : we mean the circles corresponding to edges and vertices of Γ respectively. Slightly more improperly we speak of faces of L , by which we mean the portions of the plane delimited by edges of L .

Now we wish to apply the Fourier transform in a diagrammatic way. This is done via the following relation (obtained from the connected sum formula for the Kauffman bracket):

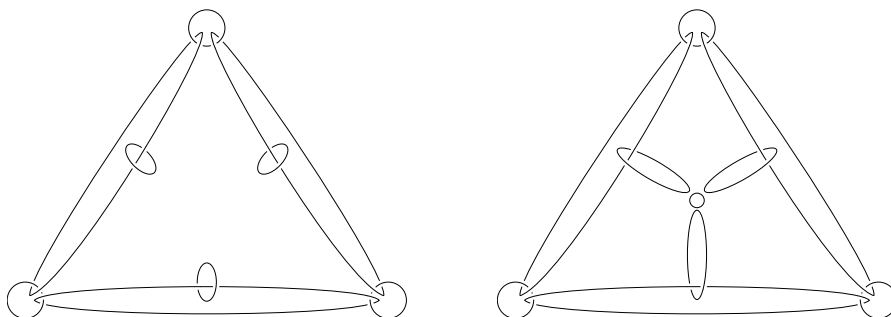


Figure 6.4: Stretching edges towards the center and adding an extra component.

$$\sum_{i \in I_r} H(i, j) \text{---} \underset{i}{\text{---}} = \frac{\Omega}{\text{---}} \text{---} \underset{j}{\text{---}} \quad (6.2)$$

to each component of L that corresponds to an edge of Γ : this gives us the Fourier transform of $Y_r(\Gamma, \text{col})$. We call the meridional circles added via this process the *transverse* circles; they will correspond to edges of Γ^* .

Take a face F of L and stretch the circles transverse to its edges so that they are close to the center of F (see Figure 6.4). Add an unknot U colored with Ω at the center of F and handleslide it along all the edges of F ; the result is that U gets linked to each transversal circle and remains unlinked from any edge or vertex of Γ as in the left part of Figure 6.5. The circle U will correspond to a vertex in Γ^* . Repeat this procedure for every face of L .

Now apply the inverse of the chainmail relation in Figure 6.2 to each circle corresponding to a vertex of Γ and each circle corresponding to a vertex of Γ^* . The result is going to be 4 unlinked graphs (and several unlinked unknots that for now we ignore), 2 of which give $Y_r(\Gamma^*, \text{col}'')$ and two of which give $Y_r(\Gamma, \Omega)$ (where we still denote with Ω the coloring of Γ with color Ω on each edge).

Lemma 6.8. *The following equality holds:*

$$Y_r(\Gamma, \Omega) = N^g.$$

Proof. The Yokota invariant does not change when performing a Whitehead move on an edge colored with Ω (Proposition 3.18.2). Therefore, we can change Γ to be a “bicycle” graph as in 6.6, with some circles connected linearly by segments; since a Whitehead move does not change the genus of the regular neighborhood, there are g circles. Because of the bridge rule 5, the Kauffman bracket is 0 unless the colors of every connecting edge is 0, and therefore

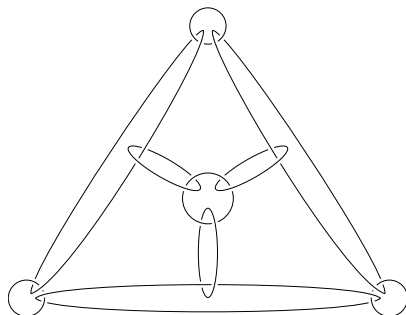


Figure 6.5: The central component gets linked by handleslides.

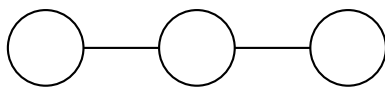


Figure 6.6: Bicycle with 3 wheels

$$Y_r(\Gamma, \Omega) = \left(\sum_{i_1, \dots, i_g \in I_r} \Delta_{i_1}^2 \cdots \Delta_{i_g}^2 \right) = N^g$$

which concludes the proof. \square

To conclude the proof it only remains to check how many factors of N are added or lost through this procedure. At the beginning we added an unknot for each vertex of Γ , and then for each face. However when we applied the inverse of the chainmail relation we removed the exact same number of components; therefore there is no additional N factor. \square

Proposition 6.9. *We have*

$$\lim_{r \rightarrow \infty} \frac{TV_r(\Gamma)}{TV_r(\Gamma^*)} = O(r^n)$$

for some $n \in \mathbb{N}$.

Proof. Let col_{max} be a coloring of Γ such that $|Y_r(\Gamma, col)|$ is maximum.

Thanks to Proposition 6.7

$$\begin{aligned} \frac{TV_r(\Gamma^*)}{TV_r(\Gamma)} &\leq \frac{\sum_{col} |Y_r(\Gamma^*, col)|}{|Y_r(\Gamma, col_{max})|} = N^{-g} \sum_{col} \left| \sum_{col'} H(col, col') \frac{Y_r(\Gamma, col')}{|Y_r(\Gamma, col_{max})|} \right| \leq \\ &N^{-g} \sum_{col, col'} |H(col, col')| \end{aligned}$$

and the latter is a sum of polynomially many polynomial terms. \square

Corollary 6.10. *If $\lim_{r \rightarrow +\infty} \frac{\pi}{r} \log(TV_r(\Gamma))$ exists, then $\lim_{r \rightarrow +\infty} \frac{\pi}{r} \log(TV_r(\Gamma^*))$ also exists; moreover the two quantities are equal.*

Corollary 6.11. *The Maximum Volume Conjecture is true for Γ if and only if it is true for Γ^* .*

Proof. Corollary 5.5 states that the maximum volume of Γ is the same as the maximum volume of Γ^* ; this and Corollary 6.10 imply the thesis. \square

Theorem 1.7. *Conjecture 6.5 (hence, the Maximum Volume conjecture) is verified for any planar graph obtained from the tetrahedron by applying any sequence of the following two moves:*

- *blowing up a trivalent vertex (see Figure 1.1) or*
- *triangulating a triangular face (see Figure 1.2).*

Proof. The proof is by induction on the number g of blow-ups or triangulations needed to construct Γ . Notice that if Γ is obtained from Γ' via a blow-up, Γ^* is obtained from $(\Gamma')^*$ by a triangulation of a triangular face, and vice-versa.

We first prove that $\text{Vol}(\bar{\Gamma}) = (g+1)v_8$. The case of $g = 0$ is well known and appears in [51]. Take now any Γ obtained from Γ' by a blow-up of a vertex v ; we can take the rectification $\bar{\Gamma}'$ and glue a right-angled ideal octahedron to the face corresponding to v . Notice that the gluing is done along an ideal triangular face, and along right dihedral angles. It is immediate to see that this gluing gives the truncation of $\bar{\Gamma}$: the 1-skeleton is the same and there are only right angles. Therefore, by blowing up a vertex the maximum volume grows by v_8 . Dually, triangulating a triangular face makes the maximum volume grow by v_8 as well.

We now prove that

$$\frac{\pi}{r} \log |Y_r(\Gamma, col)| \leq (g+1)v_8 + O\left(\frac{\log(r)}{r}\right).$$

The base case $g = 0$ is Theorem 1.8.

If Γ is obtained from Γ' as a blow-up of a single vertex, then

$$Y_r(\Gamma, col) = Y_r(\Gamma', col_1)Y_r(T, col_2)$$

where T is a tetrahedron, and col_1, col_2 are the colorings induced by col on Γ' and T respectively. Therefore, $Y_r(\Gamma, col) \leq Y_r(\Gamma', col_1)Y_r(T, col_2)$ and by induction

$$\frac{\pi}{r} \log |Y_r(\Gamma, col)| \leq (g+1)v_8 + O\left(\frac{\log(r)}{r}\right).$$

By duality, this inequality also holds if Γ is obtained from Γ' by triangulating a single triangular face.

The sharpness of the upper bound is proven in the following proposition.

Proposition 6.12. *If Γ is as above and $col = (\frac{r-2\pm 1}{2}, \dots, \frac{r-2\pm 1}{2})$ (where the signs are chosen so that $r-2\pm 1$ is a multiple of 4), then*

$$\lim_{r \rightarrow +\infty} \frac{\pi}{r} \log(Y_r(\Gamma, col)) = (g+1)v_8.$$

Proof. The proof is once again by induction; the base case is Theorem 1.8. Suppose Γ is obtained from the tetrahedron by g blow-ups and triangulations, and at least 1 blow-up. Then, Γ is a vertex sum of Γ_1 and Γ_2 , with both graphs obtained from the tetrahedron via g_1 and g_2 blow-ups or triangulations respectively, and $g_1 + g_2 = g - 1$. Since $Y_r(\Gamma, col) = Y_r(\Gamma_1, col_1)Y_r(\Gamma_2, col_2)$ (with col_1, col_2 the colorings induced by col on Γ_1, Γ_2 respectively), we have

$$\begin{aligned} \lim_{r \rightarrow +\infty} \frac{\pi}{r} \log(Y_r(\Gamma, col)) &= \lim_{r \rightarrow +\infty} \frac{\pi}{r} \log(Y_r(\Gamma_1, col_1)Y_r(\Gamma_2, col_2)) = \\ &= (g_1 + 1 + g_2 + 1)v_8 = (g+1)v_8. \end{aligned}$$

We need to deal with the case of Γ being obtained via g triangulations. In this case, Γ^* is obtained from the tetrahedron via g blow-ups. Apply the Fourier transform to $Y_r(\Gamma, col)$:

$$Y_r(\Gamma, col) = \sum_{col'} H(col, col') Y_r(\Gamma^*, col');$$

however, since col is constantly $\frac{r-2\pm 1}{2}$ and even,

$$\begin{aligned} H\left(\frac{r-2\pm 1}{2}, j\right) &= (-1)^j \frac{\sin\left(\frac{2\pi}{r} \frac{r\pm 1}{2}(j+1)\right)}{\sin(2\pi/r)} = \\ (-1)^j \frac{\sin\left(\pi(j+1) \pm \frac{\pi}{r}(j+1)\right)}{\sin(2\pi/r)} &= -\frac{\sin\left(\pm \frac{\pi}{r}(j+1)\right)}{\sin(2\pi/r)} \end{aligned}$$

which has \mp sign since $0 \leq j \leq r-1$. Moreover, since Γ^* is a trivalent graph, $Y_r(\Gamma^*, col') = |\langle \Gamma^*, col' \rangle|^2$ is non-negative for every coloring; therefore, $Y_r(\Gamma, col)$ is a sum with constant sign of $Y_r(\Gamma^*, col')$ over all possible colorings. This shows that $Y_r(\Gamma, col)$ grows as the maximum growth of $Y_r(\Gamma^*, col')$ over all colorings, which is $(g+1)v_8$. \square

□

Remark 6.13. Proposition 6.12 actually proves the Conjecture 1.3 for a large family of polyhedra (albeit for a single sequence of colors each) since the volume of a polyhedron with internal angles 0 is the volume of its rectification (notice how $2\pi \frac{r \pm 1 - 2}{2} \rightarrow \pi$). Moreover, because of 3.20, Conjecture 1.3 is verified (for the sequence above) for any graph obtained from the tetrahedron via blow-ups, triangulations and doubles.

6.3 The Turaev-Viro volume conjecture

In this section we apply Theorem 1.7 to prove the Turaev-Viro volume conjecture for an infinite family of examples. The manifolds for which we prove the conjecture have Reshetikhin-Turaev invariants closely related to the Yokota invariant of the graphs of Theorem 1.7.

Proposition 6.14. *Let $\Gamma \subseteq S^3$ be a graph obtained from the tetrahedron by a sequence of $g-1$ blow-ups of vertices or triangulations of triangular faces as in the hypothesis of Theorem 1.7; let e_1, \dots, e_k be its edges, and denote with h the number of vertices of Γ . Then there is a k -component link $L = L_1 \sqcup \dots \sqcup L_k$ in $S^3 \#^{h-1} (S^1 \times S^2)$ such that for any $col \in I_r^k$ coloring (seen both as a coloring of Γ and as a coloring of L) we have*

$$Y_r(\Gamma, col) = \left(\sqrt{\frac{2}{r}} \sin(2\pi/r) \right)^h RT_r(S^3 \#^{h-1} (S^1 \times S^2), L, col)$$

Proof. We have seen in the proof of Proposition 6.7 that there is a way to associate to any (Γ, col) a skein element \mathcal{L} in $\mathcal{S}(S^3)$ such that $Y_r(\Gamma, col) = \langle \mathcal{L} \rangle$. The skein \mathcal{L} is a link with $k+h$ components; k of these components are in bijection with the edges of Γ and are colored with the corresponding color of col . The other h are unknotted components in bijection with the vertices of Γ and are colored with Ω . Pick a component of \mathcal{L} colored with Ω : it is possible to handleslide it along each other Ω -colored component without modifying the Kauffman bracket. After it is handleslid along each component, it becomes unlinked from everything, therefore $\langle \mathcal{L} \rangle = \langle U \rangle \langle \mathcal{L}' \rangle = \left(\sqrt{\frac{2}{r}} \sin(2\pi/r) \right) \langle \mathcal{L}' \rangle$ where U is an unknotted, unlinked component colored with Ω and \mathcal{L}' is the remaining part of the skein. By the definition of the Reshetikhin-Turaev invariant of links

$$\langle \mathcal{L}' \rangle = \left(\sqrt{\frac{2}{r}} \sin(2\pi/r) \right)^{h-1} RT_r(S^3 \#^{h-1} (S^1 \times S^2), L, col)$$

where L is the link obtained from \mathcal{L}' by doing a 0-framed Dehn surgery on the components of \mathcal{L} colored with Ω . Notice that L only depends on Γ and not on the coloring. \square

As we did previously to simplify the notation, when writing the formulas we drop the factor $\left(\sqrt{\frac{2}{r}} \sin(2\pi/r)\right)^{h-1}$; since this is a factor that grows polynomially in r , dropping it is inconsequential when proving the volume conjecture.

Proposition 6.15. *If Γ is as in Proposition 6.14, then the link L obtained from Γ by the construction of Proposition 6.14 is hyperbolic, and its hyperbolic structure is obtained by gluing $4g$ right-angled hyperbolic ideal octahedra.*

Proof. Let $\bar{\Gamma}$ be the rectification of Γ , and let P be its truncation. We have seen in the proof of Theorem 1.7 that P can be obtained by gluing g right-angled hyperbolic octahedra. Take two copies of P and glue them along each corresponding truncation face. This gives a manifold homeomorphic to a handlebody of genus $h - 1$ with some annuli removed from the boundary; the decomposition into octahedra makes it into a finite volume manifold M with geodesic boundary. Take the double of M along the geodesic boundary: this gives a manifold N which is homeomorphic to $S^3 \#^{h-1} (S^1 \times S^2) \setminus L$.

To see this, take the octahedron O and truncate a small link of each of its vertices. This truncation can be seen as the basic building block of the fundamental shadow links (see Figure 2.13): each truncated vertex corresponds to an arc, four of the faces of the octahedron correspond to the discs and the remaining four faces correspond to the regions of the spheres delimited by the arcs.

The polyhedron P is obtained by gluing octahedra together; glue the building blocks in the same pattern to obtain a ball with h discs on its boundary and some arcs connecting the discs. If we take the double of this ball along the discs we obtain a genus $h - 1$ handlebody with a link in its boundary. Doubling the handlebody gives $S^3 \#^h (S^1 \times S^2)$ and the link in the boundary is exactly L . \square

We will soon prove that the Turaev-Viro Volume Conjecture holds for the complements of the links just introduced; we need to show that this result is interesting by proving that some of these complements are not diffeomorphic to complements of Fundamental Shadow Links. We do this by counting how many thrice punctured spheres there are in each complement.

Proposition 6.16. *Let Γ be a graph as in the hypotheses of Proposition 6.14; let t be the maximal number of disjoint triangular faces in the truncation of $\bar{\Gamma}$. Let L be the link associated to Γ by the construction of Proposition 6.14, and*

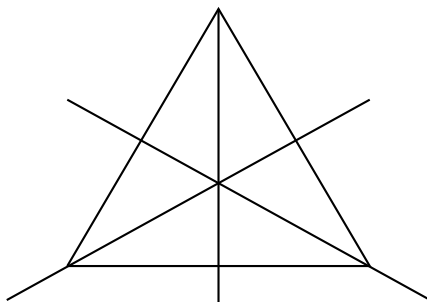


Figure 6.7: The 6 geodesic in a thrice punctured sphere cutting it into triangles.

E_L be its exterior. Then E_L contains at most $t+2g-2$ disjoint thrice-punctured spheres.

Proof. The reasoning in this proof is similar to the proof of [15, Proposition 3.4].

Let P be the truncation of $\bar{\Gamma}$; we have seen that E_L is obtained by doubling P along the truncation faces (to obtain a hyperbolic manifold with geodesic boundary H) and doubling again along the geodesic boundary.

Since it is the rectification of Γ , the truncation faces of P can be colored with black and the remaining with white; this way two faces of the same color never share an edge.

As we have seen E_L decomposes into octahedra; take O an octahedron in this decomposition, and let S be any thrice-punctured sphere.

Claim: $S \cap O$ is either the empty set or a facet of O .

We first look at $S \cap O$ as a subset of S . It must be a convex region of S delimited by geodesics. Since S contains exactly 6 close geodesics the possible configurations are easy to list. Figure 6.7 shows the 6 geodesics cutting S into triangles; the possibilities for $S \cap O$ can be obtained by looking at all the possible ways to glue these triangles to obtain a convex set. The convex subsets of S obtained by gluing triangle regions are:

1. a triangle with 1 ideal vertex (obtained by taking a single triangle region);
2. a triangle with 2 ideal vertices (obtained by gluing two triangle regions without an ideal vertex in common);
3. a square with 1 ideal vertex and 2 right angles (obtained by gluing two triangle regions with an ideal vertex in common);
4. a triangle with 2 ideal vertices and a right angle (obtained by gluing a triangle region to the triangle in 2);

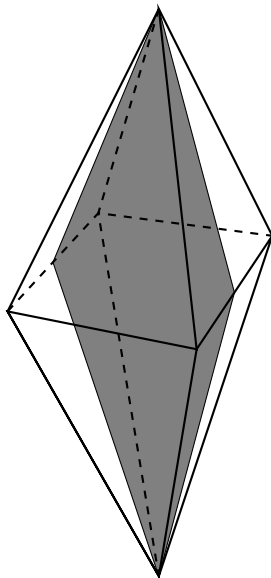


Figure 6.8: A square arising as the intersection of a thrice-punctured sphere and an octahedron of E_L .

5. a square with 2 ideal vertices (obtained by gluing two triangles in 2 along a common geodesic side);
6. a bigon with 1 ideal point (obtained by gluing all triangle regions sharing an ideal vertex);
7. a triangle with 3 ideal vertices (obtained by gluing 6 triangle regions);
8. the whole thrice-punctured sphere S .

Every other possible way of gluing together the triangle regions of Figure 6.7 does not give a convex subset.

On the other hand, $S \cap O$ as a subset of O must coincide with the intersection of O with a plane $\Pi \subseteq \mathbb{H}^3$; therefore it cannot be either a bigon with an ideal point nor the whole S . Moreover, $\Pi \cap O$ cannot be a triangle with one or two ideal vertices, nor can it be a square with one ideal vertex and two right angles. The remaining possibilities are that it is a vertex, an edge, an ideal triangle (which is to say, a face) or a square with two ideal vertices (see Figure 6.8). However, every octahedron that is glued to O must be distinct by construction; therefore the latter case is impossible since the intersection of S with four of these octahedra must also be a square with 2 ideal vertices, which would contradict the fact that S is a thrice-punctured sphere.

Let \mathcal{S} be a set of disjoint thrice-punctured spheres. This determines a set of disjoint ideal triangles in each of the four copies of P that make up E_L . Each

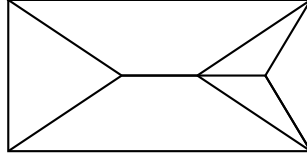


Figure 6.9: A graph whose link is not a fundamental shadow link.

polyhedron contains exactly $g - 1$ properly embedded geodesic triangles (the ones that decompose P into octahedra). These glue up to give $2g - 2$ disjoint thrice-punctured spheres in E_L . Furthermore, a disjoint collection T_1, \dots, T_t of triangles in ∂P induces a set of disjoint thrice-punctured spheres. Therefore, there are at most $2g - 2 + t$ disjoint thrice-punctured spheres in E_L . \square

Remark 6.17. If M is the exterior of a fundamental shadow link with volume $2nv_8$, then it contains exactly $2n$ disjoint thrice-punctured spheres. This can be used to show that some of the exterior of the links provided by Proposition 6.14 are not fundamental shadow links; the simplest such example is the link associated to the graph shown in Figure 6.9. An easy check shows that the truncation of $\bar{\Gamma}$ contains at most 6 disjoint triangular faces, which means that E_L contains at most 10 thrice-punctured spheres; on the other hand a fundamental shadow link with the same volume as E_L must contain 12 spheres.

More in general, if Γ as above is obtained from the tetrahedron through at least one triangulation and at least one blow-up, then the associated manifold is not diffeomorphic to the exterior of a fundamental shadow link.

Theorem 6.18. *Let $L \subseteq S^3 \#^{h-1} (S^1 \times S^2)$ obtained from Γ by applying the construction of Proposition 6.14. Then the Turaev-Viro volume conjecture holds for the exterior of L .*

Proof. Theorem 1.7 implies that

$$\frac{\pi}{r} \log |RT_r(S^3 \#^{h-1} (S^1 \times S^2), L, col)| = \frac{\pi}{r} \log |Y_r(\Gamma, col)| \leq gv_8 + O(\log(r)/r).$$

Furthermore if we denote with c the coloring $(\frac{r+1}{2}, \dots, \frac{r+1}{2})$ (where the sign is chosen so that the color is always even), we have

$$\frac{\pi}{r} \log |RT_r(S^3 \#^{h-1} (S^1 \times S^2), L, c)| = \frac{\pi}{r} \log |Y_r(\Gamma, c)| = gv_8 + O(\log(r)/r).$$

If E_L is the exterior of L ,

$$TV_r(E_L) = \sum_{col \in I_r^k} |RT_r(S^3 \#^{h-1} (S^1 \times S^2), L, col)|^2$$

by 3.14, and $\text{Vol}(E_L) = 4gv_8$ by Proposition 6.15, which implies the thesis by the same reasoning used in the proof of Theorem 1.8. \square

Remark 6.19. There is an overlap between Theorem 6.18 and Theorem 1.8. Some links of Theorem 6.18 are also Fundamental Shadow Links (FSL); namely, those links corresponding to graphs obtained from the tetrahedron by blow-ups. However many other are not.

Appendix A

Numerical evidence for Conjecture 1.3

Supporting evidence for Conjecture 1.3 in the case of simple polyhedra can be found in [29]. In this appendix we show numerical computations supporting the conjecture for the square and pentagonal pyramids; all the calculations are performed with the Mathematica software.

The ideal regular square pyramid.

By Theorem 2.15 there is a unique square pyramid such that the angles at the base are $\frac{\pi}{4}$ and the vertical angles are $\frac{\pi}{2}$. Such a pyramid is ideal and is maximally symmetric; it is decomposed into two ideal tetrahedra with angles $\frac{\pi}{4}, \frac{\pi}{4}, \frac{\pi}{2}$ hence its hyperbolic volume is equal to $4\Lambda\left(\frac{\pi}{4}\right) = \frac{v_8}{2} \cong 1.83193$ (where Λ is the Lobachevski function). Consider the coloring of Figure A.1; it converges to the angles of the ideal pyramid in the sense of Conjecture 1.3.

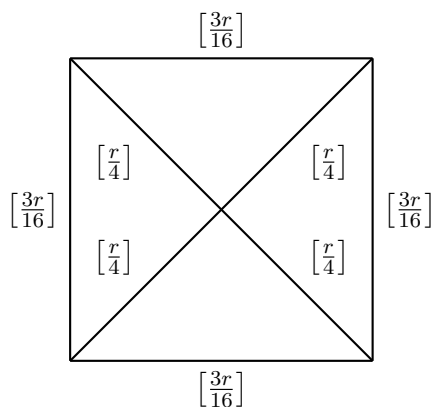
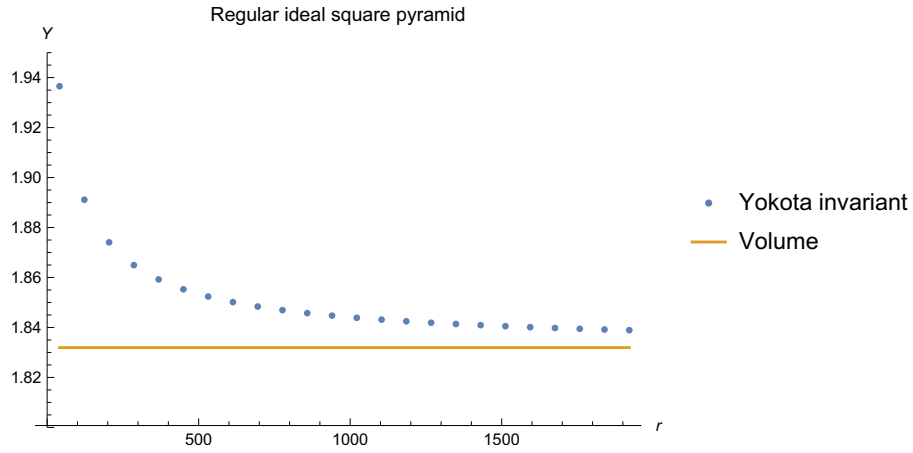


Figure A.1: The coloring of a square pyramid associated to the ideal regular pyramid

Its Yokota invariant is given by

$$\sum_{i \in I_r} \Delta_i \left| \begin{bmatrix} \lceil \frac{r}{4} \rceil \\ \lceil \frac{3r}{16} \rceil \\ \lceil \frac{3r}{16} \rceil \end{bmatrix} \begin{bmatrix} \lceil \frac{r}{4} \rceil \\ \lceil \frac{3r}{16} \rceil \\ \lceil \frac{3r}{16} \rceil \end{bmatrix} \begin{bmatrix} i \\ \lceil \frac{3r}{16} \rceil \\ \lceil \frac{3r}{16} \rceil \end{bmatrix} \right|^4$$

where $\lceil x \rceil$ is the rounding of x to the nearest integer.



The 0-angled squared pyramid

Because of the arguments of Section 2.2, the square pyramid with every dihedral angle equal to 0 exists and attains the maximum volume of any square pyramid (it is in fact the rectified pyramid). Its truncation is the right-angled ideal antiprism. The volume of a right-angled ideal antiprism with n -gonal face is given by

$$2n \left(\Lambda \left(\frac{\pi}{4} + \frac{\pi}{2n} \right) + \Lambda \left(\frac{\pi}{4} - \frac{\pi}{2n} \right) \right)$$

and for $n = 4$ this gives $\cong 6.02305$.

Color the pyramid with the color $\lceil \frac{r}{4} \rceil$ at every vertex; this coloring converges to the angles of the rectified pyramid.

Its Yokota invariant is given by

$$\sum_{i \in I_r} \Delta_i \left| \begin{bmatrix} \lceil \frac{r}{4} \rceil \\ \lceil \frac{r}{4} \rceil \\ \lceil \frac{r}{4} \rceil \end{bmatrix} \begin{bmatrix} \lceil \frac{r}{4} \rceil \\ \lceil \frac{r}{4} \rceil \\ \lceil \frac{r}{4} \rceil \end{bmatrix} \begin{bmatrix} i \\ \lceil \frac{r}{4} \rceil \\ \lceil \frac{r}{4} \rceil \end{bmatrix} \right|^4$$

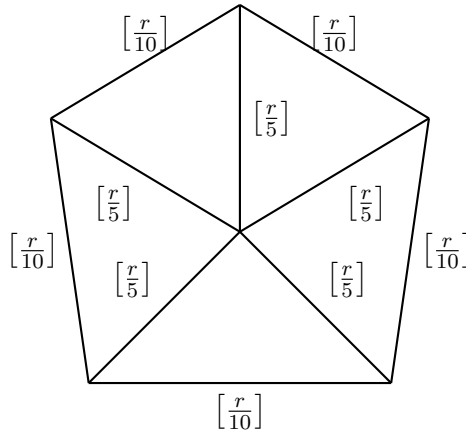
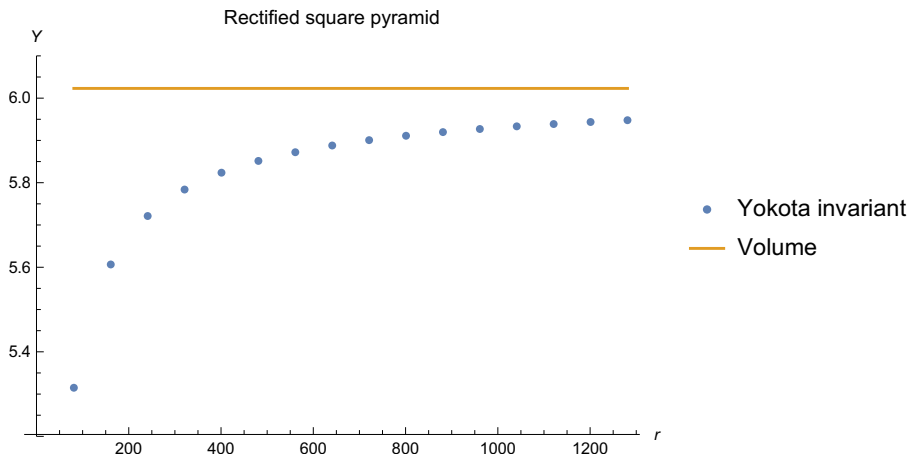


Figure A.2: The coloring of the pentagonal pyramid corresponding to an ideal regular pyramid



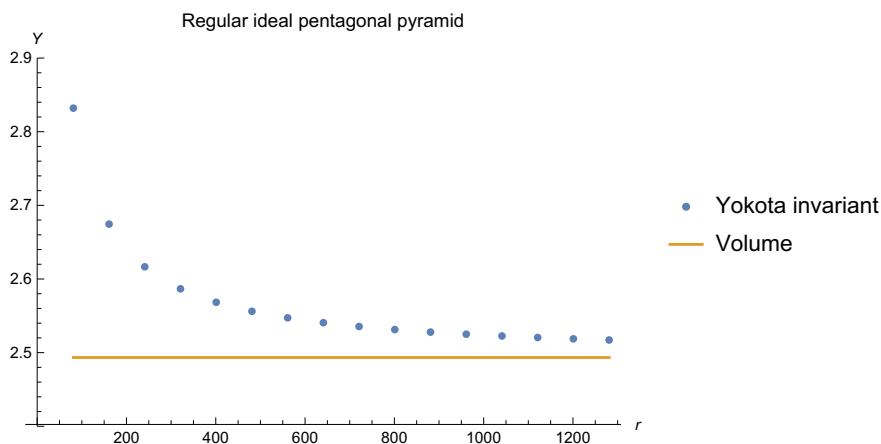
The ideal regular pentagonal pyramid.

As before there is a unique ideal pentagonal pyramid with vertical angles $\frac{3\pi}{5}$ and base angles $\frac{\pi}{5}$; this pyramid is maximally symmetric. We can decompose it into 3 ideal tetrahedra, two with dihedral angles $\frac{\pi}{5}, \frac{\pi}{5}, \frac{3\pi}{5}$ and the remaining with dihedral angles $\frac{\pi}{5}, \frac{2\pi}{5}, \frac{2\pi}{5}$. Its volume then is

$$5\Lambda\left(\frac{\pi}{5}\right) + 2\Lambda\left(\frac{2\pi}{5}\right) + \Lambda\left(\frac{3\pi}{5}\right) \cong 2.49339.$$

Consider the coloring in Figure A.2, converging to the angles of the ideal pyramid. Its Yokota invariant is

$$\sum_{i,j \in I_r} \Delta_i \Delta_j \left| \left(\left| \begin{bmatrix} \left[\frac{r}{10}\right] & \left[\frac{r}{10}\right] & i \\ \left[\frac{r}{5}\right] & \left[\frac{r}{5}\right] & \left[\frac{r}{5}\right] \end{bmatrix} \right| \left| \begin{bmatrix} \left[\frac{r}{10}\right] & \left[\frac{r}{10}\right] & j \\ \left[\frac{r}{5}\right] & \left[\frac{r}{5}\right] & \left[\frac{r}{5}\right] \end{bmatrix} \right| \left| \begin{bmatrix} \left[\frac{r}{10}\right] & i & j \\ \left[\frac{r}{5}\right] & \left[\frac{r}{5}\right] & \left[\frac{r}{5}\right] \end{bmatrix} \right| \right) \right|^2.$$

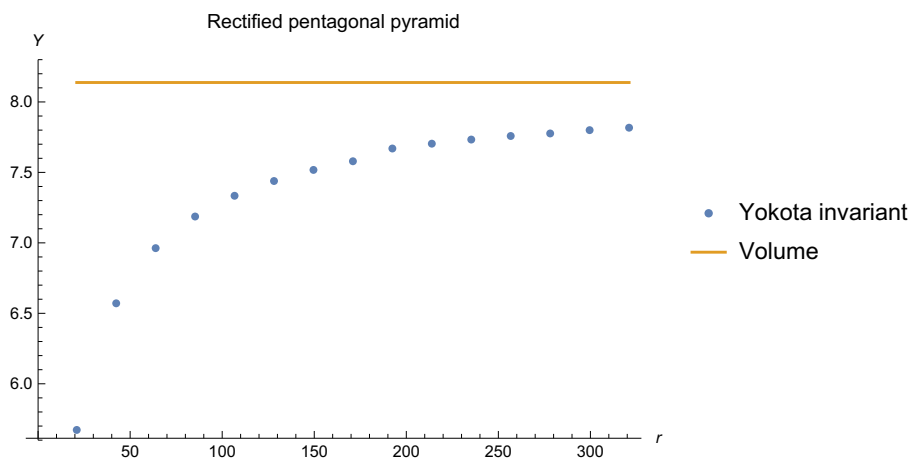


The 0-angled pentagonal pyramid

The volume of the rectified pyramid is $\cong 8.13789$, and the corresponding Yokota invariant is

$$\sum_{i,j \in I_r} \Delta_i \Delta_j \left| \left(\left| \begin{bmatrix} r \\ \frac{r}{4} \\ \frac{r}{4} \end{bmatrix} \begin{bmatrix} r \\ \frac{r}{4} \\ \frac{r}{4} \end{bmatrix} \begin{bmatrix} i \\ \frac{r}{4} \end{bmatrix} \right| \left| \begin{bmatrix} r \\ \frac{r}{4} \\ \frac{r}{4} \end{bmatrix} \begin{bmatrix} r \\ \frac{r}{4} \\ \frac{r}{4} \end{bmatrix} \begin{bmatrix} j \\ \frac{r}{4} \end{bmatrix} \right| \left| \begin{bmatrix} r \\ \frac{r}{4} \\ \frac{r}{4} \end{bmatrix} \begin{bmatrix} i \\ \frac{r}{4} \end{bmatrix} \begin{bmatrix} j \\ \frac{r}{4} \end{bmatrix} \right| \right)^2.$$

Because of the greater range of the sum, it is considerably slower to compute than the other examples; we were only able to arrive to level $r = 321$, and the Yokota invariant is within 4% of the volume. However this is similar to the error (at level 321) in the previous examples.



Bibliography

- [1] E. M. Andreev. On convex polyhedra in Lobachevskii spaces. *Matematicheskii Sbornik*, 123(3):445–478, 1970.
- [2] X. Bao and F. Bonahon. Hyperideal polyhedra in hyperbolic 3-space. *Bulletin de la Société mathématique de France*, 130(3):457–491, 2002.
- [3] J.W. Barrett. Geometrical measurements in three-dimensional quantum gravity. *International Journal of Modern Physics A*, 18(supp02):97–113, 2003.
- [4] J.W. Barrett, J. Faria Martins, and J.M. García-Islas. Observables in the Turaev-Viro and Crane-Yetter models. *Journal of Mathematical Physics*, 48(9):093508, 2007.
- [5] G. Belletti. A maximum volume conjecture for hyperbolic polyhedra. *arXiv:2002.01904*, 2020.
- [6] G. Belletti. The maximum volume of hyperbolic polyhedra. *arXiv:2002.00174*, 2020.
- [7] G. Belletti, R. Detcherry, E. Kalfagianni, and T. Yang. Growth of quantum 6j-symbols and applications to the Volume Conjecture. *arXiv:1807.03327*, accepted for publication at the Journal of Differential Geometry, 2018.
- [8] R. Benedetti and C. Petronio. On Roberts’ proof of the Turaev-Walker theorem. *J. Knot Theory Ramifications*, 5(4):427–439, 1996.
- [9] L. Charles and J. Marché. Knot state asymptotics I: AJ conjecture and Abelian representations. *Publications mathématiques de l’IHÉS*, 121(1):279–322, 2015.
- [10] L. Charles and J. Marché. Knot state asymptotics II: Witten conjecture and irreducible representations. *Publications mathématiques de l’IHÉS*, 121(1):323–361, 2015.

- [11] Q. Chen and J. Murakami. Asymptotics of Quantum $6j$ -Symbols. *arXiv preprint math.GT/1706.04887*.
- [12] Q. Chen and T. Yang. Volume conjectures for the Reshetikhin–Turaev and the Turaev–Viro invariants. *Quantum Topology*, 9(3):419–460, 2018.
- [13] F. Costantino. $6j$ -symbols, hyperbolic structures and the volume conjecture. *Geom. Topol.*, 11:1831–1854, 2007.
- [14] F. Costantino. Colored Jones invariants of links in $S^3 \#_k S^2 \times S^1$ and the volume conjecture. *J. London Math. Soc.*, 76(2):1–15, 2007.
- [15] F. Costantino, R. Frigerio, B. Martelli, and C. Petronio. Triangulations of 3-manifolds, hyperbolic relative handlebodies, and Dehn filling. *Comment. Math. Helv.*, 82(4):903–933, 2007.
- [16] F. Costantino, F. Guéritaud, and R. van der Veen. On the volume conjecture for polyhedra. *Geometriae Dedicata*, 179(1):385–409, 2015.
- [17] F. Costantino and D. Thurston. 3-manifolds efficiently bound 4-manifolds. *J. Topol.*, 1(3):703–745, 2008.
- [18] R. Detcherry and E. Kalfagianni. Gromov norm and Turaev-Viro invariants of 3-manifolds. GT. arXiv:1705.09964.
- [19] R. Detcherry, E. Kalfagianni, and T. Yang. Turaev-Viro invariants, colored Jones polynomials, and volume. *Quantum Topology*, 9(4):775–813, 2018.
- [20] R. Díaz. Non-convexity of the space of dihedral angles of hyperbolic polyhedra. *Comptes Rendus de l'Académie des Sciences - Series I - Mathematics*, 325(9):993 – 998, 1997.
- [21] H. Fleischner. The uniquely embeddable planar graphs. *Discrete Mathematics*, 4(4):347–358, 1973.
- [22] S. Garoufalidis and T.T.Q. Lê. Asymptotics of the colored Jones function of a knot. *Geometry & Topology*, 15(4):2135–2180, 2011.
- [23] L. Jeffrey. Chern-Simons-Witten invariants of lens spaces and torus bundles, and the semiclassical approximation. *Communications in mathematical physics*, 147(3):563–604, 1992.
- [24] V. Jones. A polynomial invariant for knots via von Neumann algebras. *Bulletin of the American Mathematical Society*, 12(1):103–111, 1985.
- [25] R. Kashaev. The hyperbolic volume of knots from the quantum dilogarithm. *Letters in Mathematical Physics*, 39(3):269–275, 1997.

- [26] L.H. Kauffman and S. Lins. *Temperley-Lieb recoupling theory and invariants of 3-manifolds*. Princeton University Press, 1994.
- [27] Robion Kirby. A calculus for framed links in S^3 . *Invent. math.*, 45(1):35–56, 1978.
- [28] A. Kirillov and N. Reshetikhin. Representations of the algebra $U_q(\mathfrak{sl}_2)$, q -orthogonal polynomials and invariants of links. *Infinite-dimensional Lie algebras and groups*, 1989.
- [29] A. Kolpakov and J. Murakami. Combinatorial Decompositions, Kirillov–Reshetikhin Invariants, and the Volume Conjecture for Hyperbolic Polyhedra. *Experimental Mathematics*, 27(2):193–207, 2018.
- [30] W.B.R. Lickorish. The skein method for three-manifold invariants. *Journal of Knot Theory and Its Ramifications*, 2(02):171–194, 1993.
- [31] W.B.R. Lickorish. *An introduction to knot theory*, volume 175. Springer Science & Business Media, 2012.
- [32] B. Martelli. An introduction to geometric topology. *arXiv preprint arXiv:1610.02592*, 2016.
- [33] J.W. Milnor. *Collected papers. 1. Geometry*. Publish or Perish, 1994.
- [34] Y. Miyamoto. On the volume and surface area of hyperbolic polyhedra. *Geometriae Dedicata*, 40(2):223–236, 1991.
- [35] G. Montcouquiol. Deformations of hyperbolic convex polyhedra and cone-3-manifolds. *Geometriae Dedicata*, 166(1):163–183, 2013.
- [36] J. Murakami and M. Yano. On the volume of a hyperbolic and spherical tetrahedron. *Communications in analysis and geometry*, 13(2):379–400, 2005.
- [37] T. Ohtsuki. On the asymptotic expansion of the Kashaev invariant of the 5_2 knot. *Quantum Topol.*, 7(4):669–735, 2016.
- [38] T. Ohtsuki. On the asymptotic expansions of the Kashaev invariant of hyperbolic knots with seven crossings. *International Journal of Mathematics*, 28(13):1750096, 2017.
- [39] T. Ohtsuki. On the asymptotic expansion of the quantum $SU(2)$ invariant at $q = \exp(4\pi\sqrt{-1}/N)$ for closed hyperbolic 3-manifolds obtained by integral surgery along the figure-eight knot. *Algebraic & Geometric Topology*, 18(7):4187–4274, 2018.

- [40] T. Ohtsuki and Y. Yokota. On the asymptotic expansions of the Kashaev invariant of the knots with 6 crossings. In *Mathematical Proceedings of the Cambridge Philosophical Society*, volume 165, pages 287–339. Cambridge University Press, 2018.
- [41] N. Reshetikhin and V. Turaev. Ribbon graphs and their invariants derived from quantum groups. *Communications in Mathematical Physics*, 127(1):1–26, 1990.
- [42] N. Reshetikhin and V. Turaev. Invariants of 3-manifolds via link polynomials and quantum groups. *Inventiones mathematicae*, 103(1):547–597, 1991.
- [43] I. Rivin. Euclidean structures on simplicial surfaces and hyperbolic volume. *Annals of mathematics*, 139(3):553–580, 1994.
- [44] I. Rivin. A characterization of ideal polyhedra in hyperbolic 3-space. *Annals of mathematics*, pages 51–70, 1996.
- [45] I. Rivin and C. Hodgson. A characterization of compact convex polyhedra in hyperbolic 3-space. *Inventiones mathematicae*, 111(1):77–111, 1993.
- [46] E. Steinitz. Polyeder und raumeinteilungen. *Encyk der Math Wiss*, 12:38–43, 1922.
- [47] W. Thurston. *The geometry and topology of three-manifolds*. Princeton University Princeton, NJ, 1979.
- [48] V. G. Turaev. Shadow links and face models of statistical mechanics. *J. Differential Geom.*, 36(1):35–74, 1992.
- [49] V. G. Turaev. *Quantum invariants of knots and 3-manifolds*, volume 18 of *de Gruyter Studies in Mathematics*. Walter de Gruyter & Co., Berlin, 1994.
- [50] V. G. Turaev and O. Y. Viro. State sum invariants of 3-manifolds and quantum $6j$ -symbols. *Topology*, 4:865–902, 1992.
- [51] A. Ushijima. A volume formula for generalised hyperbolic tetrahedra. In *Non-Euclidean geometries*, pages 249–265. Springer, 2006.
- [52] R. van der Veen. The volume conjecture for augmented knotted trivalent graphs. *Algebraic & Geometric Topology*, 9(2):691–722, 2009.
- [53] A. Vesnin and A. Egorov. Ideal right-angled polyhedra in Lobachevsky space. *preprint arXiv:1909.11523*.
- [54] H. Weiss. The deformation theory of hyperbolic cone-3-manifolds with cone-angles less than 2π . *Geometry & Topology*, 17(1):329–367, 2013.

- [55] E. Witten. Quantum field theory and the Jones polynomial. *Communications in Mathematical Physics*, 121(3):351–399, 1989.
- [56] Y. Yokota. Topological invariants of graphs in 3-space. *Topology*, 35(1):77–87, 1996.